WASHINGTON UNIVERSITY

SEVER INSTITUTE OF TECHNOLOGY

INTEGRAL TRICKLE-BED REACTOR PERFORMANCE

by

Ahmed A. Elhisnawi

Prepared under the direction of Professor M. P. Duduković

A research proposal presented to the Sever Institute of Washington University in partial fulfillment of the requirement for the degree of

DOCTOR OF SCIENCE

May, 1980

Saint Louis, Missouri

WASHINGTON UNIVERSITY
SEVER INSTITUTE OF TECHNOLOGY

ABSTRACT

INTEGRAL TRICKLE-BED REACTOR PERFORMANCE

by

Ahmed A. Elhisnawi

ADVISOR: Professor M. P. Duduković

May, 1980

Saint Louis, Missouri

The effect of superficial velocities and liquid physical properties on a trickle-bed reactor performance operated at high conversion per pass will be investigated. It is of particular interest to determine whether reactor performance can be predicted from the information given on contacting efficiency, rate and transport coefficients.

Reaction and tracer experiments will be performed in a laboratory scale glass column with two phase flow over both 0.5% and 2.5% palladium on alumina catalyst. The selected reaction system is the catalytic hydrogenation of α-methylstyrene to cumane in various hydrocarbon solvents.

The solvents selected are cyclohexane, hexane, and tetrahydrofurane which will also be used in the tracer experiments as the carrier liquids. Nitrogen or helium will serve as the gas phase for tracer experiments. The gas and liquid superficial velocities will be varied over ranges that are comparable to those utilized in pilot scale and industrial size trickle-bed reactors.

The results will be interpreted by a suitable model which accounts for the various transport processes between the three phases, and contacting effectiveness.

TABLE OF CONTENTS

LIST OF FIGURES

LIST OF FIGURES
(continued)

LIST OF TABLES

CHAPTER 1

Introduction

1-1. GENERAL:

A trickle-bed reactor is a multiphase reactor in which liquid and gaseous reactants in cocurrent flow are contacted over a fixed bed of catalyst particles. The presence of a three phase system in such a reactor adds more complexity to the design and prediction of the reactor performance. The main problems are related to the areas of heat and mass transfer, liquid holdups. pressure drop, solid-liquid contacting effectiveness, catalyst utilization and reaction nature.

Several studies have appeared in the literature regarding the physical aspects of the problem such as pressure drop, residence time distribution and hydrodynamic models. These studies are summarized by Charpentier et al (28)*, Satterfield (8), Hoffman (9, 10) and recently discussed by Mills (110). Chemical aspects of the operation of such a reactor have received little attention in the past except for the studies of Goto and Smith (35), Sedriks and Kenney (49), Satterfield and co-workers (66, 62) and Germain et al (63).

The selection of a proper heterogeneous reaction system is important for the success of this project. The reaction system chosen must satisfy the following requirements:

1. Reaction proceeds only in the liquid phase and is catalyzed by solid.

* The numbers in parentheses in the text indicate references in the Bibliography.

2. No homogeneous reaction takes place.

3. Reactants or products do not poison the catalyst.

In addition to the above requirements, it is desirable that the reaction system chosen proceeds at normal conditions and in the presence of an inert liquid solvent in order to avoid or minimize heat effects and hot spots that otherwise could exist in the case of an exothermic reaction.

Based on preliminary experiments, literature survey and the work of previous investigators on trickle-bed reactors, we have chosen the hydrogenation of α-methylstyrene to cumene as a reaction model. The hydrogenation reaction will be carried out using 0.5% and 2.5% palladium on alumina catalyst in various hydrocarbon solvents at atmospheric pressure and a temperature range of 15°C to 30°C. The selection of this reaction system was also based upon the low volatility and ease of hydrogenation resulting in an appreciable rate at these conditions in the liquid phase.

1-2. RESEARCH OBJECTIVES:

The main objectives of the proposed research are to: (*i*) determine the effects of liquid physical properties (ℓ, μ, σ) and mass velocities on the performance of an integral packed bed reactor operated in trickle-flow regime, and to (*ii*) develop an appropriate model for trickle-bed reactor performance. A list of specific goals which will allow these objectives to be achieved is summarized below:

1. Establish the kinetics of the reaction free of any external or internal mass transfer effects.

2. Establish the effect of solvent on the reaction rate.
3. Establish the effect of palladium concentration on the reaction rate.
4. Determine the effect polymerization inhibitor and purified-aged α-methylstyrene on the reaction rate.
5. Determine the effectiveness factor of completely wetted pellets.
6. Determine contacting efficiency in a trickle-bed reactor using tracers in various hydrocarbon solvents as a function of liquid mass velocity and liquid carrier physical properties.
7. Determine the effects of liquid mass velocity and physical properties on integral trickle-bed reactor performance.
8. Develop a model for predicting reactor performance and test the model against experimental data.

Successful completion of this research will provide a systematic method of experimentally evaluating an isothermal trickle-bed reactor performance under reaction conditions. It will also allow an assessment of whether or not external solid-liquid contacting obtained by both reaction and tracer based methods is quantatively equivalent. This information is necessary for proper reactor modeling.

CHAPTER 2

Background

The term trickle-bed reactor is usually used to describe a reactor in which the liquid phase is allowed to trickle over a fixed bed of catalyst particles with cocurrent flow of the gas phase.

Trickle-bed reactors have been developed and widely used by the petroleum industry for such processes as catalytic treatment with hydrogen of various petroleum fractions. In particular they are frequently used in hydrodesulfurization or hydrotreating of heavy or residual oil stocks and the hydrofinishing or hydrotreating of lubricating oils (1, 2, 3).

Applications of trickle-bed reactors have also increased in the chemical industry such as in synthesis of butyendial from aqueous formaldehyde and acetylene (4, 5). Trickle-bed reactors are also used for selective hydrogenation of acetylene (6), hydrogenation of benzene to cyclohexane, hydrogenation of α-methylstyrene to cumene, etc.

In recent years the importance of trickle-bed reactors has increased due to their potential use in the removal of dissolved organic compounds from industrial waste water as an alternative to biological oxidation, in addition to their potential use in hydrotreating and hydrodenitrogenation of coal liquids (7). In general this type of reactor is applicable to all processes where gaseous and liquid reactants have to be contacted in the presence of solid catalyst.

The catalyst particles generally used in trickle-bed reactors are in the form of cylinders, spheres, extrudates or granuli, with particles diameter ranging from 0.08 to 0.64 cm. Typical catalyst used in trickle-bed operations include cobalt-molybelenum on alumina support for hydrodesulfurization processes, palladium, platinum, rhodium or ruthenium deposited on alumina or activated carbon for hydrogenation processes. Various metal oxides such as Nio, Fe_2O_3, Cr_2O_3, Cuo or Zno are commonly used for oxidation processes.

Accurate characterization of the processes which occur in trickle-bed reactors are extremely difficult, because of the complex interaction between the flowing phases and the stationary catalyst bed. The main problems in predicting trickle-bed performance are in evaluating a number of variables as functions of design parameters and physical properties. These variables are: holdup, pressure drop, transport rates, catalyst contacting efficiency, catalyst effectiveness factor in addition to heat transfer, liquid residence time distribution and dispersion effects. The subject as a whole has been reviewed by Satterfield (8), Hofmann (9, 10), Smith et al (11) and Gianette et al (105).

In trickle flow regime, the liquid is allowed to trickle over the packing in the discontinuous shape of films, rivulets and drops near a stagnant continuous gas phase. If the gas flow rate is further increased, the drag effects between the two phase increase. This results in a greater velocity in the

liquid phase as a consequence of the drag force on the liquid by the increased gas flow rate.

Various flow maps have been presented in the literature for two phase flow in a packed bed. The hydrodynamic regimes set up in a packed bed for foaming and non-foaming liquids have been defined by Charpentier and Favier (28), Midoux et al (106), Weekman and Myers (13), Chou et al (107), Larkins et al (27), Specchia and Baldi (32). Basically four flow regimes have been identified by the above mentioned investigators for both foaming and non-foaming liquids. These regimes are trickling flow, pulsing flow, dispersed bubble flow and spray flow. The transitions from one flow regime to the other has shown to be dependent on the fluid properties, bed porosity and wetting characteristic of the packing.

The problem of liquid distribution in trickle-bed reactors has been the subject of many investigations (12-18). The liquid velocity profile has been generally obtained by measuring the liquid flow from several annular collectors at the bottom of the column. The liquid velocity profile reaches a steady state after a certain bed depth known as the calming bed depth and does not change with an increase in bed depth. The calming bed depth was found to be a function of the packing shape and size, column diameter, gas and liquid flow rates, liquid physical properties and the design of liquid inlet distributor. However, it is a generally recognized fact that the calming depth is shorter for a uniform liquid distributor than for a single point liquid source inlet.

The recent study of Herskowitz (12) in which the local volumetric flow rate was measured over a wide range of the ratio of column diameter to particle diameter, using different type of packing material and sizes, concluded that for a ratio of (d_c/d_p) higher than 18, the liquid flow distribution was uniform. This ratio was lowered to 12 when the water surface tension was changed from 73.1 to 38 dgnes/cm. This indicates a strong dependence of the column diameter to particle diameter ratio on the liquid physical properties.

In the gas continuous regime at low gas and liquid flow rates, the liquid distribution on the packing is quite uniform for particle diameters of less than 6 mm and for $12 \leq d_c/d_p \leq 48$ regardless of the packing shape. Baldi and Specchia (18) and Specchia et al (14) observed that at large gas flow rate, the liquid velocity profile depends on the gas superficial velocity. The liquid tends to gather in the center with gas flowing preferentially along the walls as the pulsing flow regime is approached. Further increase in the gas flow rate again led to a liquid redistribution.

It is important to note that most of the above mentioned studies on liquid distribution were carried out using air-water system and the packing generally used in absorption columns. A summary of these studies is given in table 2-1. It was observed that there is a lack of experimental data in hydrodynamic regimes other than the gas continuous flow when particles with the same shape and size as in commercial reactors are used. In addition, more investigation is needed

Table 2-1

Summary of Liquid Distribution Studies for
Two-Phase Concurrent Down Flow in Packed Beds

Reference	System	Column Diameter (mm)	Packing	Comments
Herskowitz (12)	air-water	40.8	2.58, 3.52, 7.15, 8.75 and 11.1 mm granular activated carbon. 6.35 and 9.53 mm ceramic balls.	Uniform liquid distribution when $\frac{d_c}{d_p} > 18$.
	air-water	114	3 mm glass beads, 6.35 x 6.35, 4.76 x 4.76 and 3.18 x 3.18 mm alumina cylinders.	
Weekman and Myers (13)	air-water	80	4.7 mm glass beads 6.5 mm alumina spheres.	Liquid flow tended to concentrate near the wall and the center of the column.
Specchia et al (14)	air-water	141	6 mm glass beads	Liquid distribution is uniform for $d_p \leq 6$ mm, and $12 \leq \frac{d_c}{d_p} \leq 48$.
Baldi and Specchia (18)	air-water	141	6 mm Berl saddles 6 and 12.5 mm Raschig rings.	
Sylvester et al (15)	air-water	150	3 x 3 mm cylinders, 6 mm Raschig rings and 6 mm Intalox saddles.	Approximate plug flow of the liquid in the column.
Reiss (16)	air-water	400	12-75 mm Raschig rings	Radial liquid distribution is a function of bed height and gas and liquid flow rates.
Hochman and Effron (17)	N_2-Me Oh	150	4.8 mm glass beads	No liquid or gas velocity gradients exist in trickle-flow regime.

to study the effect of physical properties of liquid and gas on liquid distribution.

Liquid holdup is an important parameter in modeling and design of trickle-bed reactors regardless of the nature of the reaction. For reactions occurring in the liquid phase only, dynamic holdup or operating holdup is important for kinetic data interpretation. On the other hand if reactions occur in both liquid and vapor phases both dynamic and static holdups affect the reaction rate.

Shah (19) summarized a large number of holdup studies that appeared in the literature and some of the available correlation for liquid holdup are presented in Table 2-2. A large number of investigators have attempted to correlate liquid holdup with liquid superficial mass velocity, particles Reynolds number, or single phase friction losses. The system studied has been predominantly air-water and glass beads.

Despite the significant discrepancies in the prediction of liquid holdup by various published correlations they all indicate that the liquid holdup under trickle flow conditions increases with liquid velocity and essentially is independent of the gas flow rate.

The role of gas-liquid and liquid-solid mass transfer as applicable to trickle-beds is very important. Such studies related to gas liquid mass transfer have been reported by several investigators (21-25, 108 and 109). The more recent correlations have been summarized by Charpentier (20) and Shah (19).

Table 2-2

Correlations for Liquid Holdup

Reference	Correlation	Comments
Soto et al (26)	$\frac{H_E}{\epsilon} = 0.4\ a_E^{1/3}\ X_1^{0.22}$, for $0.1 < X_1 < 20$	2.6 to 24.3 glass spheres $X_1 = \frac{\Delta P_L}{\Delta P_G}$
Larkins et al (27)	$\log_{10} \frac{H_E}{\epsilon} = -.774 + 525 \log_{10} X_1 - .109(\log_{10} X_1)^2$	$.05 < X_1 = \frac{\Delta P_L}{\Delta P_G} < 30$
Charpentier and Favier (28)	$\log_{10} \frac{H_E}{\epsilon} = -.28 + .175 \log_{10} X - .047(\log_{10} X)^2$	3 mm glass spheres
	$\log_{10} \frac{H_E}{\epsilon} = -.363 + .168 \log_{10} X - .043(\log_{10} X)^2$	1.8 x 6 and 1.4 x 5 mm cylinders
	$.05 < X = \frac{L/G}{(\Delta P_G/\rho_G\ g_C\ Z) + 1} < 100$	
Way (30)	$H_E \propto L^{.33}$	3 mm glass spheres and 3.2 x 3.2 mm cylinders
Hochman and Effron (17)	$H_D = 0.00445\ (Re_L)^{.76}$	4.8 mm glass spheres

Table 2-2
(continued)

Reference	Correlation	Comments
Otake and Okada (29)	$H_D = 1.295(Re_L)^{.676}\ (Ga_L)^{-.44}\ (a_E\ d_p)$	6.2 - 22 mm spheres. 12.7, 25.4 mm Raschig rings, Berl saddles. $10 < Re_L < 2000$
	and	
	$H_D = 15.1(Re_L)^{.676}\ (Ga_L)^{-.44}\ (a_E\ d_p)$	Broken solids $10 < Re_L < 2000$
Specchia and Baldi (32)	$\frac{H_D}{\epsilon} = 3.86\ (Re_L)^{.545}\ (Ga^*_L)^{-.42}\ \left(\frac{a_S\ d_p}{\epsilon}\right)^{.65}$	poor interaction regime $3 < Re_L < 470$
	$\frac{H_D}{\epsilon} = a'\ [\bar{z}/\psi^{1.1}]^{-6}\ \left(\frac{a_S\ d_p}{\epsilon}\right)^{.65}$	high interaction regime. $a' = .125$, $b = .312$ non-foaming liquid. $a' = .0616$, $b = .172$ foaming liquid. particles = 6 mm glass spheres, 5.4 x 5.4 and 2.7 x 2.7 mm glass cylinders, 6.4, 10.3 and 22 mm Rasching rings.
Colombo et al (33)	$\frac{H_E}{\epsilon} = 3.86(Re_L)^{.565}\ (Ga_L)^{-.42}\ \left(\frac{a_S\ d_p}{\epsilon}\right)^{.65}$	0.1 cm crushed carbon particles and 3.8 x 4.8 mm carbon cylinders.

Giametto et al (21) determined gas-liquid interfacial areas for cocurrent down flow over all possible hydrodynamic regimes using various types and sizes of packing materials. At low combined gas-liquid loading, the values of the interfacial areas obtained were within the same order of magnitude as those obtained for countercurrent flow. This work was extended further by determination of individual gas film and liquid film mass transfer coefficients (22). It was observed by Specchia et al (23), for the case of upward cocurrent flow, that the interfacial area and liquid mass transfer coefficient were found to be higher for upward cocurrent than for downward cocurrent flow for the same gas and liquid flow rates.

A large number of investigators have attempted to correlate the volumetric mass transfer coefficient $K_L a_g$ based on energy dissipation and some of the available correlations are presented in Table 2-3. Reiss (16) proposed a relation for $K_L a$ evaluation in both pulse and spray flow. Satterfield (8) suggested that the Reiss correlation be valid only when the diffusivity of the solute in the liquid is 2.4×10^{-9} m^2 sec^{-1} and the viscosity of the liquid is close to that of water. A correlation in terms of dimensionless gas-liquid mass transfer coefficient and energy parameter has been proposed by Gianetto et al (21, 22). More recently Goto and Smith (34), Mahajani and Sharma (109) used the correlating procedure of Sherwood and Holloway (37) to fit their experimental results in terms of liquid flow rate and physical properties.

Table 2-3

Summary of Some Existing Correlation for Gas-Liquid Mass Transfer Coefficient in Cocurrent Downflow Packed Beds

Reference	dp (mm)	Superficial Velocity (10^{-2} m/sec) Liquid	Gas	Correlation (MKS units)
Reiss (16)	12.5-76	4-30	60-450	$K_G a_L = 2 + 0.1(E_G)^{.66}$, $E_G = \left(\frac{\Delta P}{\Delta Z}\right)_{LG} U_G$; $K_L a_L = 0.03\ (E_L)^{.5}$, $E_L = \left(\frac{\Delta P}{\Delta Z}\right)_{LG} U_L$
Gianetto et al (21, 22)	6	:08-4.4	40-230	$\frac{K_G \epsilon}{U_L} = 0.035\left[\frac{(\Delta P/\Delta Z)_{LG}}{\bar{\psi}(\ell_G U_G^2 + \ell_L U_L^2}\right]$; $\frac{K_L \epsilon}{U_L} = .03\left[\left[\frac{\epsilon(\Delta P/\Delta Z)_{LG}}{a_S(1-\epsilon)\ell_L U_L^2}\right]^{.07} - 1\right]$
Goto and Smith (34)	4.1 spheres	105-.5	0-.8	$\frac{K_L a_L}{D_A} = 4440\left(\frac{\rho_L U_L d_p}{\mu_L}\right)^{.4}\left(\frac{\mu_L}{\ell_L D_L}\right)^{.5}$
	2.9 rings	~	~	$\frac{K_L a_L}{D_A} = 9080\left(\frac{\rho_L U_L d_p}{\mu_L}\right)^{.41}\left(\frac{\mu_L}{\ell_L D_L}\right)^{.5}$

Table 2-3
(continued)

Reference	dp (mm)	Superficial Velocity (10^{-2} m/sec) Liquid	Gas	Correlation (MKS units)
Ufford and Perona (38)	6.3 rings	.4-8.3	4.3-12	$K_L a_L = 13.5\ U_L^{1.06}\ U_G^{.75}$
	12.7 rings	~	~	$K_L a_L = 2.96\ U_L^{.93}\ U_G^{.42}$
	19 saddles	~	~	$K_L a_L = 2.73\ U_L^{.82}\ U_G^{.46}$
Sylvester and Pitayagulsarn (36)	3.2 pellets	.3-1.7	18-75	$K_L a_L = 1.295 \times 10^{-6}\ Q_L^{1.2}\ Q_G^{.3}$ Q is flow rate in $\frac{lb}{ft^2\text{-}Hr}$

The liquid-solid mass transfer coefficient under trickle flow conditions was first measured by Van Krevelen and Krekels (39) from the rate of dissolution of benzoic acid with no gas flow. Their correlation was in reasonable agreement with the data of Sato et al (40) for benzoic acid system with 5.5 and 12.2 mm particles at low gas flow rate. Hirose et al (41) made an extensive measurement in trickle, pulsed and bubble flow regimes, concluded that in the case of catalytic oxidation of ethanol to acetic acid, large particles give more resistance at the liquid-solid interface compared with gas-liquid interface.

It is interesting to note that the data of Van Krevelen and Krekels (39) for trickle-bed and those of Evans and Gerald (42) for liquid full bed indicate that the values of $K_s a_s$ are greater in trickle-bed than in liquid full bed at the same flow rate for the larger particles. This is possible because of the larger linear liquid velocities in trickle-beds where part of the volume is occupied by the flowing gas. Goto and Smith (34) observed the reverse effect for small particles (0.054 cm), which is primarily due to the fact that the entire external surface area was not utilized for liquid-solid mass transfer in trickle-beds packed with small particles. A summary of existing correlations in the literature is presented in Table 2-4.

It is a generally recognized fact that many factors influence the performance of trickle-bed reactors. One of the most important factors in the design of trickle-bed reactors is the degree to which the catalyst pellets are actively wetted by the

Table 2-4

Some of the Available Correlations for
Liquid-Solid Mass Transfer Coefficients

Reference	Correlation	
Van Krevelen and Krekels (39)	$\frac{K_{LS}}{D_A a_S} = 1.8 \left(\frac{\ell_L u_L}{a_S \mu_L}\right)^{0.5} \left(\frac{\mu_L}{\ell_L D_A}\right)^{1/3}$	
Goto and Smith (34)	$\frac{K_{LS} a_S}{D_A} = 45\ Sc^{1/3} \left(\frac{L}{\mu_L}\right)^{.56}$	For .241 cm B-Naphthol
	$= 153\ Sc^{1/3} \left(\frac{L}{\mu L}\right)^{.67}$	For .054 cm particles
Dwivedi and Upadhyay (114)	$\epsilon_B J_D = 1.1068\ Re_L^{-.72}$	For $Re_L < 10$
	$= .4548\ Re_L^{-.4069}$	$Re_L > 10$
Specchia et al (111)	$\ln[Sh' (Sc)^{-1/3}] = 7.82 \sqrt{\ln(We \times 10^3)} - 1.29 \ln(We' \times 10^3) - 7.61$	
	$Sh' = \frac{K_{LS} a_S d_P}{a_t D_A}$	
	$We' = \frac{U_L^2 \ell_L d}{\sigma_{L\ T}^2}$	

flowing liquid phase. The importance of the catalyst effective wetting on the performance of trickle-beds have been investigated by several researchers (43-50). It is believed that higher liquid dynamic holdup leads to better contacting efficiency. However, up to now it is not clear what effects the wettability of particles and heat effects occurring during exothermic reaction have on contacting efficiency.

All correlations reported in the literature for contacting efficiency are for nonporous packing. Some data for porous packing were reported by Schwartz (48), who utilized a tracer method to measure contacting efficiency and by Colombo et al (33). Recently Mills (110) utilized both methods of Schwartz (48) and Colombo et al (33) to measure contacting efficiency in trickle flow regime and confirmed the dependence of contacting efficiency on liquid flow rates. A summary of the established correlations on contacting efficiency is presented in Table 2-5.

Theoretical investigations of the effect of catalyst wetting on the performance and catalyst effectiveness factor of trickle-bed reactors have been reported by Duduković (46), Mills and Duduković (47, 104), Sylvester and Pitayagulsarn (15, 36). Further details of these studies are given in Appendix A.

Table 2-5

Contacting Efficiency Correlations for Nonporous Packing

Reference	Correlation	
Onda et al (112)	$\eta_c = 1-\text{Exp}[-1.45\ Re_L^{0.1}\ Fr_L^{-0.05}\ We_L^{0.2}\left(\frac{\sigma_c}{\sigma_L}\right)^{.75}]$	$8 < d_p < 50.8$ mm $50 \leq L \leq 3\times10^3 \frac{g}{cm^2\text{-Hr}}$
Onda et al (43)[zz]	$\eta_c = 1-1.02\ \text{Exp}(-.278(L/a_S\ \nu_L))$	For column packed with Raschig rings.
Puranik and Vogelpohl (44)	$\eta_c = 1.05\ Re_L^{.047}\ We_L^{.135}\left(\frac{\sigma_L}{\sigma_c}\right)^{-.206}$	(dynamic)
	$\eta_{cE} = 1.045\ Re_L^{.041}\ We_L^{.133}\left(\frac{\sigma_L}{\sigma_c}\right)^{-.182}$	(Total)
Shulman et al (45)	$\eta_c = .24\ (L/G)^{.25}$	Rasching rings
	$\eta_c = 0.35\ (L/G)^{.2}$	Berl Saddles

CHAPTER 3

Proposed Methods for Evaluation of Trickle-Bed Reactor Data

The following transport steps in a trickle-bed reactor for a gas limited reaction are assumed to occur:

1. Transfer of gaseous reactant from the flowing gas phase to the liquid phase across the gas-liquid interface.
2. Transfer of gaseous reactant from the flowing gas phase to the externally dry surface of the catalyst particles across the gas-solid interface.
3. Transfer of gaseous reactant which is present in the liquid phase to the actively wetted part of the catalyst across the liquid-solid interface.
4. Transfer of liquid reactant in the flowing liquid phase to the actively wetted part of catalyst pellet across the liquid-solid interface.
5. Diffusion of reactants into the interior of the catalyst particles, where adsorption and reaction takes place.

In addition to the above mentioned transport steps, the following assumptions are made:

A. Isothermal operation of the trickle-bed.

B. Physical properties, flow rates, transport coefficients and liquid holdup are constant throughout the bed.

C. Solubility of the reactant gas is adequately described by Henry's law.

D. Mixing in both liquid and gas flowing streams is adequately described the axial dispersion model.

E. The catalyst pores are completely filled with liquid due to capillary effects and particle scale incomplete contacting occurs on the exterior surface of the catalyst.

Based on the above assumptions and transport steps a proposed model for the trickle-bed reactor performance is derived for the case of a gas limited reaction. For the case of α-methylstyrene hydrogenation, the steady state model derived based on hydrogen concentration is:

$$\tilde{D}_g \frac{d^2 C_{H_2,g}}{dZ^2} - U_{sg} \frac{dC_{H_2,g}}{dZ} - K_L a_{gl} \left[\frac{C_{H_2,g}}{H_i} - C_{H_2,L} \right]$$

$$- K_{gs}\, a_{gs} \left[C_{H_2,g} - H_i\, C_{H_2,i|r=R} \right] = 0 \qquad (1)$$

$$\tilde{D}_L \frac{d^2 C_{H_2,L}}{dZ^2} - U_{sL} \frac{dC_{H_2,L}}{dZ} + K_L\, a_{gl} \left[\frac{C_{H_2,g}}{H_i} - C_{H_2,L} \right] +$$

$$K_{LS}\, a_{LS} \left[C_{H_2,i|r=R} - C_{H_2,L} \right] = 0 \qquad (2)$$

and on the pellet

$$K_{gs}\, a_{gs} \left[C_{H_2,g} - H_i\, C_{H_2,i|r=R} \right] + K_{Ls}\, a_{Ls} \left[C_{H_2,L} - H_i\, C_{H_2,i|r=R} \right] = K(1 - \varepsilon_B)(C_{H_2,i|r=R})\, \eta_{TB} \qquad (3)$$

where $$a_{LS} = \frac{S_{ext}}{V_p} \eta_{ce}(1 - h_g - H_{LE}) \quad (4)$$

$$a_{gs} = \frac{S_{ext}}{V_p}(1 - \eta_{ce})(1 - h_g - H_{LE}) \quad (5)$$

with the boundary conditions

at Z = o $$\tilde{D}_g \frac{dC_{H_2,g}}{dZ} = U_{sg}(C_{H_2,g} - C_{H_2,g,f})$$

$$\tilde{D}_L \frac{dC_{H_2,L}}{d_Z} = U_{SL}(C_{H_2,L} - C_{H_2,L,f})$$

at Z = L $$\frac{dC_{H_2,g}}{dZ} = \frac{dC_{H_2,L}}{dZ} = 0$$

Other models have recently been proposed in the literature which allow the steady state performance of trickle-bed reactor to be evaluated in terms of appropriate rate and transport coefficients (94, 95, 96). However, in all of the previous proposed models the gas-solid mass transfer has been neglected. This transport step (gas-solid) is of importance in hydrogenation reactions where gaseous reactants are limiting for the following reasons:

1. In the case where liquid reactants are nonvolatile, the dry areas of the catalyst particles act as a major supplier of gas reactant to the liquid filled pores (12).
2. In the case of volatile liquid reactants, the dry areas of the catalyst serve as a supply area for

both reactants in the vapor phase as well as a surface where corresponding vapor phase reaction may occur (49, 63).

3. In the case of extremely exothermic reactions, gas-solid mass transfer might occur between the liquid vapor in the liquid filled pores and the main body of the gas stream.

Catalyst effectiveness factor of partially wetted surface in trickle-bed reactors have been studied by Dudukovic and co-workers (104, 46, 47). Approximate expressions for the catalyst effectiveness factor for finite resistances on dry and wetted surfaces and incomplete external solid-liquid contacting were shown to yield accurate estimate of $\eta_{T.B}$ when compared to more exact numerical results (104) in certain instances. These approximate formulas for different geometries are listed in Table 3-1. The approximate formulas for slab geometry has been used to interpret the data of Herskowitz (12) for α-methylstyrene hydrogenation in trickle-bed reactor. The results obtained for the external contacting efficiency are displayed on Figure 3-1, and were found to be less than 2% from the actual results of Herskowitz who used a more rigorous cube model.

Based on preliminary results for completely wetted pellets and the analysis performed on Herskowitz data, it will be possible to use the approximate formulas to extract contacting efficiency and liquid-solid mass transfer coefficients when equilibrium feed is used in trickle-bed experiments.

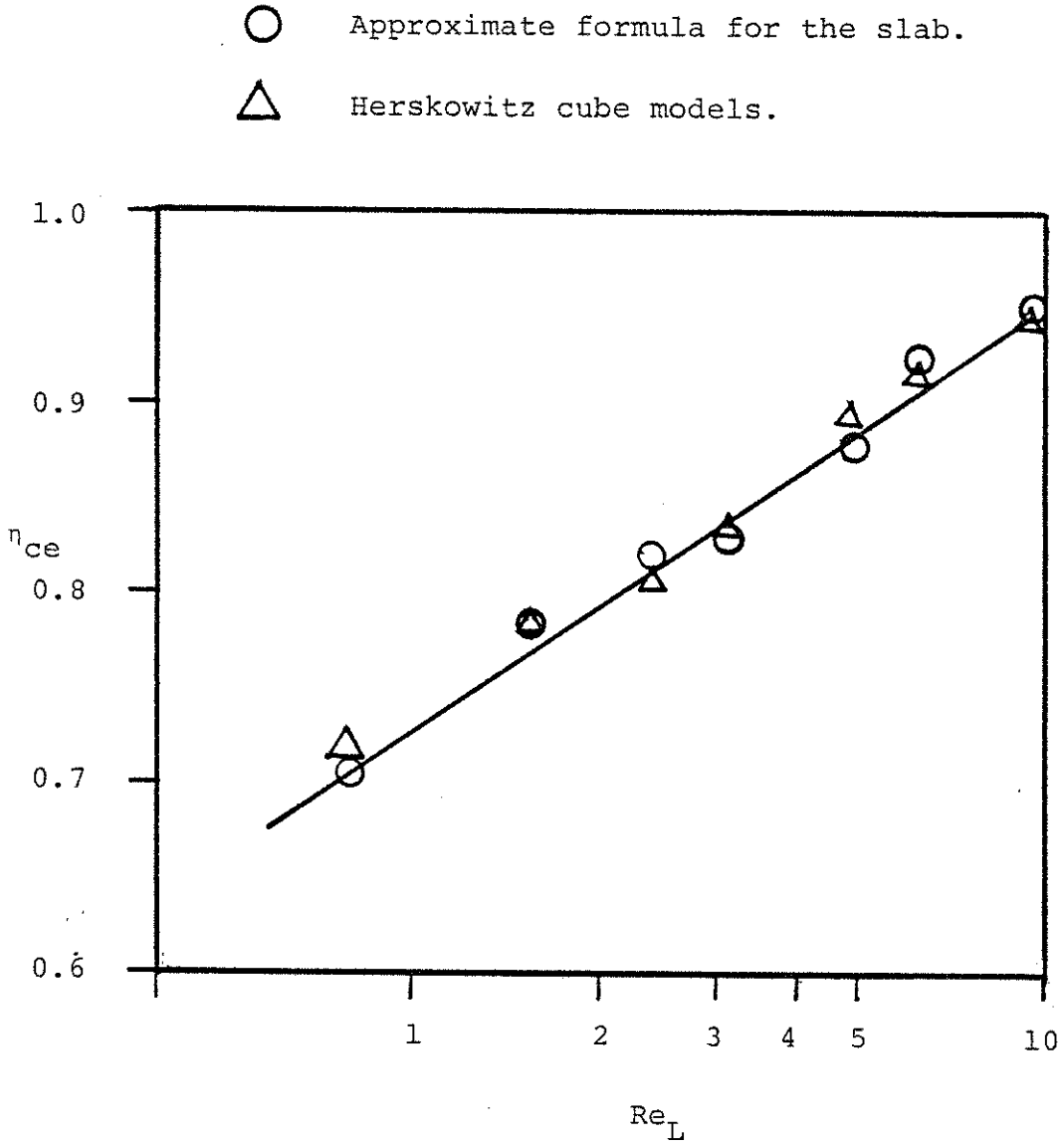

Figure 3-1. Contacting efficiency as a function of Reynolds number.

Table 3-1

Approximate Forms of the Effectiveness Factor in Partially Wetted Catalyst Pellets

Geometry	Effectiveness Factor, η_{TB}	
	In terms of Thiele Modulus ϕ	In terms of Modified (Aris) Modulus Λ
Slab	$\dfrac{\eta_{CE}}{\frac{\phi^2}{(Bi_w)_s}+\frac{\phi}{\tanh\phi}}+\dfrac{1-\eta_{CE}}{\frac{\phi^2}{(Bi_d)_s}+\frac{\phi}{\tanh\phi}}$	$\dfrac{\eta_{CE}}{\frac{\Lambda^2}{\tilde{B}i_w}+\frac{\Lambda}{\tanh\Lambda}}+\dfrac{1-\eta_{CE}}{\frac{\Lambda^2}{\tilde{B}i_d}+\frac{\Lambda}{\tanh\Lambda}}$
Cylinder	$\dfrac{\eta_{CE}}{\frac{\phi^2}{2(Bi_w)_c}+\frac{\phi I_0(\phi)}{2I_1(\phi)}}+\dfrac{1-\eta_{CE}}{\frac{\phi^2}{2(Bi_d)_c}+\frac{\phi I_0(\phi)}{2I_1(\phi)}}$	$\dfrac{\eta_{CE}}{\frac{\Lambda^2}{\tilde{B}i_w}+\Lambda\frac{I_0(2\Lambda)}{I_1(2\Lambda)}}+\dfrac{1-\eta_{CE}}{\frac{\Lambda^2}{\tilde{B}i_d}+\Lambda\frac{I_0(2\Lambda)}{I_1(2\Lambda)}}$
Sphere	$\dfrac{\eta_{CE}}{\frac{\phi^2}{3(Bi_w)_{sp}}+\frac{\phi^2}{3[\phi\coth\phi-1]}}+\dfrac{1-\eta_{CE}}{\frac{\phi^2}{3(Bi_d)_{sp}}+\frac{\phi^2}{3[\phi\coth\phi-1]}}$	$\dfrac{\eta_{CE}}{\frac{\Lambda^2}{\tilde{B}i_w}+\frac{3\Lambda^2}{3\Lambda\coth(3\Lambda)-1}}+\dfrac{1-\eta_{CE}}{\frac{\Lambda^2}{\tilde{B}i_d}+\frac{3\Lambda^2}{3\Lambda\coth(3\Lambda)-1}}$

Contacting efficiency will also be evaluated using tracer methods under conditions similar to those encountered in reaction experiments. From the tracer experiments other parameters can also be evaluated such as liquid holdups and a measure of backmixing.

CHAPTER 4

Equipment and Procedure

The equipment, which will be utilized for the present work, consists mainly of two separate experimental apparatuses. These apparatuses are designed for the purpose of experimental investigation of both intrinsic and apparent kinetics of α-methylstyrene hydrogenation in a stirred reactor, and for dynamic and steady state experiments for the same reaction in a trickle-bed.

4-1. STIRRED-REACTOR APPARATUS:

A schematic diagram of the reactor system and the experimental setup is shown on Figure 4-1. The reactor vessel was constructed of pyrex glass with a capacity of about 2800 cc. The reactor vessel bottom was modified from a dished type to a flat type bottom in order to eliminate dead space and to enhance catalyst suspension when the reactor is operated as a slurry reactor.

Eight equally spaced baffles were constructed of 300 series stainless steel and soldered on two rigs in such a fashion so that the whole baffle assembly can be mounted to the reactor top cover. The clearance between the baffles and the reactor wall was about 0.16 cm and the baffle assembly ended about 1.27 cm from the reactor flat bottom. The baffle assembly was designed in such a fashion that a stationary catalyst basket could be mounted to the baffle assembly for studies involving catalyst pellets or can be removed for studies involving

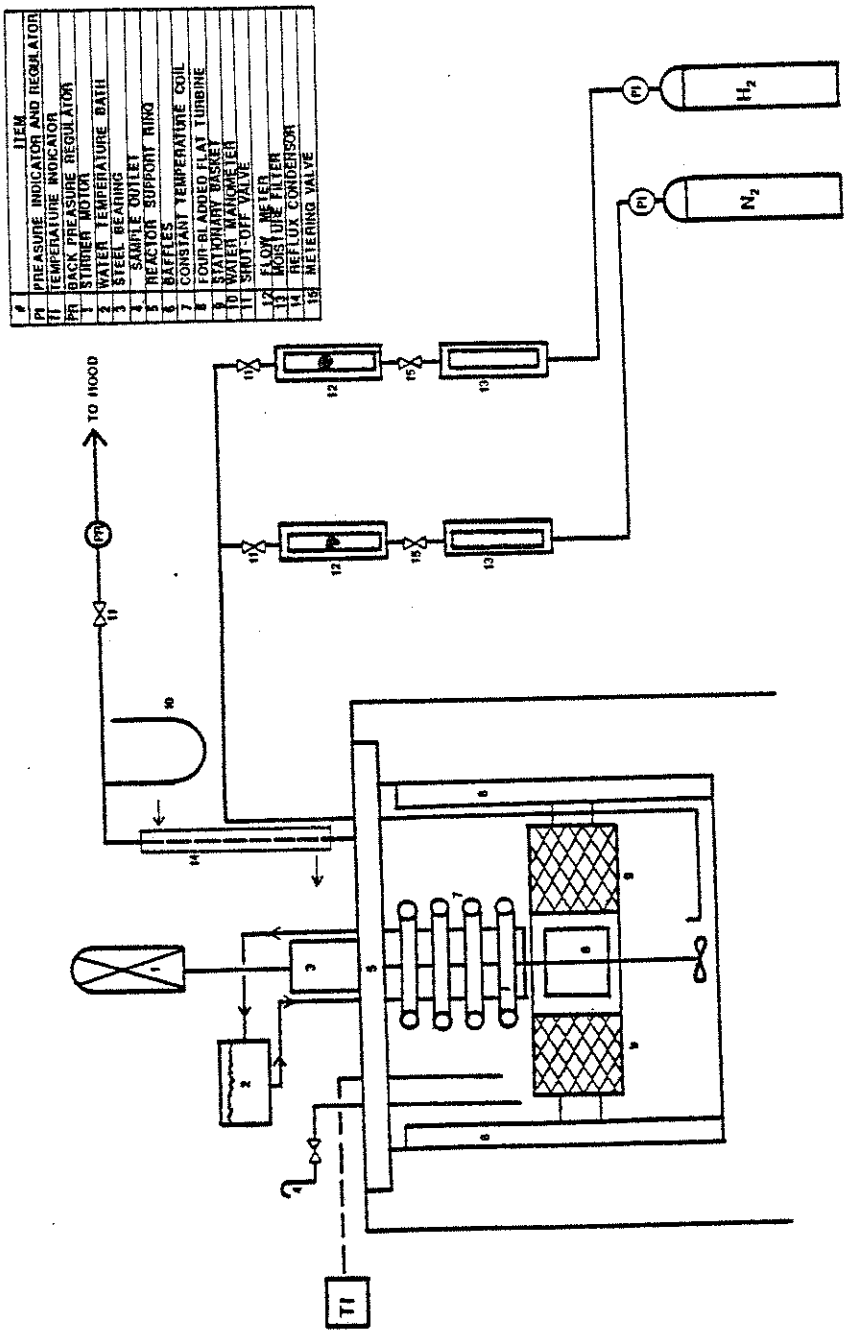

Figure 4-1. Experimental equipment for intrinsic and apparent reaction studies.

slurries as shown on Figure 4-2.

The catalyst basket was made out of two-20 wire mesh screens soldered on both sides of a 1.03 cm thick stainless steel O-ring. The basket cover was also made out of 1.03 cm thick stainless steel ring and can be fastened to the basket via four-hold-down screws. Four side support arms are soldered to the basket outer screen at 90° intervals for which the basket can be mounted to the baffle assembly. The dimensions and view of the stationary catalyst basket are shown on Figures 4-3 to 4-5.

A one-fourth horsepower motor was used to drive the 0.79 cm diameter agitator shaft. The stirring speed was measure using a strobe motor and controlled by means of a Variac. The agitator shaft was constructed of stainless steel and connected to the motor through a bearing support chamber, which kept the shaft from vibrating. Special made seals (Grane Packing Company) are used to protect the shaft bearing from corrosive fluids and granuli.

Agitation of the liquid is accomplished by using two turbines. A flat four-bladed turbine was constructed (Figure 4-6) and placed in the annular region of the basket forcing the liquid over the catalyst pellets and through the basket. The second turbine is placed about 2 cm from the bottom of the reactor. It was observed during experimental runs, that this type of agitator arrangement gave an excellent mixing of the fluid and uniform catalyst suspension, in case of slurry operation, was maintained throughout the runs.

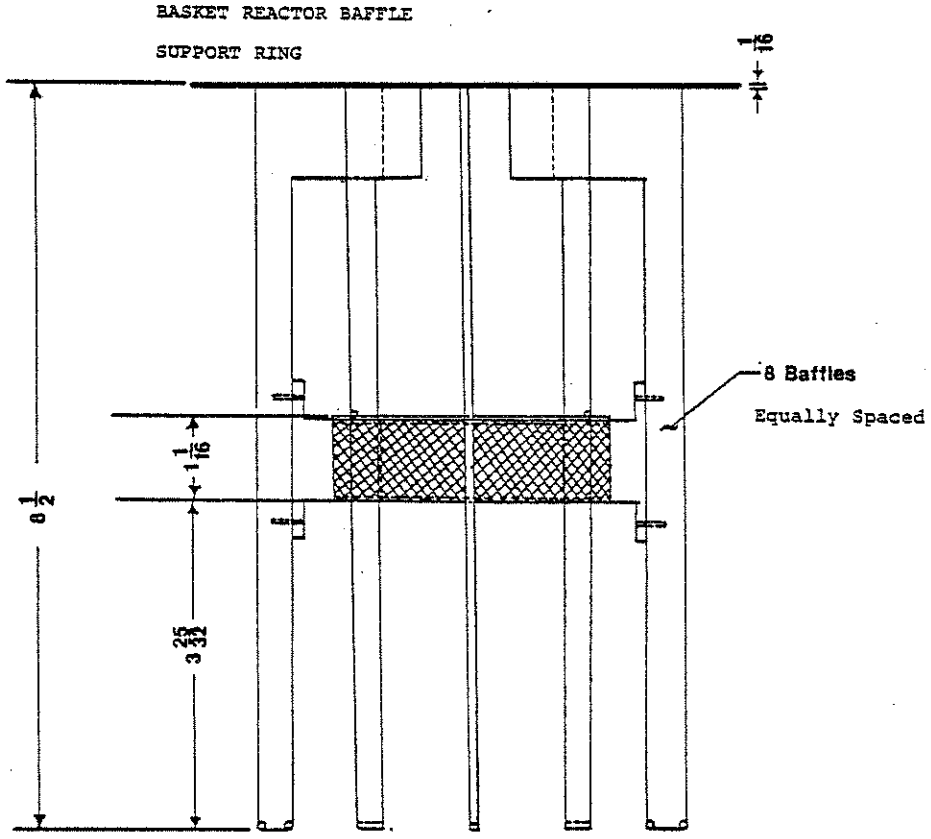

Note: 1.) Baffle support ring not shown.

2.) Basket may be removed for slurry applications.

Figure 4-2.

BASKETT REACTOR

BAFFLE - ASSEMBLY

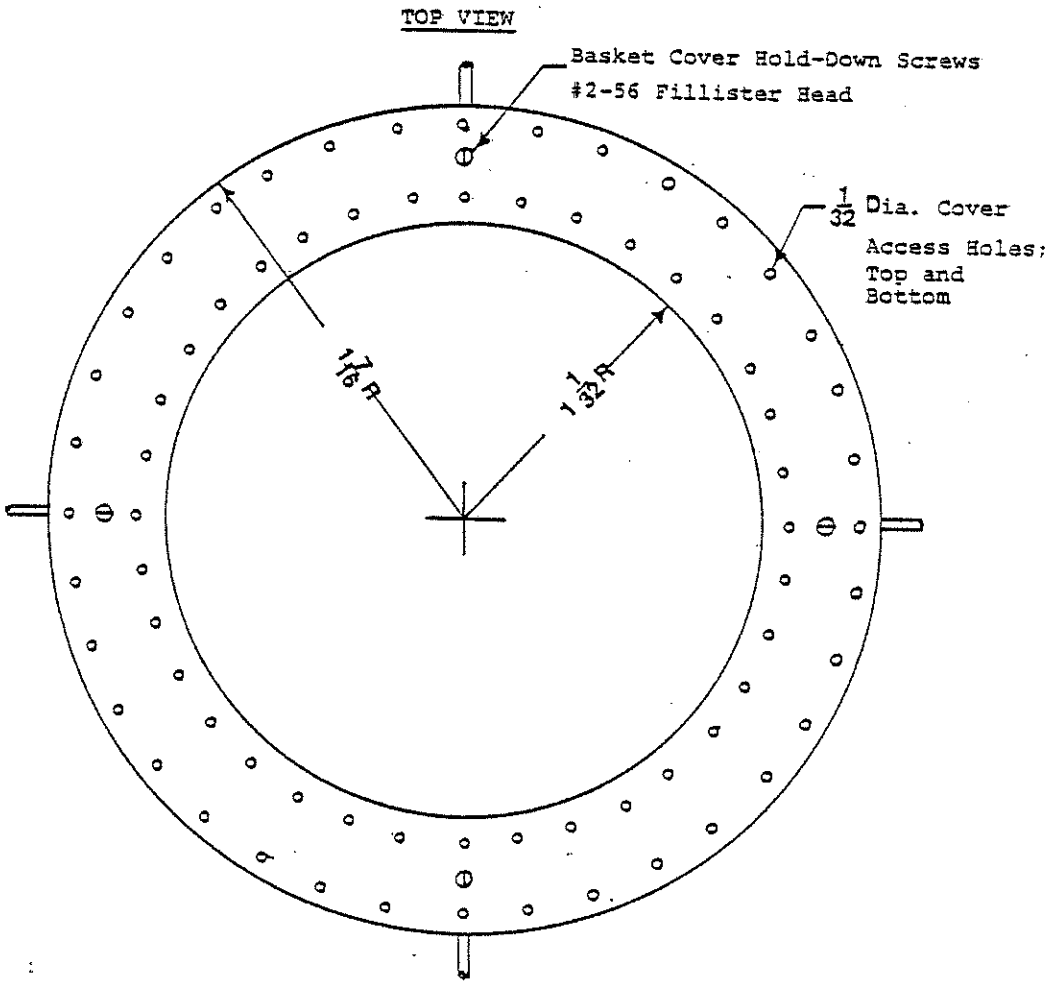

Figure 4-3. STATIONARY CATALYST BASKET COVER

2 REQUIRED

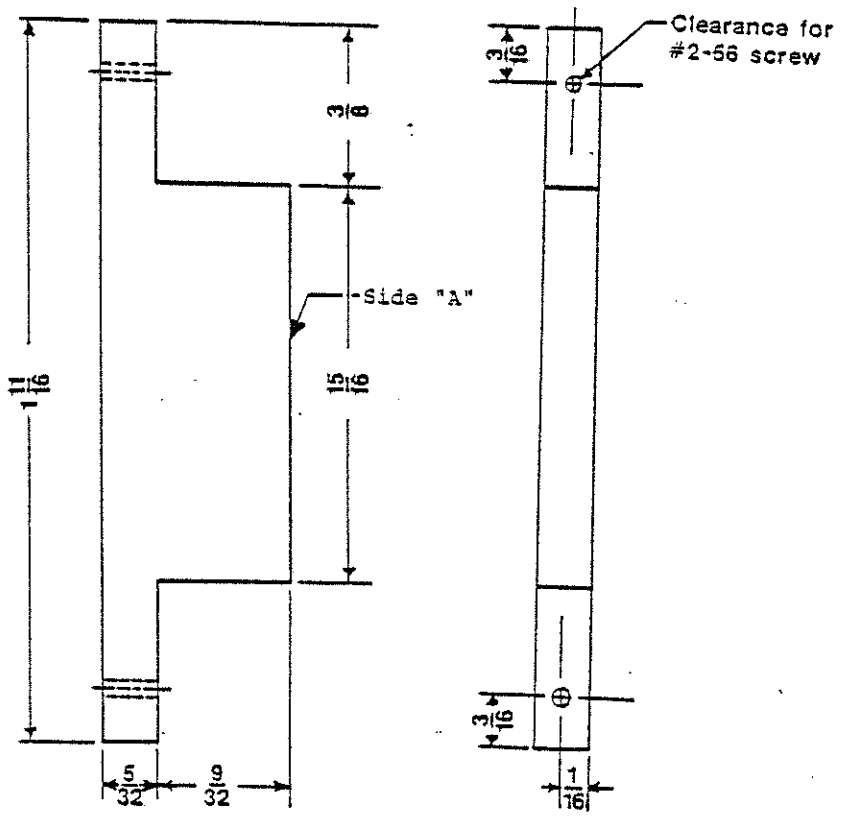

Notes: 1. Material to be 300 series SS.

2. Silver Solder to Basket at 90° Intervals on Side "A".

3. Attachment Arm Screw Locations Given on baffle drawing.

Figure 4-4. BASKET REACTOR

BASKET ATTACHMENT ARMS

4 REQUIRED

Scale: None

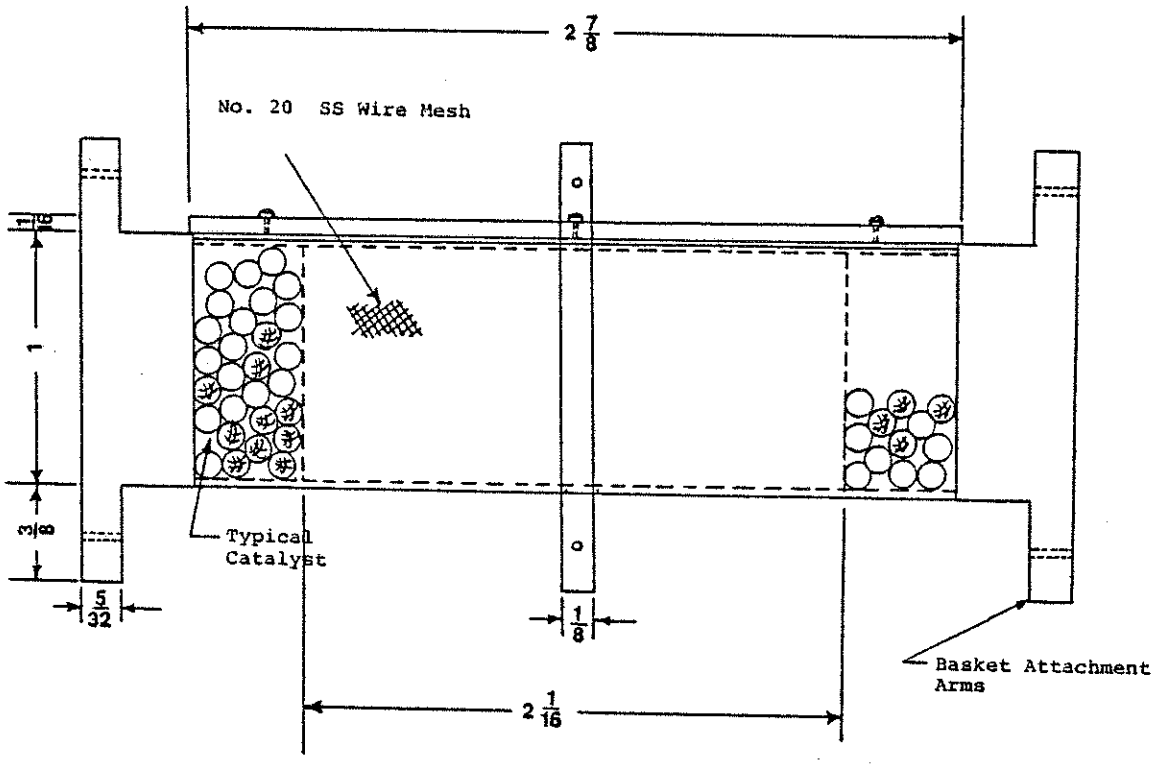

Figure 4-5.

STATIONARY CATALYST BASKET

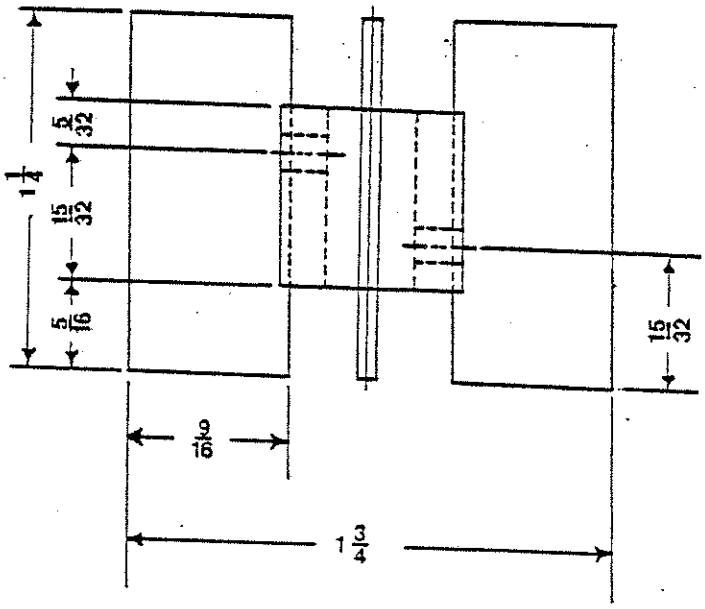

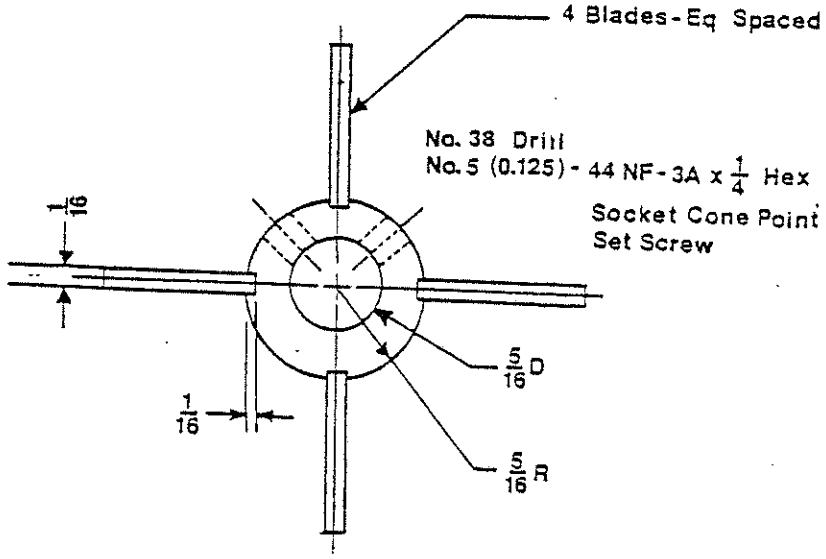

Figure 4-6.
BASKET REACTOR TURBINE
Scale: 2" = 1"

The temperature inside the reactor was monitored using thermocouples connected to a digital readout. The inside reactor temperature was maintained within ±0.3°C during reaction runs by circulation of water through the reactor coils from a constant temperature bath. The constant temperature bath is a Haake NK22 model equipped with both heating and refrigeration units and can be maintained within ±0.02°C at 70°C.

The reactor system is operated as a semi-batch reactor using a single batch of liquid and continuous flow of gas. Gas is supplied to the reactor system from standard gas cylinders and allowed to flow through an oxygen trap and moisture removal unit. The purpose of this unit is to remove oxygen, water and hydrocarbon moisture because of their effect on catalyst performance. The gas inlet pressure to the reactor can be regulated at the cylinder by means of two-stage regulator and the gas flow is controlled by means of a needle valve. Two rotameters are used to monitor the flow of hydrogen and nitrogen gases to the reactor system. The calibration curve for each rotameter is displayed on Figures 4-9 and 4-10.

During reaction experiments, reactor pressure was maintained at 24 cm of water above atmospheric pressure by means of a back pressure regulator. Several reactor ports were utilized for gas inlet, gas outlet, sampling and liquid feed.

A reflux condenser is installed on the gas exit line to prevent liquid carry-over by the flowing gas phase, in order to

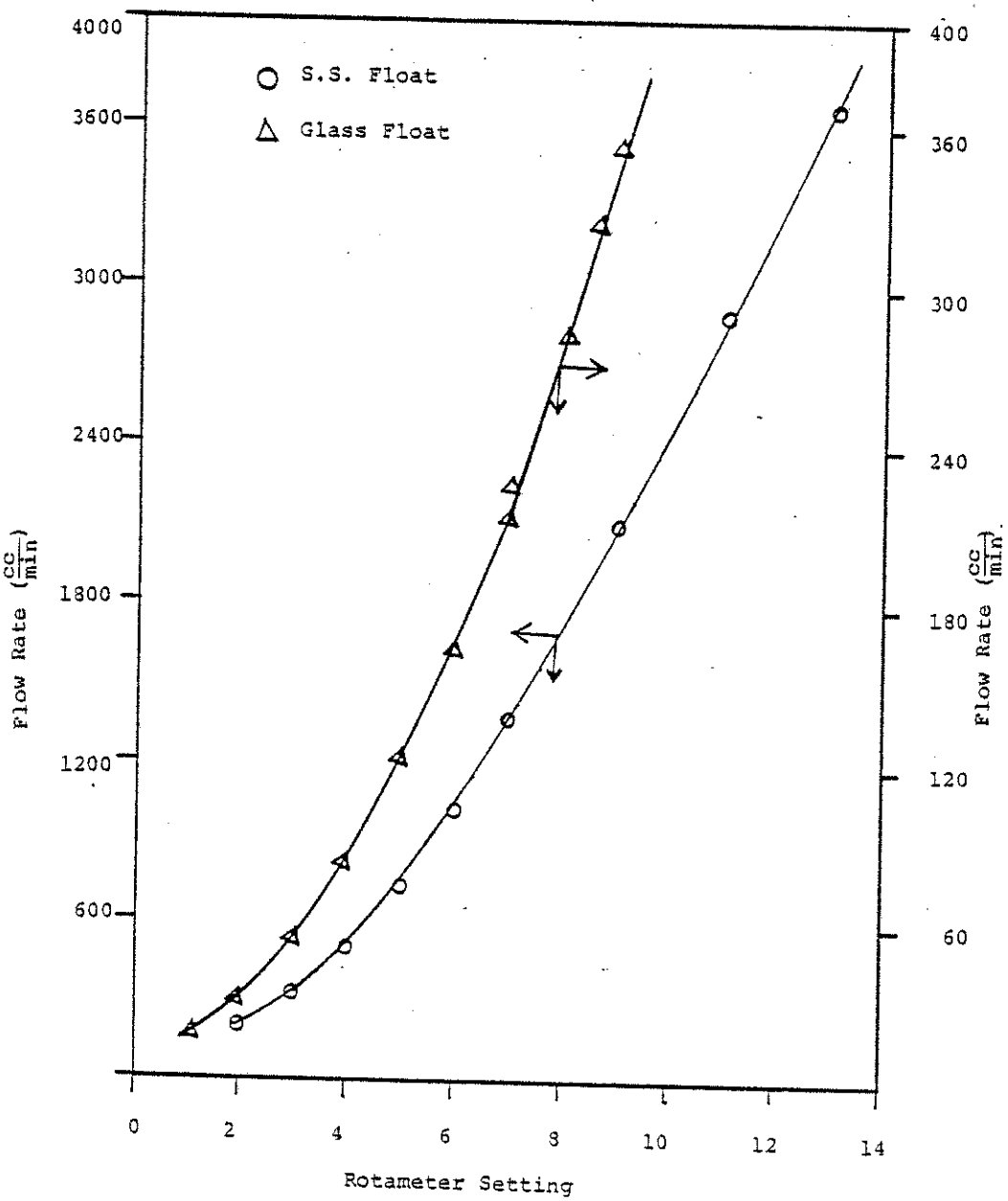

Figure 4-9. Calibration Curve for hydrogen flow

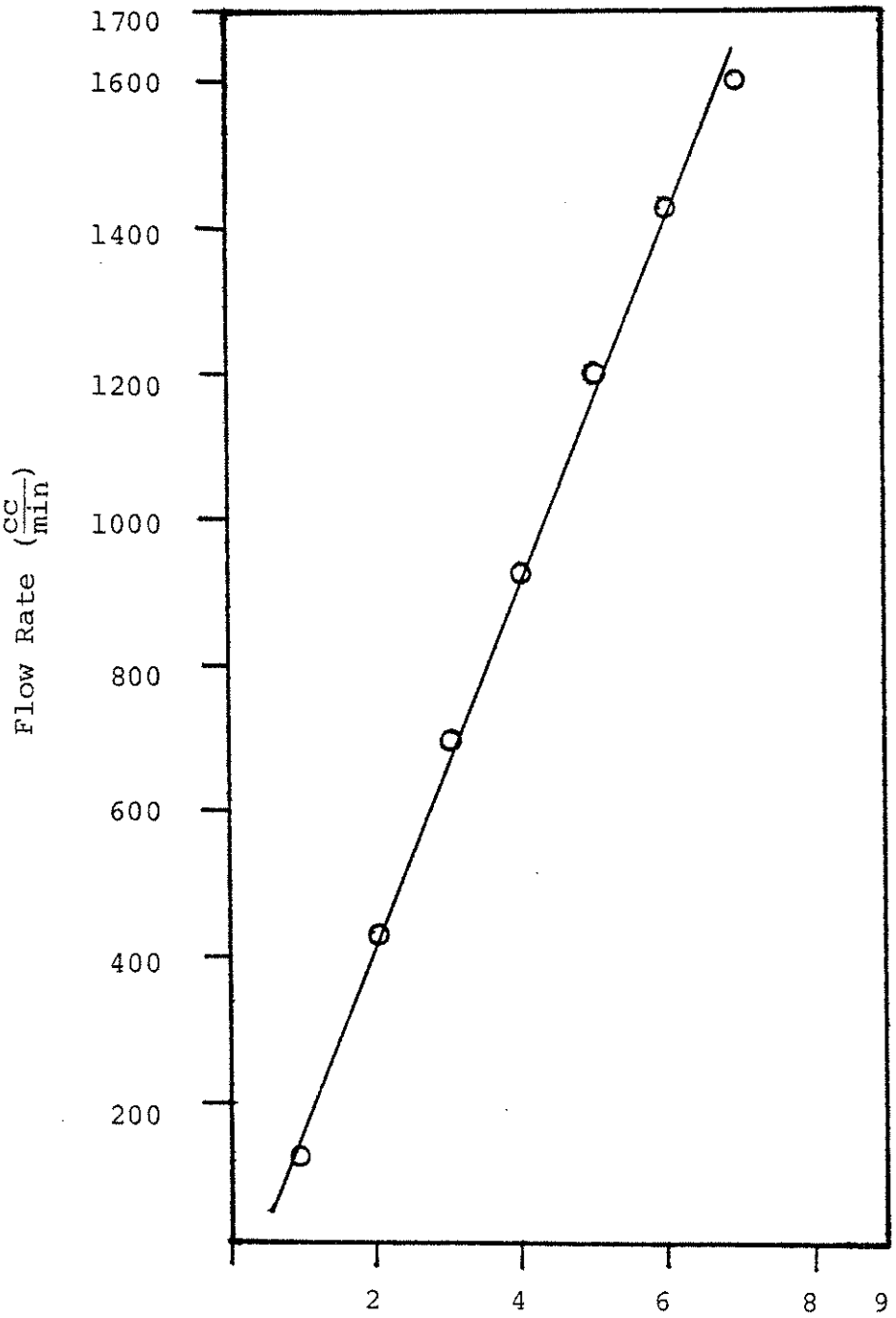

Figure 4-10. Calibration Curve for nitrogen flow.

keep the volume of the liquid in the reactor as constant as possible and to prevent condensation of liquid in the gas exit lines.

During the catalyst activation process, the reactor assembly was heated to the desired activation temperature by means of a 470 watt heater controlled by Fischer proportional temperature controller.

A gas chromatograph (Gow Mac) and digital integrator (Infotronic) were used to allow for quick and accurate analysis of the reaction mixture. The appropriate column, injection port, and detector temperatures which resulted in good peaks reparation in the shortest possible time were found by repeated trials. These settings are given in Table 4-1.

The gas chromatograph unit was calibrated using known solutions concentration of α-methylstyrene and cumene in cyclohexane. A 2-μl samples were withdrawn from each solution and injected into the gas chromatograph. The results from the calibration solutions are displayed on Figures 4-7 and 4-8, and do exhibit a linear relation between concentration and peak area.

4-2. EXPERIMENTAL PROCEDURE FOR THE STIRRED-REACTOR:

In order to obtain accurate and reproducible experimental results for α-methylstyrene hydrogenation, we have devised a systematic procedure to follow during the course of each experimental run. The procedure can be outlined as follows:

1. Charge the reactor with a known amount of catalyst.

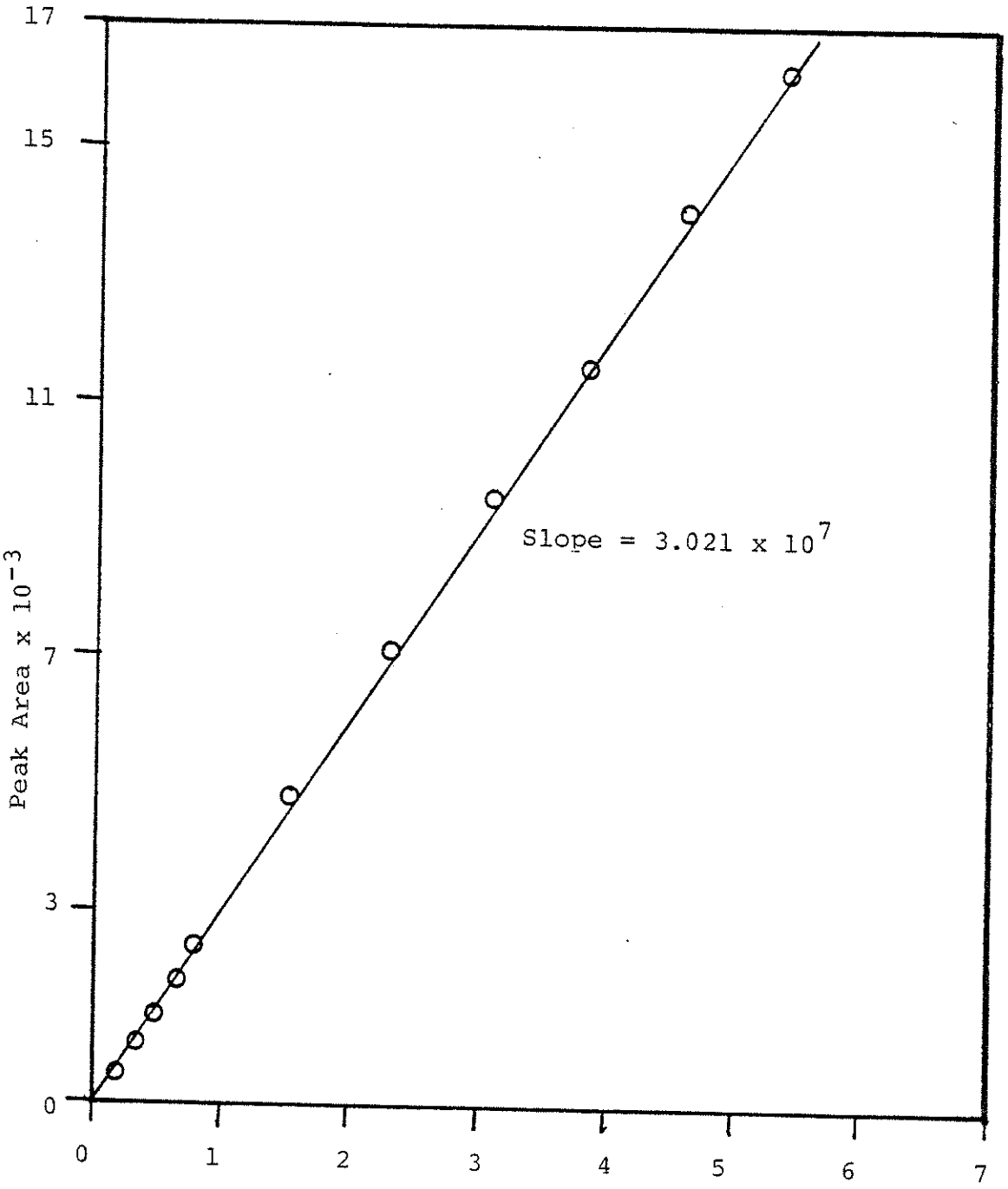

Figure 4-7 G.C. Calibration Curve

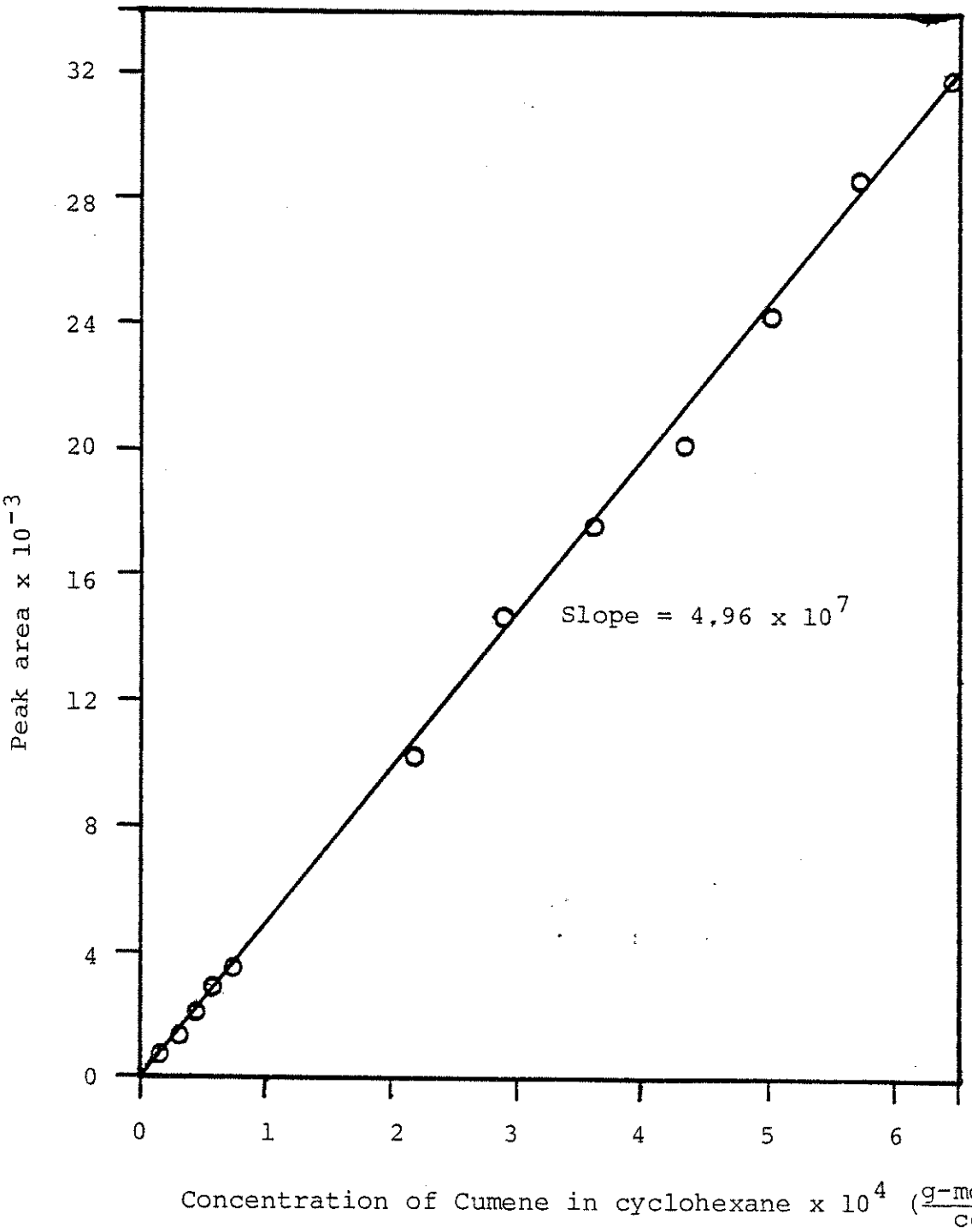

Figure 4-8 G.C. Calibration Curve

Table 4-1

Settings on Gas Chromatograph

Column temperature	110°C
Injection port temperature	190°C
Detector temperature	185°C
Bridge Current	100 ma.
Attenuator setting	1
Polarity	+
The flow rate on both sides of the detector	60 cc/min.
Sample volume	2 µl.

2. Place the heating mantel onto the reactor and check for gas leaks using nitrogen gas.
3. Heat the reactor to a temperature of 140°C with nitrogen gas flowing through the reactor at a rate of 250 cc/min., for a period of three hours in order to remove any moisture adsorbed by the catalyst.
4. Switch from nitrogen to hydrogen gas flowing at a rate of 250 cc/min., for a period of two hours without agitation and for a period of three hours with agitation rate of 150 R.P.M.
5. During hydrogen gas flow, keep the reactor at 5-10 cm of water back pressure.
6. Allow the reactor to cool down to the desired reaction temperature in the presence of flowing nitrogen gas in order to avoid any contact between the activated catalyst and air. The cooling process can be achieved faster if cold water is circulated from the constant temperature bath through the reactor.
7. Charge the reactor under slightly positive pressure with cyclohexane and purified α-methylstyrene.
8. Adjust hydrogen flow rate to the desired setting and stop the flow of nitrogen through the reactor.
9. Allow the reaction to reach equilibrium state before withdrawing samples at predetermined time intervals.
10. Inject 2-μl of each sample taken into the gas chromatograph and determine reaction mixture composition.

It should be mentioned at this point, that the above outlined procedure gave a reproducible result within ±3% or less. Addition of purified α-methylstyrene was essential if true intrinsic and apparent rate form was to be obtained. The purification procedure consists of passing α-methylstyrene over a fixed bed of activated F-1 porous alumina in order to remove the anti-polymerization inhibitor.

4-3. EXPERIMENTAL PLAN FOR INTRINSIC AND APPARENT KINETIC STUDIES OF α-METHYLSTYRENE HYDROGENATION:

The first objective of this work is to study both intrinsic and apparent reaction kinetics of α-methylstyrene hydrogenation free of any external mass transfer limitations, and also free of any internal mass transfer limitation when intrinsic reaction kinetics are to be determined. In order to achieve this objective, we believe that intrinsic reaction studies should be carried out first, for two reasons:

1. Experimental settings (agitation rate and hydrogen flow rate) at which external mass transfer limitations are not present in the intrinsic studies are usually higher than those for apparent studies.
2. The effect of internal diffusion resistance can be readily estimated for the apparent reaction, once the intrinsic rate form is known.

Factors which would influence external and internal mass transfer in our reactor system are particle size, agitation rate and gas flow rate. Experiments will first be performed using crushed catalyst pellets of uniform particle diameter

and a specific set of operating conditions (agitator speed, hydrogen flow rate, and temperature) for the purpose of reproducing several experimental runs to ensure the validity of the devised procedure. Once reproducibility is achieved, experiments will be carried out at the same operating conditions except that the catalyst particles will now be crushed to a smaller particle diameter and rate measurements will be obtained. This procedure will be followed up to the point where there is no change in the rate measurements for two successive particle sizes.

Experiments will then be performed at the smallest particle size and various agitator speeds and gas flow rates in order to determine the optimum operating conditions which ensure the absence of any external mass transfer limitations. Once the optimum operating condtions are experimentally determined (dp, R.P.M. and hydrogen flow rate), experiments will be performed to study the effect of reaction temerpature, hydrogen partial pressure and initial α-methylstyrene concentration on the reaction rate.

From the experimental results, it would be possible to evaluate the extent of pore diffusion at any given particle size by evaluation of the Wagner modulus.

Apparent reaction studies will consist mainly of studying the same reaction using 0.5% and 2.5% palladium on alumina pellets for the cases where palladium is deposited only in a thin layer on the outer pellet surface and also throughout the pellet. The same operating conditions determined previously in

the intrinsic study will be used in this set of experiments. The effect of temperature and hydrogen partial pressure on the reaction rate will also be investigated.

The catalyst pellets that will be utilized for both apparent reaction and trickle-bed studies are cylinderical pellets of 0.13 cm in diameter and 0.563 cm long. The catalyst film thickness on the 2.5% pd pellets is 0.257 mm and on 0.5% pd pellets is 0.0703 mm. For both apparent and intrinsic reaction studies, the rate will be measured only in the temperature range of 15 to 30°C.

4-4. TRICKLE-BED APPARATUS:

The trickle-bed apparatus which will be utilized in the present study is given in Figure 4-11 and 4-12. The main components are, the liquid and gas delivery system, controls for setting and adjusting liquid and gas flow rates and the analytical and recording equipment for continuous and discrete monitoring of the reactor exit concentration in the liquid effluent.

The liquid delivery system consists of two ten gallon tanks. The tank is filled with liquid by, first pulling a vacuum using a single stage vacuum pump connected to the top of the tank. A cold trap is installed between the vacuum pump and the feed tank in order to condense any hydrocarbon vapor, which could pass into the vacuum pump oil. A flexible hose is connected to a small valve located at the bottom of the feed tank. After vacuum has been drawn, the flexible hose is dipped into a fresh purified liquid and the valve is opened. This procedure not only serves to fill the tank, but also to mix its content.

The liquid feed tank is pressurized with gas after it has been filled with liquid. The gas chosen to pressurize the tank is either nitrogen, hydrogen or helium depending on the particle objective of the experimental set. The liquid feed tank pressure is kept constant by maintaining a constant cylinder supply pressure.

Figure 4-11. Experimental equipment for tracer and reaction studies.

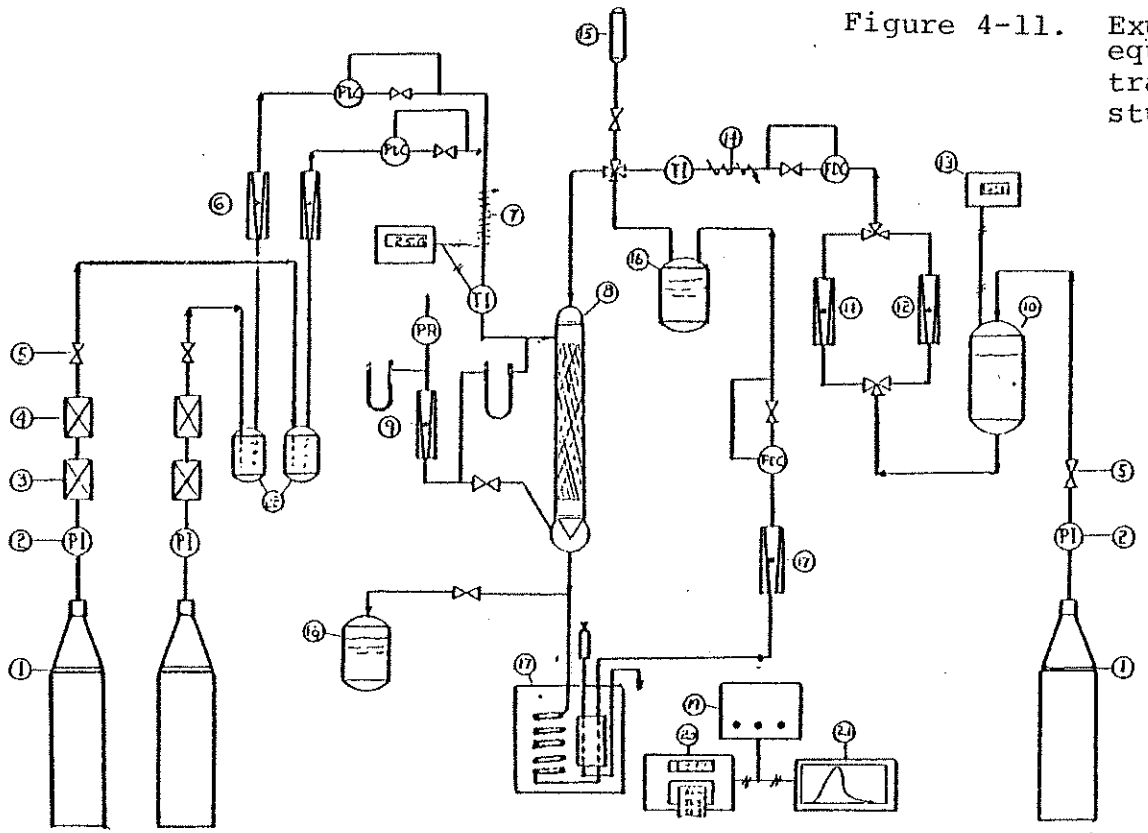

No.	Item	No.	Item	No.	Item
1	Gas Supply Cylinder	8	Trickle-Bed Column	15	Tracer Supply Tank
2	Pressure Indicator and Regulator	9	Outlet Gas Flowmeter	16	Waste Tank
3	Oxygen Trap	10	Liquid Supply Tank	17	Water Bath
4	Moisture Filter	11	Low Range Liquid Flowmeter	18	Optical Detector
5	Shut-Off Valve			19	Control Module
6	Inlet Gas Flowmeter	12	High Range Liquid Flowmeter	20	Voltmeter-Printer
7	Gas Heater	13	Bourdon Gauge	21	Recorder
		14	Liquid Feed Heater	22	Saturation Tanks

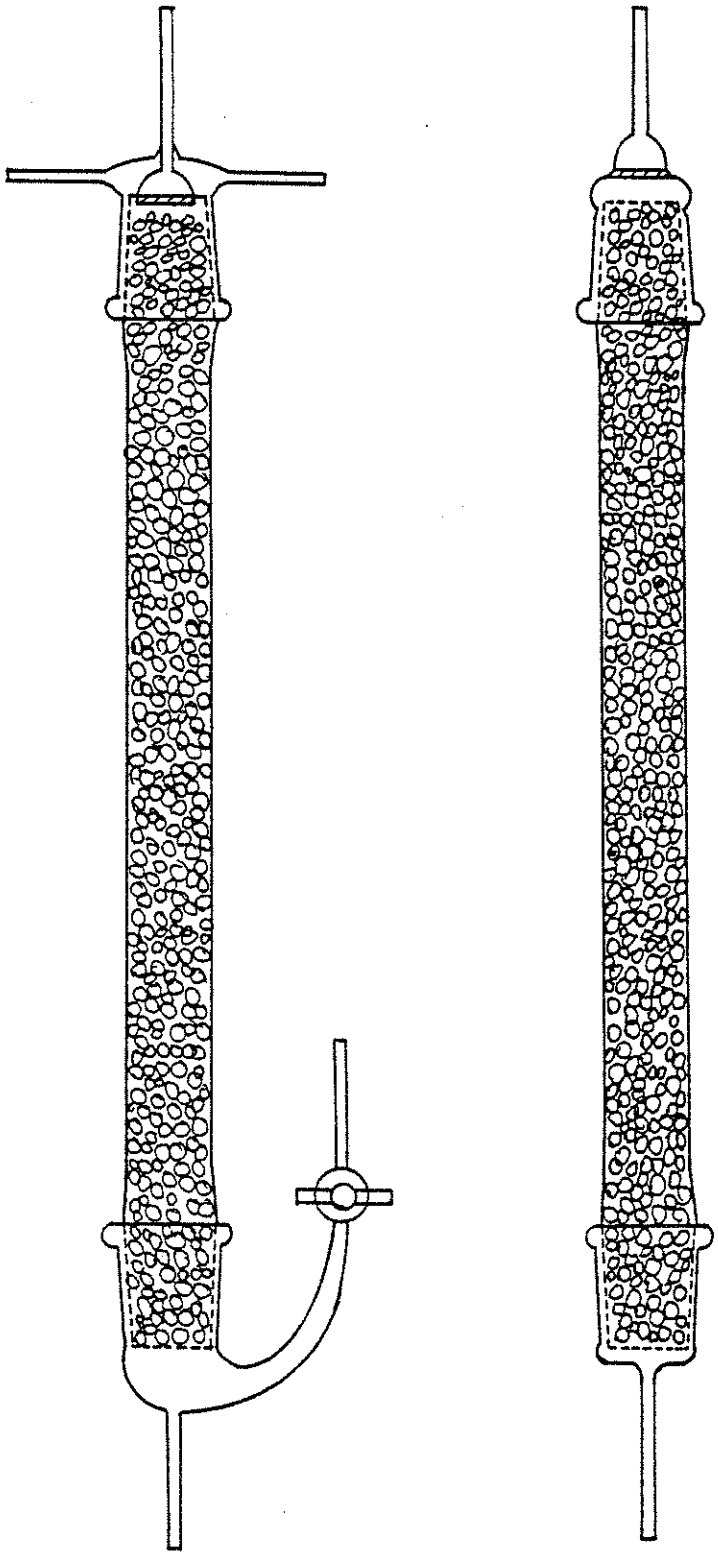

Figure 4-12. Trickle-bed reactor 40 cm long and 1.905 cm in diameter.

Upon exiting from the liquid feed tank, the liquid flow rate can be diverted by means of a three-way ball valve to either one of the two flow meters, depending on the range of liquid superfacial mass velocity required. The liquid flow rates are set by means of a needle valve to the desired flow rate. It is essential to maintain a constant liquid head delivery system for the liquid stream in order to avoid any fluctuation in the flow rate.

For the case where tracer experiments are being performed, a six-port stainless steel sampling valve equipped with a 0.606 cm^3 loop volume will be used to introduce an impulse disturbance in the liquid stream. The sampling valve is located in close proximity of the trickle-bed column.

The second phase flowing to the trickle-bed is gas whose source is a standard gas cylinder. The gas pressure is regulated at the cylinder by means of a two-stage regulator and allowed to pass through an oxygen trap and moisture removal unit prior to entering the trickle-bed column. The gas flow rate is controlled by a needle valve and monitore- by a rotameter. Depending on the gas flow rate, the rotameter float can be easily changed to accommodate higher flow rates.

The present experimental set up will be used, such that the gas and liquid streams are only allowed to flow co-currently downward through the catalyst bed. Upon exiting

from the packed section of the column both liquid and gas streams enter a glass bulb equipped with side arm where separation of the two phases takes place.

The gas exits through the side arm and flows through a needle valve, rotameter and back pressure regulator, and then is vented to the fume hood. The back pressure regulator is utilized to maintain the column pressure to be set slightly above atmospheric pressure.

In the case of tracer experiments a slightly positive pressure in the column is required to force the exiting liquid out of the system with sufficient pressure so that a sample stream can be diverted to the instrument used to monitor the tracer concentration in a continuous fashion. The liquid level in the exit downpipe must be maintained at a specific level to prevent gas from flowing to the refractometer. When high liquid flow rates are required, a split flow scheme is devised in which one stream of the exit liquid is allowed to flow to the analytical instrument and the other stream to the waste tank. The flow of liquid to the refractometer is controlled by means of a flow controller and is monitored by means of a rotameter. The control valve, rotameter and flow controller are installed on the outlet side of the detector in order to prevent bubble formation and to minimize the length of tubing between the column and detector. A schematic diagram of the refractometer control scheme is given in Figure 4-13.

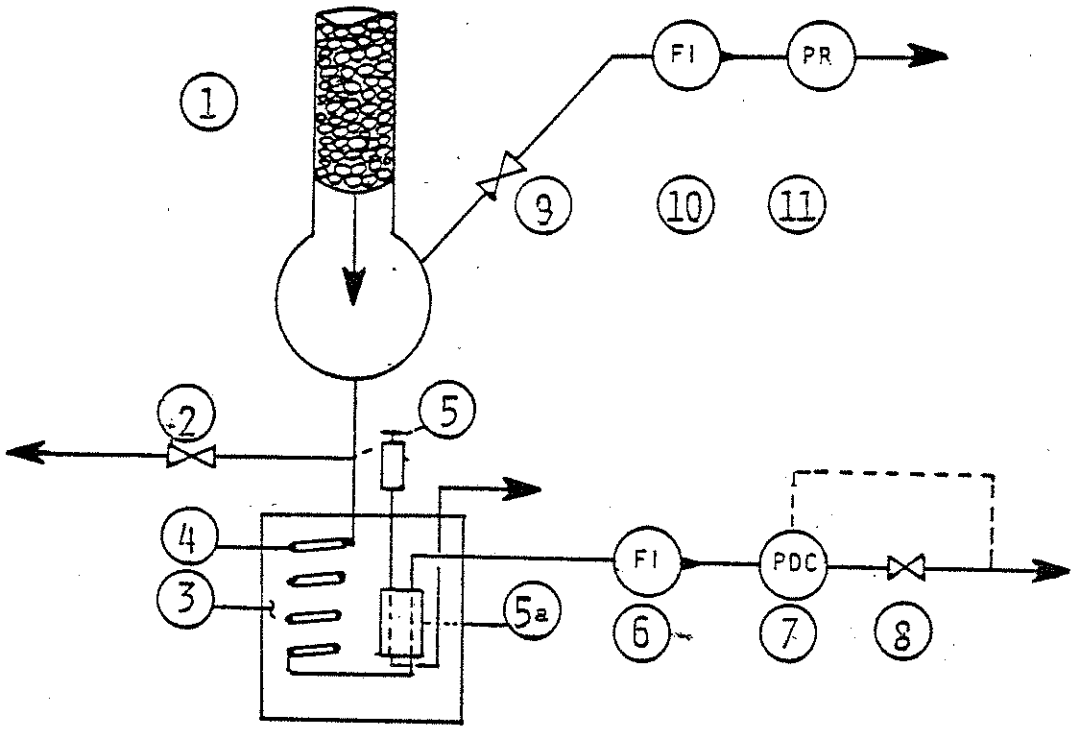

No.	Item	No.	Item
1	Trickle-Bed Column Lower Section	6	Flow Meter
2	Needle Valve	7	Flow (pressure differential) Controller
3	Constant Temp. Bath		
4	Immersed Coil	8	Metering Valve
5	Split Flow to Refractometer	9	Shut-off Valve
5a	Refractometer Optical Module	10	Flow Meter
		11	Back-Pressure Regulator

Figure 4.13 Schematic of Refractometer Control Scheme.

The instrument which will be used to monitor the tracer concentration in the liquid effluent stream is a Water Associates B-403 differential refractometer. The main components of the instruments are given in Figure 4-14. A diagonally placed piece of glass separates the two flow chambers of the optical cell. The usual configuration is to keep one side of the cell filled with the carrier fluid which serves as a reference to which liquid flowing through the other chamber in a continuous fashion is compared. The output signal from the refractometer is a 100 mv analog signal which continuously drives a strip chart recorder (Beckman). This signal is also displayed continuously on a digital voltameter (Data Technology). Interfacing hardware is available which allows the voltage displayed on the digital voltameter to be simultaneously punched at discrete time intervals in the form of paper tape. This tape can be read into the Engineering DEC-20 system for further signal processing.

In the case where reaction experiments are performed the liquid effluent from the trickle-bed is monitored both continuously by the refractometer and periodically by gas chromatograph.

4-5. TRICKLE-BED REACTOR EXPERIMENTS:

Trickle-bed reactor experiments are directed toward establishing a definite relationship between reactor

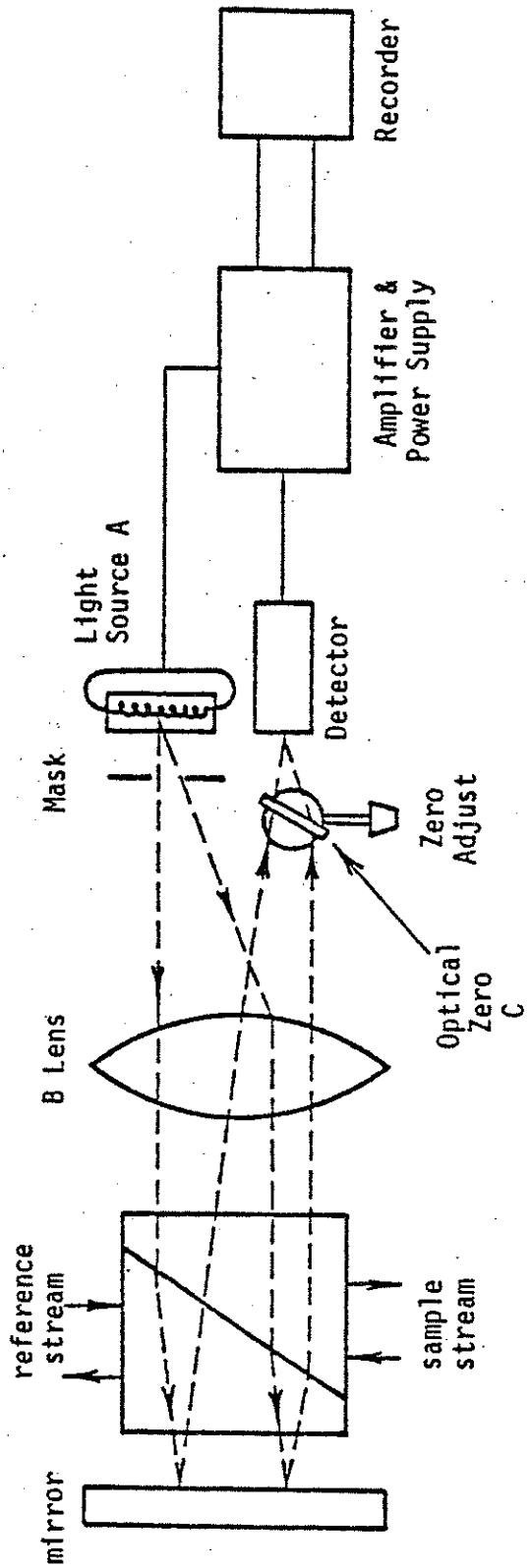

Figure 4.14 Schematic Diagram of Refractive Index Detector.

performance and solid-liquid contacting effectiveness. The main objectives of these experiments are:

1. To establish the effect of liquid mass velocity on the external solid-liquid contacting effectiveness for the same carrier liquids that will be used in reaction experiments. The tracer based method of Colombo et al (33) will be used to determine the external solid-liquid contacting effectiveness. From the tracer experiments certain parameters such as liquid hold ups, back-mixing and active bed volume can be evaluated. These parameters are required for reaction data interpretation and reactor modeling.
2. To obtain reaction conversion data for α-methylstyrene hydrogenation at various liquid mass velocities using the same carrier liquids utilized in the tracer experiments, three types of catalyst particles will be used.

In order to achieve the first objective, tracer experiments will be performed in both liquid filled column and in two phase flow trickle-bed column. Recently Mills (110) has performed tracer experiments in trickle-bed reactor has concluded that both adsorbing and nonadsorbing tracers yield the same results of contacting effectiveness if Colombo et al (33) method is utilized to interpret the results.

A suitable nonadsorbing tracer will be selected based on the solubility parameter of the tracer and the results obtained in a liquid filled column. Some possible tracers to use as nonadsorbing tracers for the various solvents to be investigated are listed in Table 4-2.

The sequence in which tracer experiments are to be performed is as follows:

A. Liquid filled column experiments are to be performed first. The objectives of these experiments are to find a suitable non-adsorbing tracer which gives the correct values of internal pore volume and external bed void volume. An effective diffisivity of the tracer as a function of liquid mass velocity will be determined in the liquid filled column.

B. Tracer experiments will be performed in two phase flow packed bed reactor at various liquid velocities and gas flow rates. The effective diffusivity of the tracer and liquid holdups will be determined as a function of liquid mass velocity.

C. The effect of liquid carrier physical properties on the contacting effectiveness will be studied using three solvents. These

Table 4-2

Some Possible Non-adsorbing Tracers

Tracer	Solubility Parameter δ (Cal/cc)$^{1/2}$	Dielectric Constant	Solvent Strength Parameter
n-decane	6.6	1.991	—
cymene	8.2	2.24	—
cyclopantene			.05
methylcyclohexane	7.8	—	—
heptane	7.4	1.924	—
pentene	7.0	1.844	0.00
xylene	8.8	2.27	0.26
toluene	8.9	2.379	0.29
benzene	9.2	2.274	0.32
cumene	9.0	2.38	
hexane	7.3	1.89	0.0
cyclohexane	8.2	2.023	0.04
tetrahydrofurane	9.1	—	0.45

are cyclohexane, hexane and tetrahydiofuran. The physical properties of these solvents are listed in Table 4-2 and 4-4.

Upon completion of the tracer experiments, reactor performance will be studied utilizing the hydrogenation of α methylstyrene to cumene in the same liquid carriers used in the tracer experiments. Reaction conversion data will be obtained at various liquid mass velocities and gas flow rates, using three different types of packings. These packings are:

1. 0.5% palladium deposited in a thin layer of 0.007 cm thick on the external surface of cylindrical alumina pellets.
2. 2.5% palladium deposited in thin layer of 0.0257 cm thick on the external surface of cylindrical alumina pellets.
3. 2.5% palladium deposited uniformally throughout, on cylindrical alumina pellets.

Three sets of reaction experiments will be directed toward obtaining reaction conversion data from which liquid-solid mass transfer coefficient and contacting effectiveness can be determined.

Prior to reaction experiments, the trickle-bed column packed with palladium on alumina catalyst will be activated in the same fashion as in the stirred-reactor studies. The

Table 4-3

Range of Variables in the Proposed Study

Variable	Range	
Q_L	0.02 - 2.5	(cc/sec)
Q_G	1 - 2	(cc/sec)
U_L	.007 - .877	(cm/sec)
U_G	0.35 - 0.7	(cm/sec)
L	.005 - .678	$\frac{\text{grams}}{\text{cm}^2\text{-sec}}$
Re_L	.079 - 9.99 ∿ 10.0	
We_L	1.76×10^{-7} - 3.25×10^{-3}	
Fr_L	3.27×10^{-7} - 6.018×10^{-3}	
σ_L	cyclohexane = 23.754	dyne/cm
μ_L	cyclohexane = 0.883	cp
ρ_L	cyclohexane = .774	grams/cc

t = 25°C

d_p = .13 cm

d_c = 1.905 cm

L_c = 40 cm

L_p = 0.563 cm

Table 4-4

Range of Physical Properties in the Proposed Study

Temp. °C	Cyclohexane			Hexane			THF		
	μ (cp)	ℓ_L ($\frac{g}{cc}$)	σ ($\frac{dyne}{cm}$)	μ	ℓ_L	σ	μ	ℓ_L	σ
15	1.052	.7832	24.593	.3219	.663	19.47	.55	.894	30.8
20	.963	.779	24.309	.3064	.659	18.95	.519	.889	30.0
25	.883	.774	23.754	.292	.6503	18.44	.49	.883	29.76
30	.812	.769	23.202	.278	.6499	17.94	.465	.878	28.5

Table 4-4
(continued)

Range of Physical Properties in the Proposed Study

Temp. °C	α-Methylstyrene			Cumene		
	μ (cp)	ℓ_L ($\frac{g}{cc}$)	σ ($\frac{dynes}{cm}$)	μ	ℓ	σ
15	.835	.915	31.9	.838	.866	29.5
20	.795	.911	31.3	.781	.862	29.0
25	.759	.906	30.8	.729	.857	28.5
30	.726	.902	30.25	.683	.853	28.0

oven of a Perkin Elmer 820 gas chromatograph will be utilized to activate and pretreat the catalyst bed.

The sequence in which reaction experiments are to be performed is as follows:

A. Pure hydrogen and presaturated liquids feed with hydrogen are introduced at the top of the reactor.

B. Pure nitrogen and presaturated liquid with hydrogen are introduced at the top of the reactor.

C. Pure hydrogen and liquid feed are introduced at the top of the reactor.

In type A. experiments, the main variables are liquid flow rates, gas flow rates, physical properties of the solvent and the percent palladium in the catalyst. The objectives of these experiments are to determine both contacting effectiveness and liquid-solid mass transfer coefficient as a function of liquid mass velocity, gas flow rate and physical properties of the liquid. Three carrier solvents will be used, namely, cyclohexane, hexane and tetrahydrofurane.

In type B. experiments, the main variables are the same as in type A., except that liquid carrier physical properties will not be investigated. Only cyclohexane solvent will be used, and the results obtained will be compared with

the one obtained for cyclohexane solvent in type A. experiments only. The objective of these experiments is to examine the effect of gas-solid mass transfer on the reactor performance. The effect of the saturated liquid feed being stripped of hydrogen on the conversion can be eliminated by the following two steps:

1. Only presaturated nitrogen with cyclohexane will be admitted to the reactor.
2. Concentration of α-methylstyrene in the feed is low enough such that the consumption of hydrogen is negligible even at contacting efficiency of one.

Finally in type C. experiments, hydrogen-deficient liquid feed and pure hydrogen gas will be utilized to measure the global reaction rate. The liquid feed will be stripped of hydrogen if any were present by pulling a vacuum and bubbling nitrogen gas. Global reaction rate will be measured as a function of liquid mass velocity and gas flow rate. The objectives of these experiments are to examine the importance of inter-particle and intra-particle mass transfer resistances on the reactor performance.

In all of the proposed studies on a trickle-bed reactor made out of a borosilicate glass cylinder 40 cm long and 1.905 cm in diameter will be utilized. The

reactor is jacketed with a 4 cm internal diameter borosilicate tube. During experiments the reactor is maintained at constant temperature by circulating water through the bed jacket from a constant temperature bath.

As mentioned earlier, the main variables introduced in both tracer and reaction experiments are liquid and gas flow rates. The range of variables and physical properties in this study is listed in table 4-3 and 4-4.

4-6 Chemicals:

Reagent grades solvents will only be used in this work. The solvents are cyclohexane, hexane and tetrahydrofuran supplied by Fisher Scientific Co. Each solvent will be purified further prior to use, by passing the liquid solvent over an activated bed of porous F-1 alumina. In the case of reaction experiments, α-methylstyrene of 98% purity (Fisher Scientific Co.) will be added to the solvent after the removal of the polymerization inhibitor. In the case of tracer experiments, only high quality reagent grade tracers will be used.

Hydrogen, nitrogen and helium gases used in this work are supplied by Acetylene Gas Company and were passed through an oxygen-trap and moisture removal unit.

The catalyst utilized in this work is 0.5% and 2.5% palladium on alumina pellets. Physical properties of the catalyst will be determined and presented in the final thesis.

4-7 PRELIMINARY EXPERIMENTS AND RESULTS:

A semi-batch slurry reactor in which the crushed catalyst particles are suspended in the liquid phase is used to determine the intrinsic kinetics of α-methyl-styrene hydrogenation in various hydrocarbon solvents. The presence of a three phase system in such a reactor allows for the possibilities of mass transfer limitations to exist. The operating conditions had to be chosen so as to ensure that mass transfer limitations on the measured reaction rate were absent.

Hydrogen gas must be absorbed from the gas bubbles and transported by liquid mixing and diffusion to the surface of the catalyst particles. The rate controlling step may be one or more of the following steps:

1. Mass transfer of hydrogen from the gas bubbles to the bulk of the liquid.
2. Mass transfer of reactants through the liquid film surrounding the catalyst particles.
3. Mass transfer of reactants in the liquid filled pores of the particles.
4. Adsorption and intrinsic kinetics of reactants on the catalyst surface.

The factors that influence either one or more of the rate controlling steps in this reaction system are, catalyst particle diameter, agitation rate and gas flow

rate. The optimum experimental settings of each of these factors must be determined first prior to any true intrinsic reaction kinetics studies.

The technique of decreasing the catalyst particle size until no further increase in the reaction rate is observed may usually be taken as a criterion for absence of pore diffusion limitations. Similarly increasing the stirring rate until no further increase in the reaction rate occurs is also taken as a criterion for absence of mass transfer limitations. However agitation does not affect the liquid-solid mass transfer appreciably when small particles size are used, but it increases the gas-liquid interfacial area and hence the rate of transfer from the gas to liquid.

Experiments were performed using 0.5% ρd- on alumina catalyst particles of 0.07 cm in diameter. The reaction rate was measured over a range of initial α-methylstyrene concentration in cyclohexane of 7.13×10^{-4} $(\frac{\text{g-mole}}{\text{cc}})$ to 1.5×10^{-4} $(\frac{\text{g-mole}}{\text{cc}})$ and at constant hydrogen flow, agitation rate, reaction volume and temperature. The measured reaction rate was 0.0069 $(\frac{\text{g-mole}}{\text{sec - gr Pd}})$ at 30.7°C and was reproduced to within ± 2.2%. The fact that straight line plots (Figure 4-15) are obtained indicates a zero order dependence of the reaction rate on α-methylstyrene concentration. Visual observations indicate

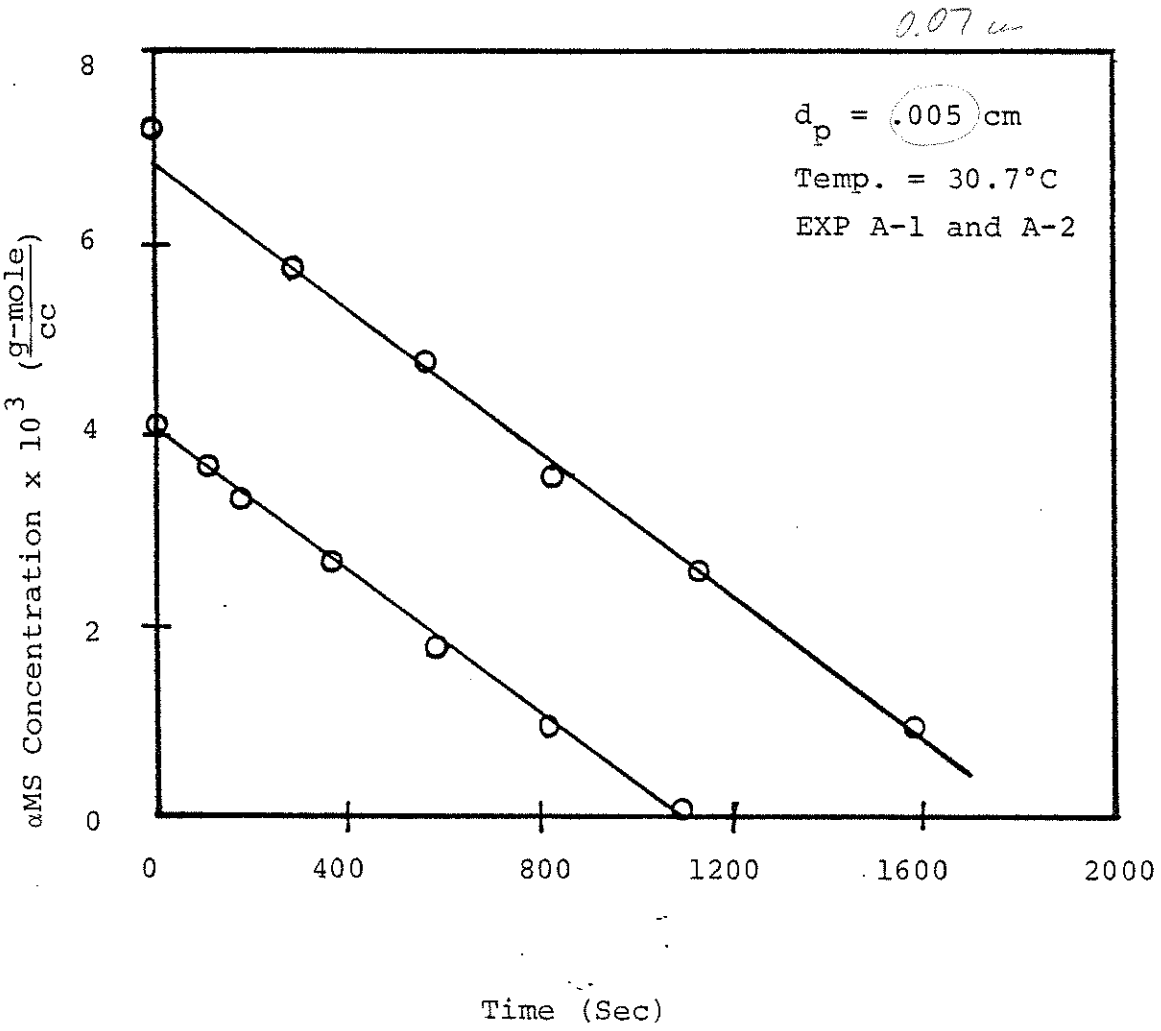

Figure 4-15. AMS Concentration as function of reaction time.

that the catalyst particles are very well suspended and the reactor was isothermal even at the highest catalyst loading of 25 grams.

A reduction in the catalyst particles size from 0.07 cm to 0.03 cm and at specified settings of experimental variables (Appendix C, set B), resulted in an increase in the reaction rate from 0.0069 ($\frac{\text{g-mole}}{\text{sec - gr pd}}$) to 0.027 ($\frac{\text{g-mole}}{\text{sec - gr pd}}$) at 30.5°C. This significant increase in the reaction rate is attributed to a decrease in one or more of the interphase or intraphase mass transfer resistances. The same dependence of the reaction rate on α-methylstyrene concentration (zero order) was also observed on the 0.03 cm particles.

$\frac{r_1}{r_2} \simeq \left(\frac{d_2}{d_1}\right)^{1.6}$

The transfer of hydrogen from the bulk gas phase to the pores of the catalyst involves a series of mass transfer steps which are characterized by corresponding mass transfer coefficients. Satterfield (51) developed an equation of the form:

$$\frac{C_{H_2,e}}{-r_A^x} = \frac{d_B}{6K_L H_i} + \frac{\ell_p d_p}{6M}\left[\frac{1}{K_{LS}} + \frac{1}{K\eta}\right]$$

to describe the transfer from gas bubbles to the catalyst surface. This equation was derived for a first order reaction with respect to gaseous reactant in a slurry reactor. In a series of runs using 0.03 cm particles of

0.5% pd-on alumina, only the catalyst loading (m) was varied. The reciprocal of reaction rate should be linear in (1/m) if the reaction rate was first order with respect to hydrogen. Such a straight line plot was obtained (Figure 4-16) which also passed through the origin indicating that the term in $1/K_L$ is negligible. The zero intercept also indicates that the hydrogen absorption is rapid and the liquid can be kept essentially saturated ($C_{H_2,e} = C_{H_2,L}$). The effect of hydrogen flow rate and agitator speed on the reaction rate was also examined using 0.03 cm particles. No effects on the rate were observed when the agitator speed and hydrogen flow rate were varied from 1400 to 1800 R.P.M. and 2100 to 3700 $(\frac{cc}{min})$ respectively. At this point it should be indicated that the rate measurements data were reproduced to within 2.2%, when particles size of 0.03 cm were used. This indicates a valid catalyst pre-treatment procedure and that the catalyst activity was essentially constant.

Finally the catalyst particles size was reduced to 0.005 cm in diameter and the reaction rate was measured over a temperature range of 15°C to 30°C at a specified set of experimental conditions (Appendix C, set-D). Two palladium catalyst concentrations were used, namely 0.5% and 2.5%. The measured reaction rate on both catalyst per gram palladium was the same at any given temperature

Temperature rate is only about ≈ 0.027 $\left(\frac{gmole}{gld\ s}\right)$.

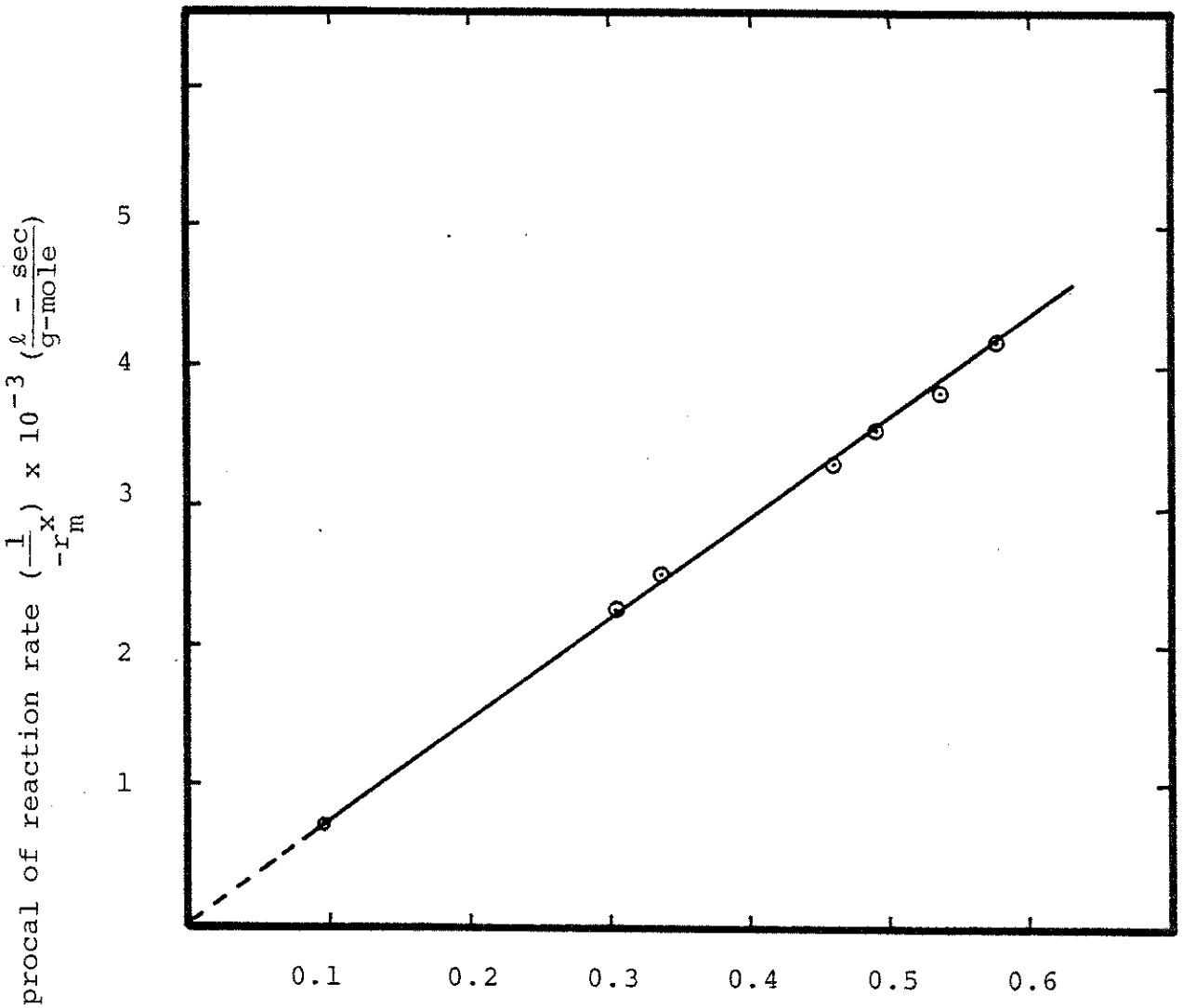

Figure 4-16. Reciprocal of reaction rate as function of reciprocal Catalyst loading (Set B).

indicating that the hydrogenation reaction appears to be structure insensitive which also has been confirmed by German et al (63) and Pexielr et al (98). The apparent reaction activation energy was calculated based on the familiar Arrhenius plot as shown in Figure 4-17A and is found to be 10.2 $\frac{\text{Kcal}}{\text{mole}}$. However, because of the increase in solubility of hydrogen in cyclohexane with temperature, the true activation energy of the reaction in cyclohexane is slightly lower than this value and can be calculated from

$$E_{true} = E_{app.} - n(\Delta H_s)$$

where

n = reaction order with respect to the gaseous reactant.

ΔH_s = heat of solution $(\frac{\text{Kcal}}{\text{mole}})$

Krayer and Nobel (113) measured the solubility of hydrogen in cyclohexane at various temperatures have calculated ΔH_s to be 1.6 $(\frac{\text{Kcal}}{\text{mole}})$.

The effect of hydrogen partial pressure on the reaction rate was also investigated. The measured reaction rate was found to be dependent on hydrogen partial pressure to the first power approximately as shown in Figure 4-18 and the reaction rate can be expressed as:

true or apparent

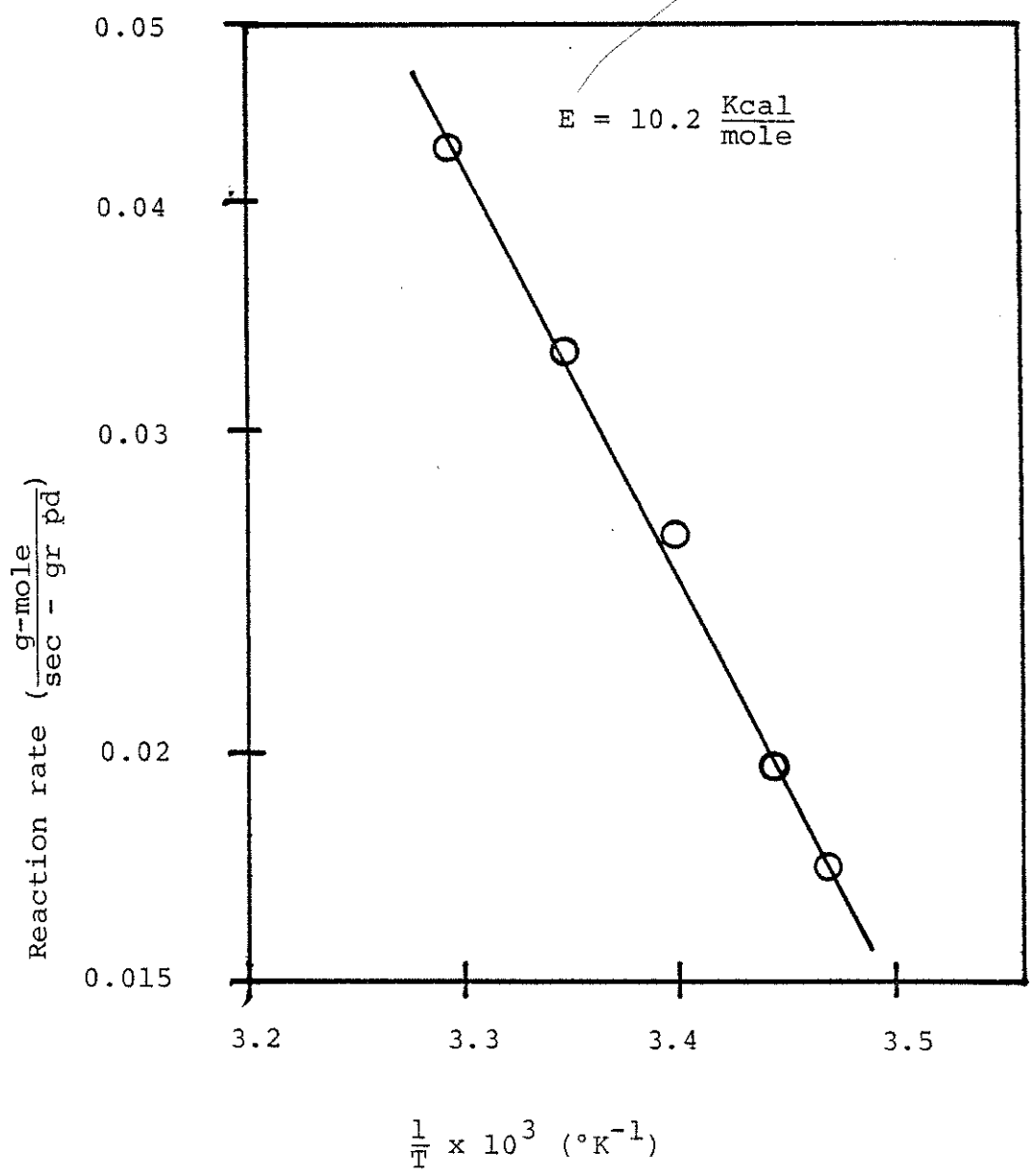

Figure 4-17A. Reaction rate as function of inverse reaction temperature in cyclohexane solvent.

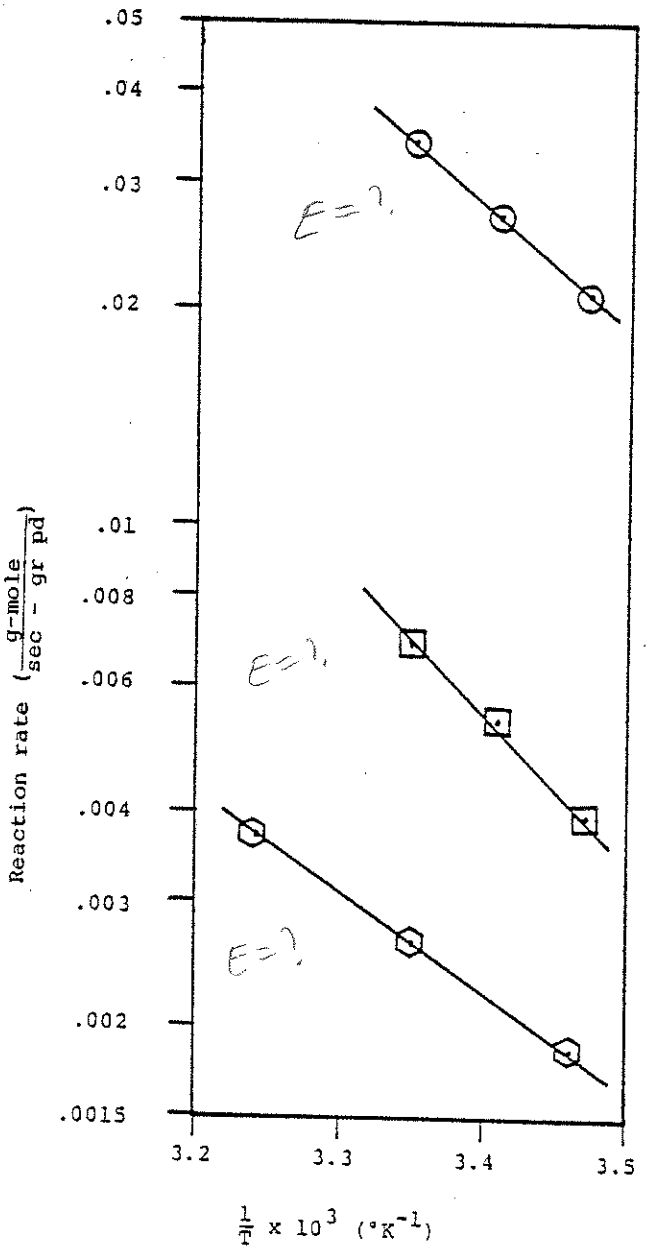

Figure 4-17B. Reaction rate as function of inverse reaction temperature.

Which solvent?
cyclohexane or
4 v. hexane?

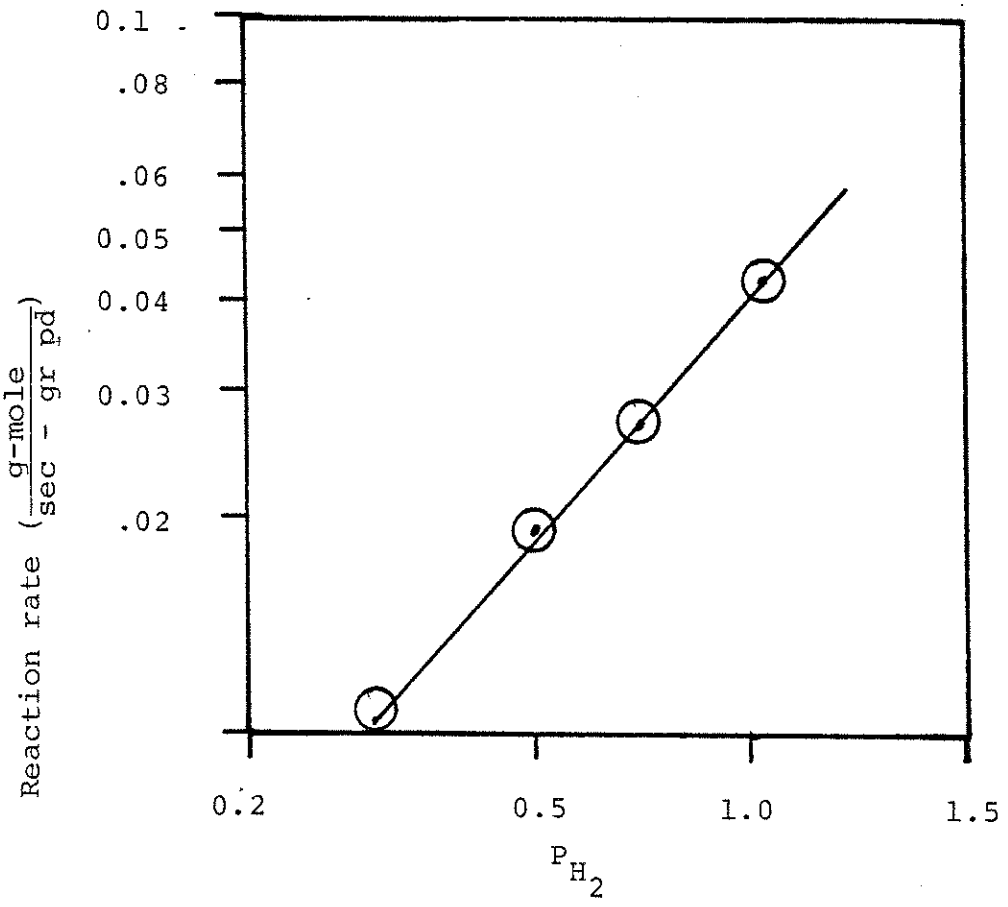

Figure 4-18. Reaction rate as function of hydrogen pressure.

$$-r_A = \frac{1}{W\beta} \frac{dN}{dt} = K_p P_{H_2}$$

or

$$-r_A = K_W C_{H_2,L}$$

where

W = Catalyst weight

Bβ = percent palladium

N = Number of moles consumed

t = time (sec)

P_{H_2} = Partial pressure of hydrogen in (atm)

$C_{H_2,L}$ = Concentration of hydrogen in the liquid phase

K_p = Reaction rate constant ($\frac{g - mole}{Sec - gr\ pd - atm}$)

Based on the results obtained for the apparent activation energy and reaction order with respect to hydrogen, the true intrinsic activation energy associated with K_W is 8.6 $\frac{Kcal}{mole}$. The first order dependence of the reaction rate on hydrogen partial pressure indicates that the surface reaction between adsorbed α-methylstyrene and hydrogen does not seem tobe the rate controlling step with regard to possible reaction mechanism.

Diffusional influences and external mass transfer limitations were apparently absent from our studies when catalyst particles diameter of 0.005 cm was used. An

apparent activation energy value of 10.2 $\frac{\text{Kcal}}{\text{mole}}$ is much higher than would be expected for a mass transfer limited process.

The effect of solvent on the reaction rate was also studied using hexane u.v and ACS grades, tetrahydrofurane, isobutyl alcohol and mixture of cyclohexane-tetrahydrofurane. In all the solvents studied the measured reaction rate was found to exhibit a zero order dependence on α-methyl-styrene concentration.

The results obtained with u.v. grade hexane solvent indicate that the measured rate exhibit a first order dependence on hydrogen partial pressure and an activation energy of 8.0 $\frac{\text{Kcal}}{\text{mole}}$ was obtained. The magnitude of the reaction rate was found to be a strong function of the solvent imparities. The measured rate in u.v. grade hexane was approximately 2.7 times the measured rate in ACS grade hexane. This reduction in the rate when ACS grade hexane is used was attributed to the presence of impurities which compete for the catalyst active sites with αmethylstyrene and hydrogen.

The results with tetrahydrofurane, mixture of cyclohexane-tetrahydrofurane and isobutyl alcohol solvents indicate that the reaction rates were lower than those obtained in cyclohexane and u.v. grade hexane at a given temperature. The experimental results show that the reaction rate does not depend only on the degree of hydrogen

solubility in a particular solvent but also on the physical properties of the solvent as shown in Table 4-5.

Attempts were made to carry out the reaction at 30°C using hydrogen donor solvent such as tetrahydrofurane were unsuccessful.

Several runs were carried out using 0.5% pd - on alumina catalyst of 0.07 cm and 0.03 cm in diameter. Only cyclohexane solvent and α-methylstyrene purified at least 24 hours prior to reaction runs were used. A significant decrease in the reaction rate was observed at 30°C and the catalyst activity was decreased further upon addition of more α-methylstyrene to the reacting system (Appendix C, Exp. F-2 and F-3). The decrease in the catalyst activity can possibly be attributed to the formation on the catalyst surface of non-desorbable dimer, trimer, or higher molecular weight polymers of α-methylstyrene. Because of the low conversion obtained in these experiments, it is very difficult to distinguish with any certainty between first or zero order reaction with respect to α-methylstyrene as shown in Figure 4-19 and 4-20. Finally 2.5% pd-on 0.005 cm alumina particles was used and the reaction was allowed to exceed 70% conversion. The measured reaction rate was found to be zero order with respect to α-methylstyrene as shown in Figure 4-21.

Table 4-5

dp = .005 cm

Solvent	t °C	$\delta\ (\frac{Cal}{cc})^{1/2}$	$-r_A\ (\frac{g\text{-mole}}{sec\text{-}g\ pd})$
Cyclohexane	25.7	8.2	.033
Hexane (U.V)	25.2	7.3	.034
70% Cyclohexane + 30% THF	24.9	8.47	.0069
THF	25	9.1	.0028
Isobutyl alcohol	25.1	11.4	.0026

same ?

how does H_2 solubility affect in hexane & cyclohexane

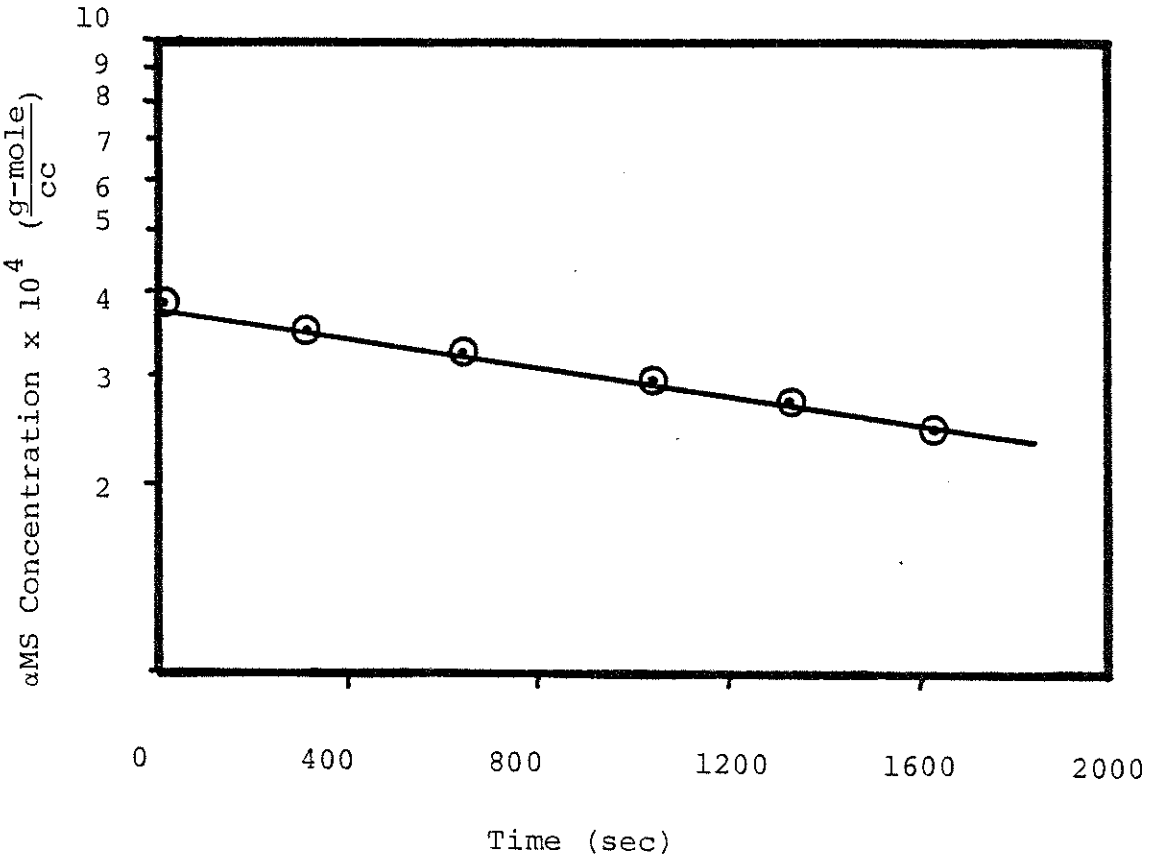

Figure 4-19. AMS Concentration as function of reaction time (Exp. F-2).

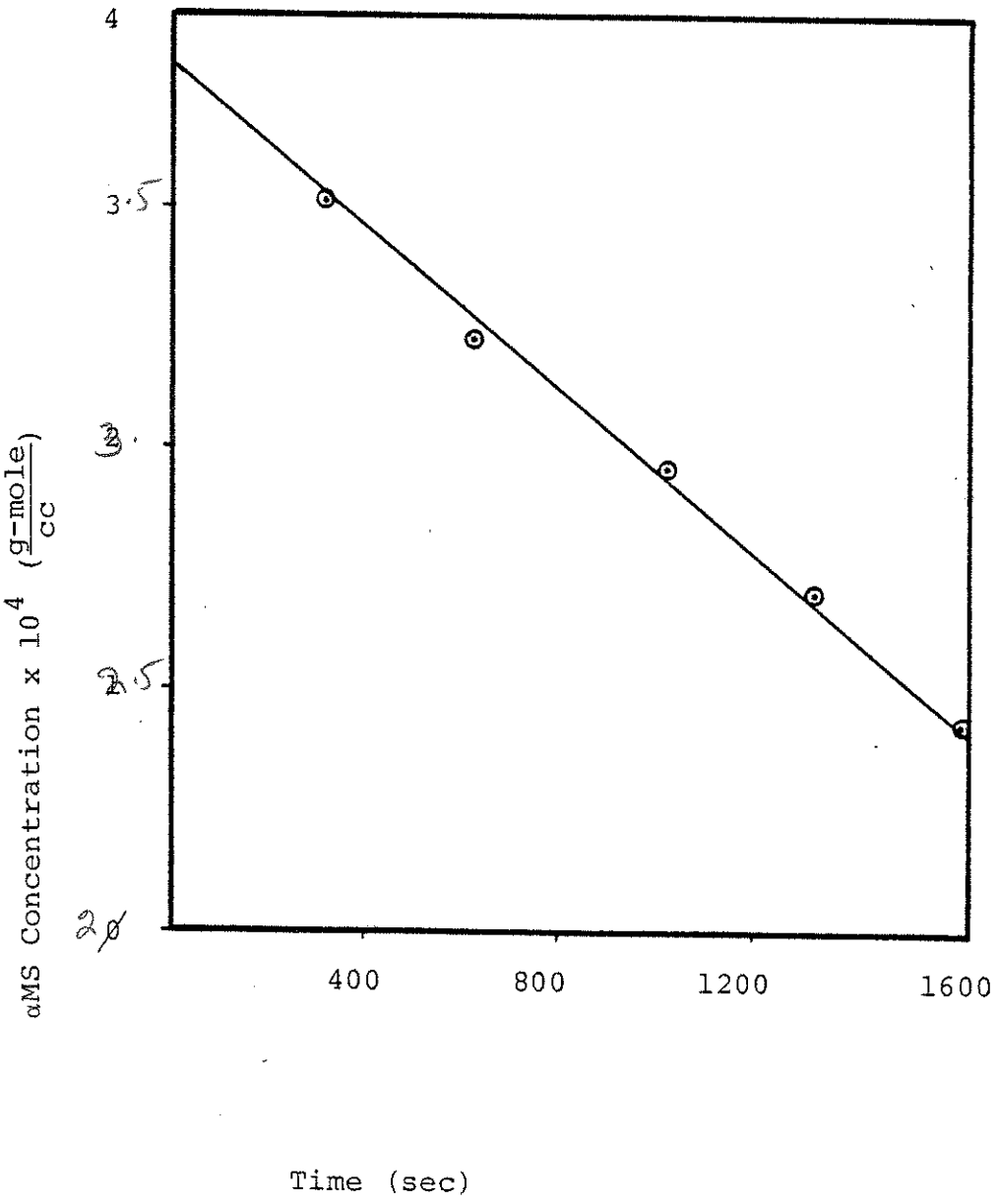

Figure 4-20. AMS Concentration as function of reaction time (Exp. F-2)

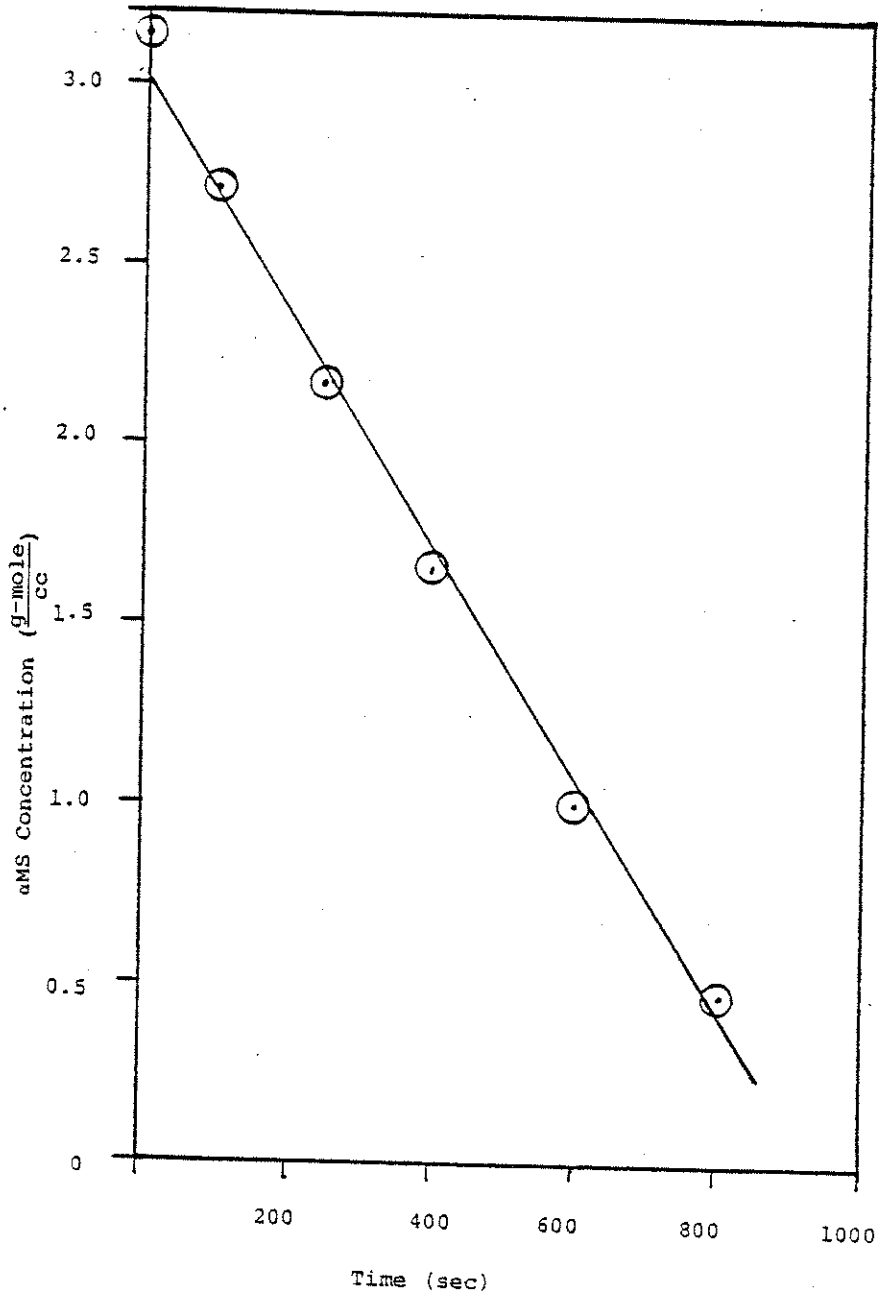

Figure 4-21. AMS Concentration as function of reaction time (Exp. F-4).

Reaction rate measurements were also made using 2.5% pd-on alumina of 0.005 cm in diameter, cyclohexane solvent, and unpurified α-methylstyrene. A decrease in the catalyst activity but no change in the reaction order were observed. The decrease in the catalyst activity is attributed to the presence of the polymerization inhibitor in the commercial α-methylstyrene used.

Based on the intrinsic study of α-methylstyrene hydrogenation, the following conclusions can be made:

1. Reaction rate was found to be zero order with respect to α-methylstyrene and first order with respect to hydrogen partial pressure.
2. Reaction rate of α-methylstyrene hydrogenation on palladium catalyst appears to be structure insensitive (Appendix C, set-D).
3. Reaction rate decreases with an increase in the solvent polarity.
4. Reaction rate is greatly affected by the presence of impurities in the solvent.
5. The presence of dimer, trimer, or higher molecular weight polymers of α-methylstyrene has a greater effect in reducing the reaction rate than the presence of polymerization inhibitor in the untreated α-methylstyrene.

Chapter 5

Appendices

Appendix A

Literature Survey:

Applications of trickle-bed reactors in the petroleum industry were first investigated by Shell and Gulf Oil Companies for the purpose of developing a low cost hydrodesulfurization process. The aim of the hydrodesulfurization process is to remove sulfur from the petroleum stock by means of a chemical reaction with hydrogen to form hydrogen sulfide. The process was developed in which the liquid oil feed was allowed to trickle over a solid catalyst bed and the gas phase (hydrogen) was the continuous phase. Frequently the hydrocarbon feed is a vapor-liquid mixture which is reacted at liquid hourly space velocity (LHSV) in the range of 0.5 - 4 (51).

The Shell hydrodesulfurization process investigated by Hoog et al (52) claimed that both capital investment and operating cost are reduced by 15 to 20% for the trickle-bed operation than for similar units operated in the vapor phase. The reduction in operating cost and capital investment was achieved mainly because less heat transfer equipments are required and the hydrogen recycle rate could be considerably reduced.

Le Nobel et al (2) in a study regarding the performance of laboratory scale trickle-bed reactors have concluded

that a reduction in both catalyst size and liquid feed viscosity increases the reaction rate. The increase in the reaction rate was attributed to a decrease in pore diffusion resistance and an increase in the diffusivity of the organo-sulfur compound through the liquid filled pores. Van Zoonen et al (53) investigated the effect of palleting pressure on pellet pore structure and on the apparent activity of the commonly utilized hydrodesulfurization catalyst $CO/MO/Al_2O_3$. Their studies were conducted using 3 x 3 mm pellets and 0.5 mm particles at reaction conditions of 35 atm pressure and 375°C. The results of their study indicate that a higher degree of desulfurization was obtained for both low density pellets than for high density pellets and on crushed catalyst than on the pellets. It was also confirmed by Van Zoonen et al (53) that the hydrodesulfurization reaction was limited by pore diffusion of the organo-sulfur molecule and the catalyst effectiveness factor was estimated to be 0.8 and 0.5 for low and higher density pellets respectively.

Under typical hydrodesulfurization reactions conditions of 57 atm pressure and 370°C, Van Deemter (54) utilized 5 mm in diameter $CO/MO/Al_2O_3$ catalyst has concluded that an average liquid film thickness around the catalyst particles was in the range of 0.01 to 0.1 mm, and an effectiveness factor of 0.36 was estimated.

The study of Adlington et al (55) on fuel oil hydrodesulfurization at 35 atm pressure and 415°C using 3.2 mm pellets, indicated that stagnant gas bubbles in the pores would decrease the effective active area and that the pores were filled with liquid for all practical purposes. They estimated an effectiveness factor of 0.6 for their study and found that the effectiveness factor did not change appreciably with feed boiling range. Their last result indicates that the decreased reactivities of the heavier sulfur compounds were roughly compensated by their decreased diffusivities. Adlington et al (55) suggested that the most effective method of increasing catalyst activity is to decrease the catalyst particle size balanced against selectivity, pressure drop and column blockage.

Cecil et al (97) performed pilot-plant experiments with several distillates, heavy vacuum gas oils, and residue. They observed no change in the reaction rate resulting from changes in mass velocity of oil in the range of about 0.13 to 0.54 Kg/m^2S. Bondi (5) have attempted to extract chemical reaction rates from conversion data obtained in a bench scale hydrodesulfurization reactor and concluded that any chemical kinetics data best be obtained in a well stirred reactor system for any liquid-gas-solid catalyst reaction.

Babcock et al (57) used a differential flow packed bed reactor operated in a countercurrent mode to study the

hydrogenation of α-methylstyrene to Cume. The reaction was carried out using 0.5% pd deposited on the external surface of 3.2 x 3.2 mm alumina pellets. They concluded that the reaction rate was limited by intrinsic reaction kinetics over the range of 1-12 atm pressure and 24-58°C, with an adiabatic temperature increase of 5.8°C for each percent conversion. It should be pointed out that Babcock et al (57) conclusions regarding the absence of mass transfer limitations is contradictory to the findings of several other investigators. However it is possible that because of the existence of less active β-phase pd-H_2 system and due to the use of commercial α-methylstyrene without further purification may result in a reduction of the catalyst activity and partial blockage of the active sites. As a consequence of a reduction in the catalytic activity of the pd catalyst a lower intrinsic reaction rate would be obtained free of mass transfer limitations.

Klassen et al (56) utilized a differential trickle-bed reactor to study air oxidation of ethanol to acetic acid in the presence of a palladium catalyst and found an appreciable resistance to the reaction encountered in both gas and liquid film. Johnson et al (58) investigated the hydrogenation of α-methylstyrene over 2% palladium powder in a slurry reactor at pressures up to 12 atm pressure.

Their data indicated the transfer of hydrogen from the gas bubbles surface to the catalyst surface to be the rate limiting step except at high agitation rates.

Sherwood et al (5) also studied the same reaction system using 55 μ particles of palladium black in a semi-batch reactor agitated by upward flow of gas. The mass transfer of hydrogen from the liquid to catalyst surface was also found to be the rate controlling step. In a similar study, Pruden et al (98) and Pexidr et al (99) also have shown the existence of mass transfer limitation to the reaction rate.

White et al (60) studied the same reaction in a rotating disk reactor. The catalyst was a palladium film-ion-plated under vacuum to the surface of a stainless steel disk. The liquid phase hydrogenation of α-methylstyrene was found to be under mix diffusion-surface reaction control at the conditions of 40-115°C, 4 atm pressure, and 5-42 radions per second disk speed. The measured kinetic parameters are independent of the degree of crystallite dispersion or crystallite size in the range of 20-200A°, but are dependent on the degree of orientation, with higher specific reactivity on the (111) relative to the (110) plane. This indicates that the olefinic group of the side-chain of α-methylstyrene would prefer adsorption on the shorter metal-metal spacing of the palladium. It is apparent that the higher specific

reactivity on the (111) relative to the (110) plane is mainly due to the greater number of the shorter of the two predominant metal-metal spacings available in face-centered cubic metals.

Biskis and Smith (61) used a pulsed-trickle-bed reactor to study α-methylstyrene hydrogenation on 0.5% pd on alumina spheres. The reaction rate was controlled by mass transfer of dissolved hydrogen to the catalyst surface and pulsation increased the mass transfer rate as much as 80%. Satterfield and Way (62) investigated the effect of the addition of an inert liquid into the gas phase catalytic reaction of isomerization of cyclopropane to propylene on a silica-alumina catalyst using three hydrocarbon solvents in a trickle-bed reactor. The ratio of the reaction rate constant under two phase flow conditions to that in gas phase alone was found to be 0.8-1.0 for Nujal solvent, 0.31 for Isopar L solvent and 0.019 for Solvesso 150 solvent. It is evident from the results of their study that cyclopropane and the inert liquid solvent compete for sites on the catalyst surface. The reduction in the reaction rate observed for the last two solvents mentioned above was attributed to both impurities in the solvents and the stronger adsorption of the solvent than cyclopropane in addition to the possible occurrence of mass transfer limitations.

Germain et al (63) have reported a detailed experimental study on the performance and mechanism of trickle-bed reactor utilizing the hydrogenation of α-methylstyrene over palladium catalyst as a reaction model. Both intrinsic and apparent reaction rate was found to be a function of hydrogen partial pressure and both rates are independent of α-methylstyrene concentration. They observed two steady state reaction rates in the operation of trickle-bed apparatus depending on the start-up procedure. The observed low reaction rate value which was lower than the rate obtained in a mix reactor, agree with the concept of mass transfer limitation through the liquid film surrounding the uniformally wetted pellet. On the other hand the higher rates obtained in the trickle-bed were even higher than those obtained in a mixed reactor indicating reaction occurrence on partially wetted pellets. The observed higher reaction rates on the partially wetted pellet than on a completely wetted pellet could be due to either vapor phase hydrogenation of α-methylstyrene or an increase in the transfer of hydrogen to the catalyst surface via gas-solid mass transfer which is greater than liquid-solid mass transfer. They also observed that in the beginning of the hydrogenation run with fresh catalyst, the packing remained dry for a long time except for some thin channels where the liquid trickled. The number of wetted pellets increased with time and the bed finally looked wetted for a temperature up to 35°C. A rapid

uniform wetting of the bed was observed if nitrogen was substituted for hydrogen flow or cumene was substituted for α-methylstyrene. Under reaction conditions, it was observed that, dry areas subsisted for any liquid flow rate if the temperature was higher than 35°C. The dry areas were always located in the active section of the packing and that some pellets were dry at a given time, wetted at another time and dry again later on.

Ware (64) in a study of benzene hydrogenation to cyclohexane observed two levels of reaction rates for apparently identical conditions in trickle-bed reactors. The low rates are attributed to diffusion plus reaction in the catalyst pures. The higher rates observed are due to vaporization or reactant, caused by highly exothermic reaction (ΔH_r = 49.8 Kcal/mole) and the subsequent gas phase reaction.

The effect of partial wetting of the catalyst pellets on trickle-bed reactor performance is very complex and not well understood yet. The study of Sedrik and Kenney (49) on partial wetting in trickle-bed reactor utilizing the selective hydrogenation of Crotonaldehyde. They observed that wetting can be incomplete and reaction on the dry particles contribute significantly or even dominate the overall rate. Reaction on the dry parts of the pellets still largely dominate the overall rate even when the extent of particles wetting was large. This

effect was attributed to the relatively higher rates of mass transfer and poorer heat transfer pertaining to gas phase reaction over a dry catalyst rather than to any difference in intrinsic kinetics.

Satterfield and Ozel (65) provided an experimental evidence of incomplete wettings in laboratory trickle-bed reactor utilizing the hydrogenation of benzene to cyclohexane. They observed through the glass-wall reactor during and in the absence of reaction that the liquid flowed downward in rivulets which tended to maintain their position with time. Some of the catalyst pellets were covered with trickling liquid film while others, although wet, were without liquid film on the surface and presumably the latter provided the mechanism for direct solid-vapor contact. The liquid film thickness of the wetted solids fluctuate in a regular manner approaching continuous film-like flow at the highest liquid flow rate, but never disappeared completely. The liquid phase reaction was diffusion limited and the contribution of the vapor phase reaction to the overall rate was considerable. The ratio of the vapor phase reactor to the liquid phase reaction decreased with an increase in the liquid flow rate, as would be expected due to an increase in liquid-solid contacting efficiency.

Herskowitz (12) studied the hydrogenation of

α-methylstyrene in both liquid full and trickle-bed reactor utilizing two different catalyst activities. He observed higher global reaction rate at low liquid velocities than for high liquid velocities when 2.5% pd on alumina and equilibrium feed was used. This was attributed to a wetting efficiency of less than one at low liquid velocities and that the contribution to the global rate was greater from the gas covered surface than from the liquid covered surface. He concluded that for the equilibrium feed operation the global reaction rate was a function of only two parameters. These are, liquid-solid contacting efficiency and liquid-solid mass transfer coefficients. The variation in liquid-solid contacting efficiency came about as the liquid flow rates were varied. For the liquid full reactor, their data indicates that both external and internal mass transfer significantly affect the global rate.

Satterfield et al (66) and Jawad Ali (50) independently have studied the α-methylstyrene hydrogenation in a trickle-bed reactor consisting of a single vertical column of spherical palladium catalyst. Both have concluded that the resistance to mass transfer through the liquid film was significant in reducing the reaction rate. Jawad Ali (50) reported that the reduction in the rate was two to three times than that in the absence of such a resistance,

while Satterfield et al (66) have reported a reduction of only a half at 50°C. Jawad Ali (50) also determined both intrinsic and apparent reaction rate. He found the rate to be dependent on the hydrogen concentration only. Ma (76) studied both intrinsic and apparent kinetics of the same reaction at 70-100°C and atmospheric pressure using 0.5% pd on alumina. The raction rate was found to be dependent on both hydrogen and α-methylstyrene concentrations to the first power. This is contradicting to the findings of several other investigators in which the rate was independent of α-methylstyrene concentration. However his results can be explained by the fact that Ma (76) operated the reactor at low α-methylstyrene conversion where both zero and first order rates cannot be distinguished. Other studies related to the performance of trickle-bed reactors including the study of Levec et al (67) and Goto et al (35) have concluded that external mass transfer effects play a vital role on the performance of such a reactor.

Sylvester et al (68) analyzed the effect of transport processes on conversion in trickle-bed reactor theoretically. A procedure was developed showing the combined effect of axial dispersion, external and internal mass transfer, and surface reaction on the conversion of a first order irreversible reaction in an isothermal trickle-bed reactor.

Hanika et al (69, 70, 71) studied the hydrogenation of cyclohexene on a flat catalytic surface which was proposed as a model for trickle-bed reactor with theoretical analysis. Hanika (72) also studied the effect of simultaneous heat and mass transfer on the hydrogenation of cyclohexene in trickle-bed reactor with particular emphasis to the problem of liquid phase evaporation and transition to the gas phase regime of operation. The measured reaction rate was a function of temperature and hydrogen flow. The measured reaction rate as a function of temperature displayed two branches between 65 and 85°C. The low values of the rates are corresponding to liquid phase reaction affected by intraparticle diffusion and the higher values of the rate are belonging to the regime of interphase diffusion in the gas phase. It was experimentally observed that the substrate concentration in the feed displayed a considerable hysteresis effect due to an abrupt increase in the reaction rate arising from temperature gradients within the bed and in the gas film surrounding the catalyst pellet. It was also observed that in both liquid phase and gas phase regimes the trickle-bed can operate in multiple steady state.

The role of mass transfer in trickle-bed reactors have been examined in the past fifteen years by by several investigators. Goto and Smith (34, 35) in a study on the

oxidation of formic acid in water with ZnO.CuO catalyst, have concluded that the performance of trickle-bed reactor depends on four transport resistances. These are, gas to liquid, liquid to solid, intraparticle and axial dispersion. Correlations for estimating various transport coefficients in such a reactor have been provided (34, 35). Generally it can be assumed that the transport process in the gas film at the gas-liquid interface will not constitute a partial limiting step. In the case of complete wetting of the catalyst particles, gaseous reactant must be transported after their absorption in the liquid from the gas-liquid interface, across the liquid up to the liquid solid interface. Under steady state condition an overall mass transfer coefficient has been defined by Satterfield et al (66) which takes into account the contribution from each of the remaining two liquid film resistances.

Calculations of the overall mass transfer coefficient on the basis of four different theoretical models have been made by Pelossef (73), who concluded that in the region of pure film flow, the overall reaction rate changes slightly in spite of considerable change in liquid flow rate.

It is interesting to note that in spite of the relatively wide scattering of Gianetto's data (22), they

all appear to be proportional to a specific transfer area. The liquid side mass transfer coefficient was independent of the flow conditions between about 0.03 to 0.08 cm/sec.

Snider and Perona (100) measured mass transfer coefficient for the hydrogenation of α-methylstyrene in a packed-bed reactor with concurrent gas and liquid upflow. Mass transfer coefficients varied from 0.006 to 0.06 cm/sec over Reynolds number ranges from 20 to 250 for the liquid phase and 2 to 75 for the gas phase. The mass transfer coefficients were found to be a function of both liquid and gas Reynolds number up to a gas Reynolds number of 50. Further studies regarding mass transfer in trickle-beds have been given in excellent review papers in the literature (8, 9, 10, 11, 33).

The effect of liquid-solid contacting efficiency on the performance of trickle-bed reactors has been determined indirectly by Herskowitz (12) for a gas limiting reaction. The high global rate obtained with equilibrium feed at low liquid flow rate was attributed to low liquid-solid contacting efficiency and high gas-solid mass transfer rate. The importance of this parameter in studying trickle-bed reactor performance has been emphasized by Mears (74), Sedriks and Kenney (49), Satterfield (8) and Schwartz (48). Based on these studies, it appears that regardless of the nature of any chemical reaction

studied in a trickle-bed reactor incomplete catalyst wetting can be singled out as the most important parameter which determine reactor performance. The importance of this parameter is primarily due to a strong connection between incomplete catalyst wetting and liquid flow rate, holdup, physical properties of reactants, exothermicity of reaction and indirectly axial dispersion.

Solid-liquid contacting efficiency has been defined for the non-porous packing as the fraction of external area contacted by the liquid. For porous packing, the solid-liquid contacting efficiency is defined based on either, the fraction of external area contacted, the fraction of total external plus internal areas contacted or the fraction of pore volume filled with liquid.

Satterfield (8) proposed a definition for the solid-liquid contacting efficiency based on the ratio of the kinetic constant obtained in a trickle-bed reactor to the true intrinsic kinetic constant. Colombo et al (33) expressed the liquid-solid contacting efficiency as the ratio of the apparent diffusivity of tracer in a porous particle determined in a trickle-bed reactor to that in a liquid full reactor.

The cyclic wetting and drying of the catalytic packing observed in different studies of hydrogenation reactions in trickle-beds can not be explained in terms

of the bed hydrodynamics only. It has been shown that the liquid flow over random packing is influenced by capillary effects at the points of contact, which are proportionally greater for small packing (75). Furthermore it is a known fact that the hydrogenation reaction products have vapor pressures greater than those of reactants as in the case of α-methylstyrene or crotonaldehyde hydrogenation. The excess pressure inside the catalyst pores tends to force the liquid out.

Models have been derived in the literature to account for partial wetting effects on the catalyst effectiveness factor. Mills et al (47) derived an expression for the catalyst effectiveness factor for the case of isothermal first order reaction with respect to a non-volatile liquid reactant. The effectiveness factor in trickle-bed was found to be a function of external contracting, pore volume fill-up and Thiele modulus. Expressions for the effectiveness factor were also derived by Mills et al (47) to account for external mass transfer limitations. Duduković (46) utilizing a modified expression of Thiele modulus has also confirmed the dependency of the effectiveness factor on contacting and pore fill-up. The problem of gas-limiting reactant was treated for slab or cube shape catalyst by Smith and co-workers (101, 102, 103). However, a more systematic general approach to the problem

of effectiveness factor in trickle-beds for different geometrics and limiting reactant cases has been treated by Mills and Dudukovic (104).

Various mathematical models for prediction of trickle-bed performance have appeared in the literature based on either plug flow model, hold-up model, effective catalyst wetting model or axial dispersion model. These models are derived for the general case of irreversible first order reaction with respect to liquid reactant, no external mass transfer limitations, isothermal reactor and no homogeneous noncatalytic liquid phase reaction.

The above mentioned models are summarized by Shah (19). The plug flow model takes into account only the case where reaction occurs at the liquid-solid interface and no condensation or vaporization of reactants occur. The proposed model can only be used to correlate data obtained in a large scale isothermal reactor such as hydrodesulfurization reactor.

Ross (77) in treating data from commercial and pilot plant hydrodesulfurization reactors, suggested the rate constant in trickle-bed is proportional to the true kinetic constant and total liquid hold-up. Henry and Gilbert (78) derived a model relating catalyst activity and parameters such as liquid superfacial mass velocity, liquid space velocity, catalyst bed depth and catalyst size.

Mears (74) questioned the validity of Henry and Gilbert's correlation based on the fact that liquid hold-up relationship in their model was derived for flow over a string of spheres. Mears (74) argued that the dependency of reactor performance on liquid velocity in pilot scale reactor is due to incomplete catalyst wetting at low liquid flow rate. Based on the wetted area correlation of Puranik and Vegelpohl (44), Mears (74) derived a correlation relating reactor performance to the system physical properties.

Bondi (5) has developed an empirical relation between the apparent rate constant and intrinsic rate constant for correlating pilot-scale data.

The above correlations do not take into account the axial dispersion effect on the performance of the reactor. In laboratory scale reactors, axial dispersion effects may have a significant effect on the reactor performance. Hochman and Effron (17) and others have shown that the axial dispersion in the liquid phase under trickle flow conditions is more significant than in a single phase reactor. Mears (74) presented a criterion for the minimum ratio of catalyst bed length to particle diameter required to hold the isothermal reactor length within 5% of that needed for plug flow reactor.

Sylvester and Pitayagulsarn (8) considered the combined effects of axial dispersion, external diffusion,

intraparticle diffusion and intrinsic kinetics on conversion for a first order, irreversible reaction in an isothermal trickle-bed reactor. They utilize a procedure developed by Suzuki and Smith (79) to derive a performance equation of such a reactor.

A summary of some studies regarding both intrinsic and apparent reaction kinetics is given in Table A-1 in addition to trickle-bed studies. Other variables affecting the performance of trickle-bed reactors such as liquid hold-up, flow regimes and pressure drops will be discussed in the final thesis.

Table A-1

Summary of Some Studies Related to Stirred and Trickle-Bed Reactors

Reference	Reactor Type	Catalyst	Reaction Conditions	Comments
Ma (76)	Semi-batch αms. hydrogenation.	0.5% pd on alumina dp = 55 μ m = 3.81 g/ℓ	70 - 100°C and 1 atm	$-r_{\alpha ms} = K\ C_{H_2}\ C_{\alpha ms}$ E ≈ 7.6 Kcal/mole
Germain et al (63)	αms hydrogenation. Semi-batch reactor	0.5% and 5% pd on alumina dp < 3μ $m = \frac{mg\ pd}{\ell}$	25 - 110°C and 0.13 - 2.6 atm	$-r_{\alpha ms} = K\ P_{H_2}^{.63}$ E ≈ 10 Kcal/mole
∿	Semi-batch	0.5% pd on alumina 3.52 x 3.24 mm cylinders	∿	$-r_{\alpha ms} = K\ P_{H_2}^{0.81}$ E ≈ 8.15 Kcal/mole
∿	Semi-batch	1% pd on alumina 3.5 x 3.32 mm cylinders	∿	$-r_{\alpha ms} = K\ P_{H_2}^{0.73}$ E ≈ 6.744 Kcal/mole
∿	Countercurrent trickle-bed reactor 45 cm long and 4 cm I.D	0.5% and 1% pd on alumina 3.52 x 3.24 mm and 3.5 x 3.32 mm cylinders	27 - 75°C and atmospheric pressure	Dc/dp ≈ 12 - 12.5 Incomplete wetting. Multiple Steady States. Mass transfer limitations in liquid phase reactions. E ∿ 8.1 Kcal/mole. Liquid flow range .008 - .16 $\frac{g}{cm^2\text{-sec}}$

Table A-1
(continued)

Reference	Reactor Type	Catalyst	Reaction Conditions	Comments
White et al (60)	Rotating disk. ams hydrogenation.	pd - film deposited on S. S. disk	40 - 115°C and 4 atm	Mix diffusion-surface reaction control. $-r_a = K C_{H_2}$ $E = 7.4 \pm 1.2$(Kcal/mole)
Lin (81)	Semi-batch ams hydrogenation	0.5% pd on alumina	93 - 170°C and 1 atm	Not enough data to determine the rate $E_{cbs} = 27.07$ (Kcal/mole)
Hanika et al (72)	Trickle-bed reactor 1.5 cm I.D. 60 cm long cyclohexane hydrogenation	3% pd on carbon 0.4 x 0.4 cm cylinders	25 - 125°C and 1 atm	Multiple steady state. Mass transfer limitations in the liquid phase reaction E = 5 Kcal/mole
Satterfield et al (66)	Trickle-bed reactor made of string of spheres. ams hydrogenation.	1% pd on spherical alumina of 0.52 cm in diameter	20 - 50°C and 1 atm	Reaction rate was function of both temperature and liquid flow rate. Mass transfer limitations. E = 5.08 Kcal/mole Molar liquid flow rate $0\text{-}5 \times 10^{-3}$ $\frac{gmole}{sec}$
Levec and Smith (67)	Trickle-bed reactor of 2.54 cm I.D. 30 cm long. oxidation of acetic acid	Ferric oxide particles of 0.0541 and 0.238 cm.	252 - 286°C 67 - 72.5 atm	Possibility of vaporization and channeling. Gas-liquid solid transport limitations. Liquid mass velocity .08-.26 g/cm^2-sec

Table A-1
(continued)

Reference	Reactor Type	Catalyst	Reaction Conditions	Comments
Sherwood and Farkus (59)	Bubble columns AMS hydrogenation	Palladium black dp = 55 μ m = .347 -2.95 $\frac{g}{\ell}$	28 - 60°C and 1.09 - 1.06 atm	Mass transfer limitations E = 4 Kcal/mole
Jawad Ali (50)	Semi-batch	25% pd on pyrumu dp = 0.1 μ m = 0.3188 g/ℓ	26-80 °C and 1 atm	$-r_{\alpha ms} = K C_{H_2}$ E = 7.5 Kcal/mole
∿	Semi-batch	25% pd on pyrumu dp = 0.95 cm	∿	$-r_{\alpha ms} = K C_{H_2}$ E = 4.4 Kcal/mole
∿	Trickle-bed made of string of spheres I.D. = 5.4 cm	25% pd on pyrumu nonporous	40 - 100	Mass transfer limitations. E = 5.5 Kcal/mole Liquid mass velocity 0.13 - 0.48 $\frac{g}{cm^2\text{-sec}}$
	∿	porous spheres	40 - 100	Mass transfer limitations. E = 4.98 Kcal/mole Liquid mass velocity .08 - .48 $\frac{g}{cm^2\text{-sec}}$
Babcock et al (57)	Trickle-bed 3.81 cm I.D. 125 cm long. αms hydrogenation.	0.5% pd on .32 x .32 cm alumina cylinders	24 - 57°C 0 - 12 atm	Surface reaction control. E = 7 Kcal/mole Liquid mass velocity $(1.5 - 7) \times 10^{-4}$ $\frac{g}{cm^2\text{-Hr}}$

Table A-1
(continued)

Reference	Reactor Type	Catalyst	Reaction Conditions	Comments
Biskis and Smith (61)	Pulsed fixed bed reactor. 2.54 cm I.D. ams hydrogenation	0.5% pd on 0.32 cm spherical alumina	55°C and 5.44 atm	Pulsation increased the mass transfer rate as much as 80%. Mass transfer of hydrogen control the reaction rate.
Goto and Smith (35)	Trickle-bed reactor 2.54 cm I.D. oxidation of formic acid in water	Cuo.Zno particles of 0.291 and 0.0541 cm	212 - 240°C and 40 atm	negligible axial dispersion effects Significant mass transfer resistance Liquid mass velocity .09 - .36 $\frac{g}{cm^2\text{-sec}}$
Herskowitz (12)	Trickle-bed reactor. 2.54 cm I.D. ams hydrogenation.	0.5% pd on 0.131 cm alumina particles	40.6°C and 1 atm	Reaction rate was a function of liquid-solid contacting efficiency and liquid flow rate. Liquid mass velocity 04 - 1.8 $\frac{g}{cm^2\text{-sec}}$

Appendix B

Nomenclature:

a_E	Total external geometric pellet surface area per unit reactor volume (cm^{-1}).
$a_L = a_{gL}$	Gas-Liquid interfacial area for mass transfer (cm^{-1}).
a_{gS}	Effective gas-solid interfacial area for mass transfer (cm^{-1}).
a_{LS}	Effective liquid-solid interfacial area for mass transfer (cm^{-1}).
a_s	Specific surface area of the packing per unit solid bed volume = $[6(1 - E)/dp]$ (cm^{-1}).
Bi_W	Biot number for mass transfer ($\bar{K}$ R/De) wetted area.
Bi_d	Biot number for mass transfer ($\frac{K_{gs} H_i R}{De}$) dry area.
$C_{H_2,g}$	Hydrogen concentration in the gas phase (g-mole/cc).
$C_{H_2,gf}$	Hydrogen concentration in the gas feed (g-mole/cc).
$C_{H_2,L}$	Hydrogen concentration in the liquid phase (g-mole/cc).
$C_{H_2,Lf}$	Hydrogen concentration in the liquid feed (g-mole/cc).
$C_{H_2,e}$	Equilibrium hydrogen concentration in the liquid phase (g-mole/cc).
$C_{H_2,i}$	Hydrogen concentration in the liquid filled pores (g-mole/cc).
d_B	Gas bubble diameter (cm).
d_c	Column diameter (cm).
d_p	Catalyst pellet diameter (cm).

D_A Molecular diffusivity (cm^2/sec).

D_e Effective diffusivity (cm^2/sec).

$\tilde{D}_g$ Axial dispersion coefficient in the gas phase (cm^2/sec).

$\tilde{D}_L$ Axial dispersion coefficient in the liquid phase (cm^2/sec).

E_g Energy of dissipation in the gas phase.

E_L Energy of dissipation in the liquid phase.

G Gas superficial mass velocity [$Kg - M^{-2} - sec^{-1}$]

H_E External liquid hold-up , dimensionless

H_D Dynamic liquid hold-up , (dimensionless)

H_T Total liquid hold-up , (dimensionless)

h_g External gas hold-up , (dimensionless)

Hi Henry's law constant , $(\frac{atm - cc}{g\text{-}mole})$

I_0, I_1 Modified Bessel function of the first kind.

K_g Gas phase mass transfer coefficient [gas-to-Liquid transfer] cm/sec.

K_{gS} Gas-Solid mass transfer coefficient (cm/sec).

K_L Liquid phase mass transfer coefficient [Liquid-to-gas] (cm/sec).

$K_{LS} = K_S$ Liquid-Solid Mass transfer coefficient (cm/sec).

$\bar{K}$ Overall mass transfer coefficient (cm/sec).

K_I Reaction rate constant.

L	Superficial liquid mass velocity, [$K_g - m^{-2} - sec^{-1}$].
M	Catalyst loading [grams/cc liquid].
Q_g, Q_L	Gas and liquid flow rates respectively (cc/min).
ΔP_G	Pressure drop for the gas phase in single phase flow (Kg - m^{-2}).
ΔP_L	Pressure drop for the liquid phase in single phase flow (Kg - m^{-2}).
S_{ext}	External surface area of the pellet (cm^2).
$U_L = U_{sL}$	Superficial liquid velocity (cm/sec).
$U_g = U_{sg}$	Superficial gas velocity (cm/sec).
V_p	Pellet volume (cm^3).
X	Pressure drop ratio defined in Table 2-2 (dimensionless).
X_1	Parameter defined in Table 2-2 (dimensionless).
Z	Reactor axial length cm.
$\bar{Z}$	Parameter defined as [$R_{e_G}^{1.67}/R_{e_L}^{.767}$] (dimensionless)

Greek Letters:

ε	Bed porosity (dimensionless).
$\eta_{CE} = \eta_C$	External contacting efficiency (dimensionless).
μ	Viscosity (poise)
ϕ	Thiele Modules

ℓ	Density	(g/cc).
σ	Surface tension	(dynes/cm).
ψ	Parameter defined as $\frac{\sigma_w}{\sigma_L} \frac{\mu_L}{\mu_w} (\frac{\ell_w}{\ell_L})^2$	1/3

Subscript:

CE	Contacting efficiency.
L	Liquid
g	Gas
W	Wetted
w	water
d	dry
E	External
T	Total
s	Solid
S	Superficial

Dimensionless Groups:

Re_L	Liquid Reynolds number [dp ℓ_L U_L/μ_L].
Ga_L	Liquid Galileo number [dp^3 g ℓ_L^2/μ_L^2].
Fr_L	Liquid Froude number [L^2/ℓ_L^2 g dp]
We_L	Liquid Weber number [L^2 dp/σ_L ℓ_L]

$G^*_{a_L}$ Modified Galileo number

$[d_p^3 \, \ell_L \, [\ell_L \, g + \delta Lg]/\mu_L^2]$

Sc Schmidt number $\mu_L/\ell_L \, D_A$

J_D Dimensionless $\dfrac{K_{L_S}}{U_L \, (Sc)^{2/3}}$

Appendix C

Data and Results

Set-A Experiments

Catalyst	= 0.5% pd on alumina
dp	= 0.07 cm
H_2 flow rate	= 2880 cc/min.
Reactor pressure	= 1.02 atm ~ 1 atm
Agitation rate	= 1400 R.P.M.
Solvent	= cyclohexane

Exp. A-1

Catalyst loading = 25 grams

Reaction temperatures = 30.7 $\pm$ 0.2°C

Reaction volume = 2300 cc

Time (sec)	A ↑ αMS x 10^4 ($\frac{\text{g-mole}}{\text{cc}}$)
0	7.133 $\pm$ .37
275	5.772 $\pm$ .11
562	4.779 $\pm$ .083
822	3.543 $\pm$ .187
1122	2.593 $\pm$ .034
1575	0.981 $\pm$ .012
1940	0

$-r_A^x = 3.868 \times 10^{-7}$ $\frac{\text{g-mole}}{\text{cc-sec}}$

$-r_A = 0.0071$ $\frac{\text{g-mole}}{\text{sec-gr pd}}$

Exp. A-2

Catalyst loading = 25 grams

Reaction temperature = 30.7 ± 0.2°C

Reaction volume = 2300 cc

Time (sec)	$\alpha MS \times 10^4$ $(\frac{g\text{-mole}}{cc})$
0	4.148 ± .133
104	3.685 ± 0.11
170	3.304 ± .09
368	2.629 ± .09
584	1.779 ± .012
812	0.932 ± .007
1095	0.1037

$-r_A^x = 3.686 \times 10^{-7}$ $\frac{g\text{-mole}}{cc\text{-sec}}$

$-r_A = 0.0068$ $\frac{g\text{-mole}}{sec\text{-gr pd}}$

Exp. A-3

Catalyst loading = 20 grams

Reaction temperature = 30.6 ± 0.1°C

Reaction volume = 2300 cc

Time (sec)	$\alpha MS \times 10^3$ $(\frac{g\text{-mole}}{cc})$
0	1.515 ± .05
112	1.24 ± .0089
315	0.564 ± .0023
415	0.274 ± .0097
500	0

$$-r_A^x = 3.054 \times 10^{-7} \quad \frac{\text{g-mole}}{\text{cc-sec}}$$

$$-r_A = 0.007 \quad \frac{\text{g-mole}}{\text{sec-gr pd}}$$

Conclusion:

$$-r_A = 0.0069 \pm .00015$$

rate is reproducible to $\pm$ 2.2%

Set-B Experiments

Catalyst	= 0.5% pd on alumina
dp	= 0.03 cm
H_2 flow rate	= 2880 cc/min
Reactor pressure	= 1.02 atm
Agitation rate	= 1400 R.P.M.
Solvent	= cyclohexane

Exp. B-1

Catalyst loading = 24 grams

Reaction temperature = 30.5 $\pm$ 0.7°C

Reaction volume = 2300 cc

Time (sec)	$\alpha MS \times 10^4$ $(\frac{\text{g-mole}}{\text{cc}})$
0	3.6339
75	2.6547
155	1.5644
245	0.3278
327	0

$-r_A^x = 13.66 \times 10^{-7}$ $\frac{\text{g-mole}}{\text{cc-sec}}$

$-r_A = 0.0262$ $\frac{\text{g-mole}}{\text{sec-gr pd}}$

Exp. B-2

Catalyst loading = 7.5 grams

Reaction temperature = 30.6 ± .3°C

Reaction volume = 2300 cc

Time (sec)	$\alpha MS \times 10^4$ $(\frac{g\text{-mole}}{cc})$
0	5.371
315	4.005
745	2.075
1005	.9501
1280	0

$-r_A^x = 4.41 \times 10^{-7}$ $\frac{g\text{-mole}}{cc\text{-sec}}$

$-r_A = 0.027$ $\frac{g\text{-mole}}{sec\text{-gr pd}}$

Exp. B-3

Catalyst loading = 6.8 grams

Reaction temperature = 30.5 ± 0.4°C

Reaction volume = 2300

Time (sec)	$\alpha MS \times 10^4$ $(\frac{g\text{-mole}}{cc})$
0	2.626
200	1.828
414	0.9134
616	0.233
752	0

$-r_A^x = 3.96 \times 10^{-7}$ $\frac{\text{g-mole}}{\text{cc-sec}}$

$-r_A = 0.0267$ $\frac{\text{g-mole}}{\text{sec-gr pd}}$

Exp. B-4

Catalyst loading = 5 grams

Reaction temperature = 30.5 ± 0.5°C

Reaction volume = 2300 cc

Time (sec)	$\alpha MS \times 10^4$ $(\frac{\text{g-mole}}{\text{cc}})$
0	3.555
202	2.911
548	1.810
855	0.928
1110	0.214

$-r_A^x = 3.015 \times 10^{-7}$ $\frac{\text{g-mole}}{\text{cc-sec}}$

$-r_A = 0.027$ $\frac{\text{g-mole}}{\text{sec-gr pd}}$

Exp. B-5

Catalyst loading = 4.7 grams

Reaction temperature = 30.3 ± 13°C

Reaction volume = 2300 cc

Time (sec)	$\alpha MS \times 10^4$ $(\frac{\text{g-mole}}{\text{cc}})$
0	1.8607
240	1.154
525	0.4161
760	0

$-r_A^x = 2.82 \times 10^{-7}$ $\frac{\text{g-mole}}{\text{cc-sec}}$

$-r_A = 0.027$ $\frac{\text{g-mole}}{\text{sec-gr pd}}$

Exp. B-6

Catalyst loading = 4.3 grams

Reaction temperature = 30.6 $\pm$ .2°C

Reaction volume = 2300 cc

Time (sec)	$\alpha MS \times 10^4$ $(\frac{\text{g-mole}}{\text{cc}})$
0	2.285
257	1.625
515	0.925
760	0.321
1020	0

$-r_A^x = 2.61 \times 10^{-7}$ $\frac{\text{g-mole}}{\text{cc-sec}}$

$-r_A = 0.027$ $\frac{\text{g-mole}}{\text{sec-gr pd}}$

Exp. B-7

Catalyst loading = 4.0 grams

Reaction temperature = 30.5 ± .3°C

Reaction volume = 2300 cc

Time (sec)	$\alpha MS \times 10^4$ $(\frac{g\text{-mole}}{cc})$
0	2.499
280	1.828
570	1.107
802	0.602
1111	0

$-r_A^x = 2.381 \times 10^{-7}$ $\frac{g\text{-mole}}{cc\text{-sec}}$

$-r_A = 0.027$ $\frac{g\text{-mole}}{sec\text{-gr pd}}$

Results of Set B Experiments

Exp. No.	Reciprocal of Catalyst loading $(\frac{1}{ms})$ $(\frac{\ell}{grams})$	Reciprocal of reaction rate $\times 10^3$ $(\frac{\ell\text{-sec}}{g\text{-mole}})$
B-1	.0958	.732
B-2	.338	2.525
B-3	.3066	2.267
B-4	.46	3.316
B-5	.489	3.546
B-6	.534	3.814
B-7	.575	4.199

Conclusions:

1. No gas-liquid mass transfer resistance.
2. $-r_A = 0.027 \pm 0.0005$

   rate is reproduced to $\pm$ 2.2%.

Set-C Experiments

Catalyst	= 0.5% pd on alumina
dp	= 0.03 cm
Reactor pressure	= 1.02 atm
Solvent	= cyclohexane

Exp. C-1

Hydrogen flow	= 2880 cc/min
Catalyst loading	= 5.0019 grams
Reaction temperature	= 30.4 $\pm$ 1°C
Reaction volume	= 2500 cc
Agitation rate	= 1400 R.P.M.

Time (sec)	$\alpha MS \times 10^4$ $(\frac{\text{g-mole}}{\text{cc}})$
0	2.877
170	2.445
390	1.763
620	1.231
820	.6869
1020	.2664

$-r_A^x = 2.64 \times 10^{-7}$ $\frac{\text{g-mole}}{\text{cc-sec}}$

$-r_A = 0.0264$ $\frac{\text{g-mole}}{\text{sec-gr pd}}$

Exp. C-2

Same conditions as in C-1 except:

Agitation rate = 1800 R.P.M.

Catalyst loading = 4.21 grams

Time (sec)	$\alpha MS \times 10^4$ $(\frac{g\text{-mole}}{cc})$
0	2.313
217	1.8252
419	1.34
624	0.939
880	0.46

$-r_A^x = 2.2 \times 10^{-7}$ $\frac{g\text{-mole}}{cc\text{-sec}}$

$-r_A = 0.0262$ $\frac{g\text{-mole}}{sec\text{-gr pd}}$

Exp. C-3

Same conditions as in C-1 except:

Agitation rate = 960 R.P.M.

Catalyst loading = 5 grams

Time (sec)	$\alpha MS \times 10^4$ $(\frac{g\text{-mole}}{cc})$
0	2.049
205	1.544
432	0.996
692	0.425

$-r_A^x = 2.35 \times 10^{-7}$ $\frac{g\text{-mole}}{cc\text{-sec}}$

$-r_A = 0.0235$ $\frac{g\text{-mole}}{sec\text{-gr pd}}$

Exp. C-4

Same conditions as in C-1 except:

Agitation rate = 555 R.P.M.

Catalyst loading = 4.723 grams

Reaction volume = 2500 cc

Time (sec)	$\alpha MS \times 10^4$ $(\frac{\text{g-mole}}{\text{cc}})$
0	2.9511
427	2.1527
940	1.2837
1200	0.8576

$-r_A^x = 1.74 \times 10^{-7}$ $\frac{\text{g-mole}}{\text{cc-sec}}$

$-r_A = 0.0184$ $\frac{\text{g-mole}}{\text{sec-gr pd}}$

Exp. C-5

Same conditions as in C-1 except:

Reaction volume = 2400 cc

Catalyst loading = 4.35 grams

Hydrogen flow = 2100 cc/min

Time (sec)	$\alpha MS \times 10^4$ $(\frac{\text{g-mole}}{\text{cc}})$
0	4.2188
475	2.934
950	1.821
1545	0.5349

$-r_A^x = 2.374 \times 10^{-7}$ $\frac{\text{g-mole}}{\text{cc-sec}}$

$-r_A = 0.0262$ $\frac{\text{g-mole}}{\text{sec-gr pd}}$

Exp. C-6

Same conditions as in C-1 except:

Hydrogen flow = 3700 cc/min

Catalyst loading = 4.1 grams

Time (sec)	$\alpha MS \times 10^4$ $(\frac{\text{g-mole}}{\text{cc}})$
0	2.511
150	2.218
350	1.764
570	1.306
800	0.804

$-r_A^x = 2.142 \times 10^{-7}$ $\frac{\text{g-mole}}{\text{cc-sec}}$

$-r_A = 0.0261$ $\frac{\text{g-mole}}{\text{sec-gr pd}}$

Conclusion: No external mass transfer limitations.

Set-D Experiments

dp = 0.005 cm

Agitation rate = 1400 R.P.M.

Reactor pressure = 1.023 atm

Solvent = cyclohexane

Exp.D-1

Catalyst loading = 5 grams of 0.5% pd

Reaction volume = 2300 cc

Hydrogen flow = 2880 cc/min

Reaction temperatures = 15.2 $\pm$ .1°C

Time (sec)	$\alpha MS \times 10^4$ $(\frac{\text{g-mole}}{\text{cc}})$
0	2.324
300	1.871
690	1.076
820	0.717

$-r_A^x = 1.95 \times 10^{-7}$ $\frac{\text{g-mole}}{\text{cc-sec}}$

$-r_A = 0.0180$ $\frac{\text{g-mole}}{\text{sec-gr pd}}$

Exp. D-2

Conditions are the same as in D-1 except:

Reaction temperature = 15°C

Time (sec)	$\alpha MS \times 10^4$ $(\frac{g\text{-mole}}{cc})$
0	3.741
204	3.334
515	2.714
815	2.2004
1100	1.7199

$-r_A^x = 1.84 \times 10^{-7}$ $\frac{g\text{-mole}}{cc\text{-sec}}$

$-r_A = 0.017$ $\frac{g\text{-mole}}{sec\text{-gr pd}}$

Exp. D-3

Catalyst loading = 2.4 grams of 2.5% pd

Reaction volume = 2300 cc

Hydrogen flow = 3700 cc/min

Agitation rate = 1400 R.P.M.

Reaction temperature = 15.7 $\pm$ 0.1

Time (sec)	$\alpha MS \times 10^4$ $(\frac{g\text{-mole}}{cc})$
0	1.649
100	1.19
200	0.765
300	0.312

$-r_A^x = 8.309 \times 10^{-7}$ $\frac{\text{g-mole}}{\text{cc-sec}}$

$-r_A = 0.0174$ $\frac{\text{g-mole}}{\text{sec-gr pd}}$

Exp. D-5

Catalyst loading = 2.54 grams of 2.5% pd

Reaction volume = 2300 cc

Hydrogen flow = 3700 cc/min

Reaction temperature = 17°C

Time (sec)	$\alpha MS \times 10^4$ $(\frac{\text{g-mole}}{\text{cc}})$
0	1.94
100	1.416
200	0.856
300	0.314

$-r_A^x = 5.438 \times 10^{-7}$ $\frac{\text{g-mole}}{\text{cc-sec}}$

$-r_A = 0.0196$ $\frac{\text{g-mole}}{\text{sec-gr pd}}$

Exp. D-6

Catalyst loading = 4.7 grams of 0.5% pd

Reaction volume = 2300 cc

Hydrogen flow = 2880 cc/min

Reaction temperature = 20.8 $\pm$ .2°C

Time (sec)	$\alpha MS \times 10^4$ $(\frac{g\text{-mole}}{cc})$
0	3.003
205	2.435
615	1.291
1000	0.3087

$-r_A^x = 2.7026 \times 10^{-7}$ $\frac{g\text{-mole}}{cc\text{-sec}}$

$-r_A = 0.0264$ $\frac{g\text{-mole}}{sec\text{-gr pd}}$

Exp. D-7

Catalyst loading = 4.6 grams of 0.5% pd

Reaction volume = 2300 cc

Hydrogen flow = 2880 cc/min

Reaction temperature = 20.8 $\pm$ 0.1°C

Time (sec)	$\alpha MS \times 10^4$ $(\frac{g\text{-mole}}{cc})$
0	3.09
253	2.441
504	1.735
804	1.3389

$-r_A^x = 2.688 \times 10^{-7}$ $\frac{g\text{-mole}}{cc\text{-sec}}$

$-r_A = 0.0268$ $\frac{g\text{-mole}}{sec\text{-gr pd}}$

Exp. D-8

Catalyst loading = 2.2 grams of 2.5% pd

Reaction volume = 2350 cc

Hydrogen flow = 3700 cc/min

Reaction temperature = 20.8 $\pm$ 0.3°C

Time (sec)	$\alpha MS \times 10^4$ $(\frac{\text{g-mole}}{\text{cc}})$
0	1.79
80	1.306
160	0.812
240	0.337

$-r_A^x = 6.066 \times 10^{-7}$ $\frac{\text{g-mole}}{\text{cc-sec}}$

$-r_A = 0.026$ $\frac{\text{g-mole}}{\text{sec-gr pd}}$

Exp. D-9

Catalyst loading = 1.75 grams of 2.5% pd

Reaction volume = 2350 cc

Hydrogen flow = 3700 cc/min

Reaction temperature = 20.8 $\pm$ .2°C

Time (sec)	$\alpha MS \times 10^4$ $(\frac{\text{g-mole}}{\text{cc}})$
0	1.536
85	1.104
160	0.733
242	0.324
300	0.07

$-r_A^x = 4.91 \times 10^{-7}$ $\frac{\text{g-mole}}{\text{cc-sec}}$

$-r_A = 0.0263$ $\frac{\text{g-mole}}{\text{sec-gr pd}}$

Exp. D-10

Catalyst loading = 4.5 of 0.5% pd

Reaction volume = 2300 cc

Hydrogen flow = 2880 cc/min

Reaction temperature = 25.7 ± 1°C

Time (sec)	$\alpha MS \times 10^4$ $(\frac{\text{g-mole}}{\text{cc}})$
0	2.967
205	2.263
404	1.552
604	0.940

$-r_A^x = 3.378 \times 10^{-7}$ $\frac{\text{g-mole}}{\text{cc-sec}}$

$-r_A = 0.0345$ $\frac{\text{g-mole}}{\text{sec-gr pd}}$

Exp. D-11

Catalyst loading = 1.9 grams of 2.5% pd

Volume of reaction = 2350 cc

Hydrogen flow = 3700 cc/min

Reaction temperature = 25.8 ± .5

Time (sec)	$\alpha MS \times 10^4$ $(\frac{g\text{-mole}}{cc})$
0	1.777
65	1.374
125	0.998
185	0.578
245	0.19

$-r_A^x = 6.506 \times 10^{-7}$ $\frac{g\text{-mole}}{cc\text{-sec}}$

$-r_A = 0.0322$ $\frac{g\text{-mole}}{sec\text{-gr pd}}$

Exp. D-12

Catalyst loading = 15 grams of 2.5% pd

Reaction volume = 2350 cc

Hydrogen flow = 3700 cc/min

Reaction temperature = 25.6 $\pm$ 0.2°C

Time (sec)	$\alpha MS \times 10^4$ $(\frac{g\text{-mole}}{cc})$
0	1.7
50	1.416
100	1.157
170	.786
235	.403
306	.066

$-r_A^x = 5.37 \times 10^{-7}$ $\frac{g\text{-mole}}{cc\text{-sec}}$

$-r_A = 0.0336$ $\frac{g\text{-mole}}{sec\text{-gr pd}}$

Exp. D-13

Catalyst loading = 4.2 grams of .5% pd

Reaction volume = 2350 cc

Hydrogen flow = 2880 cc/min

Reaction temperature = 30.7 $\pm$ .1°C

Time (sec)	$\alpha MS \times 10^4$ $(\frac{g\text{-mole}}{cc})$
0	4.223
230	3.4148
404	2.620
600	1.8307
806	1.1659

$-r_A^x = 3.878 \times 10^{-7}$ $\frac{g\text{-mole}}{cc\text{-sec}}$

$-r_A = 0.0433$ $\frac{g\text{-mole}}{sec\text{-gr pd}}$

Exp. D-14

Catalyst loading = 4.1 grams of 0.5% pd

Reaction volume = 2350 cc

Hydrogen flow = 2880 cc/min

Reaction temperature = 30.2 $\pm$ 0.1°C

Time (sec)	$\alpha MS \times 10^4$ $(\frac{g\text{-mole}}{cc})$
0	2.087
200	1.263
464	0.586
604	0

$-r_A^x = 5.969 \times 10^{-7}$ $\frac{\text{g-mole}}{\text{cc-sec}}$

$-r_A = 0.0431$ $\frac{\text{g-mole}}{\text{sec-gr pd}}$

Exp. D-16

Catalyst loading = 1.55 grams of 2.5% pd

Reaction volume = 2350 cc

Hydrogen flow = 3700 cc/min

Reaction temperature = 30.2 $\pm$ .2°C

Time (sec)	$\alpha MS \times 10^{-4}$ $(\frac{\text{g-mole}}{\text{cc}})$
0	2.582
50	2.287
100	1.854
150	1.548
200	1.181
250	0.802
300	0.474
355	0.113

$-r_A^x = 7.052 \times 10^{-7}$ $\frac{\text{g-mole}}{\text{cc-sec}}$

$-r_A = 0.0427$ $\frac{\text{g-mole}}{\text{sec-gr pd}}$

Results of Set-D

t°C	$\frac{1}{T} \times 10^3$ ($°K^{-1}$)	$-r_A$ ($\frac{g\text{-mole}}{sec\ gr\ pd}$)
15.3 ± 0.5°C	3.468	.0173 ± .00047
17°C	3.448	.0196
20.8 ± .3	3.403	.0264 ± .00033
25.7 ± 0.5	3.347	.0334 ± .0011
30.5 ± .5	3.294	.0429 ± .00033

From Figure 4-17, the reaction activation energy is 10.2 $\frac{Kcal}{mole}$.

Set-E Experiments

Catalyst	= 0.5% pd on alumina
dp	= 0.005 cm
Agitation rate	= 1400 R.P.M.
Reactor pressure	= 1.023 atm
Reaction temperature	= 30.3 $\pm$ .2°C
Solvent	= Cyclohexane

Exp. E-1

Catalyst loading	= 5.008 grams
Reaction volume	= 2300 cc
Hydrogen flow	= 2020 cc/min
Nitrogen flow	= 900 cc/min

Time (sec)	$\alpha MS \times 10^4$ $(\frac{\text{g-mole}}{\text{cc}})$
0	2.421
205	1.807
402	1.255
605	.655
850	0

$-r_A^x = 2.907 \times 10^{-7}$ $\frac{\text{g-mole}}{\text{cc-sec}}$

Exp. E-2

Catalyst loading = 4.75 grams

Reaction volume = 2300 cc

Hydrogen flow = 1420 cc/min

Nitrogen flow = 1480 cc/min

Time (sec)	$\alpha MS \times 10^4$ $(\frac{\text{g-mole}}{\text{cc}})$
0	2.383
250	1.844
504	1.315
1004	0.382

$-r_A^x = 1.9913 \times 10^{-7}$ $\frac{\text{g-mole}}{\text{cc-sec}}$

Exp. E-3

Catalyst loading = 4.517 grams

Reaction volume = 2300 cc

Hydrogen flow = 880 cc/min

Nitrogen flow = 2090 cc/min

Time (sec)	$\alpha MS \times 10^4$ $(\frac{\text{g-mole}}{\text{cc}})$
0	2.9004
404	2.527
804	2.1179
1200	1.7468
1600	1.3102

$-r_A^x = 9.91 \times 10^{-8}$ $\frac{\text{g-mole}}{\text{cc-sec}}$

Results

P_{Total} (atm)	P_{H_2} (atm)	P_{N_2} (atm)	$-r_A$ $\frac{\text{g-mole}}{\text{sec-gr pd}}$
1.023	1.023	0	.0429
1.023	0.707	0.315	.0267
1.023	0.50	0.522	.0193
1.023	0.303	0.72	.0101

From Figure 4-18, $-r_a = K_p P_{H_2}^{1.17} \sim K_p P_{H_2}$

Set-F Experiments

Solvent = cyclohexane

Agitation rate = 1400 R.P.M.

αMS purified at least 24 hours prior to reaction

Reactor pressure = 1.023 atm and 30°C

Reaction volume = 2300 cc

Exp. F-1

Catalyst loading = 25 grams of 0.5% pd

Hydrogen flow = 2880 cc/min

dp = 0.07 cm

Time (sec)	αMS x 10^4 ($\frac{\text{g-mole}}{\text{cc}}$)
0	2.446
202	2.137
340	1.945
462	1.785
603	1.624
865	1.3809

$-r_A^x = 1.234 \times 10^{-7}$ $\frac{\text{g-mole}}{\text{cc-sec}}$

$-r_A = 0.00227$ $\frac{\text{g-mole}}{\text{sec-gr pd}}$

Exp. F-2

Catalyst loading = 4.7 grams of 0.5% pd

dp = 0.03 cm

Hydrogen flow = 2880 cc/min

Time (sec)	$\alpha MS \times 10^4$ $(\frac{g\text{-mole}}{cc})$
0	3.8026
320	3.519
635	3.224
1020	2.9645
1325	2.7092
1632	2.432

$-r_A^x = 8.244 \times 10^{-8}$ $\frac{g\text{-mole}}{cc\text{-sec}}$

$-r_A = 0.00806$ $\frac{g\text{-mole}}{cc\text{-sec}}$

Exp. F-3

Same batch as in F-2 experiment.

Catalyst loading = 4.3 grams of 0.5% pd

dp = .03 cm

Hydrogen flow = 2880 cc/min

Time (sec)	$\alpha MS \times 10^4$ $(\frac{g\text{-mole}}{cc})$
0	3.47
315	3.216
630	3.0019
920	2.894
1326	2.93

$-r_A^x = 3.306 \times 10^{-7}$ $\frac{\text{g-mole}}{\text{cc-sec}}$

$-r_A = .0138$ $\frac{\text{g-mole}}{\text{sec-gr pd}}$

Exp. F-5

Reaction temperature = 32.3 ± .5°C

Catalyst loading = 2.5 grams of 2.5% pd

dp = .005 cm

αMS was not purified

H_2 flow = 3700 cc/min

Time (sec)	αMS x 10^4 ($\frac{\text{g-mole}}{\text{cc}}$)
0	1.925
50	1.565
100	1.16
150	0.812
200	0.458
250	6.079

$-r_A^x = 7.37 \times 10^{-7}$ $\frac{\text{g-mole}}{\text{cc-sec}}$

$-r_A = 0.027$ $\frac{\text{g-mole}}{\text{sec-gr pd}}$

Exp. F-6

Reaction temperature = 32.2 ± .3°C

Catalyst loading = 2.7 grams of 2.5% pd

dp = .005 cm

Hydrogen flow = 3700 cc/min

αMS was not purified

Time (sec)	αMS x 10^4 ($\frac{\text{g-mole}}{\text{cc}}$)
0	2.435
80	1.792
160	1.158
240	0.518
320	0

$-r_A^x = 7.981 \times 10^{-7}$ $\frac{\text{g-mole}}{\text{cc-sec}}$

$-r_A = 0.0271$ $\frac{\text{g-mole}}{\text{sec-gr pd}}$

Set-G Experiments

Catalyst	= 0.5% pd on alumina
dp	= 0.005 cm
Agitation rate	= 1400 R.P.M.
Solvent	= HEXANE
Reactor pressure	= 1.023 atm

Exp. G-1

Catalyst loading	= 5.0015 grams
Reaction volume	= 2300 cc
Hydrogen flow	= 2880 cc/min
Solvent U.V. grade	
Reaction temperature	= 15.1 $\pm$ .1°C

Time (sec)	$\alpha MS \times 10^4$ $(\frac{\text{g-mole}}{\text{cc}})$
0	2.065
200	1.659
400	1.127
600	0.659
800	0.15

$-r_A^x = 2.415 \times 10^{-7}$ $\frac{\text{g-mole}}{\text{cc-sec}}$

$-r_A = 0.022$ $\frac{\text{g-mole}}{\text{sec-gr pd}}$

Exp. G-2

Conditions are the same as in G-1.

Time (sec)	$\alpha MS \times 10^4$ $(\frac{\text{g-mole}}{\text{cc}})$
0	2.972
200	2.425
400	2.051
600	1.561
800	1.15

$-r_A^x = 2.254 \times 10^{-7}$ $\frac{\text{g-mole}}{\text{cc-sec}}$

$-r_A = 0.021$ $\frac{\text{g-mole}}{\text{sec-gr pd}}$

Exp. G-3

Catalyst loading = 4.4 grams

Reaction volume = 2350 cc

Hydrogen flow = 2880 cc/min

Solvent is U.V. grade

Reaction temperature = 20.5 $\pm$ .1°C

Time (sec)	$\alpha MS \times 10^4$ $(\frac{\text{g-mole}}{\text{cc}})$
0	3.044
150	2.663
355	2.1989
500	1.75

$-r_A^x = 2.54 \times 10^{-7}$ $\frac{\text{g-mole}}{\text{cc-sec}}$

$-r_A = 0.0271$ $\frac{\text{g-mole}}{\text{sec-gr pd}}$

Exp. G-4

Catalyst loading = 4.6 grams

Reaction volume = 2285 cc

Hydrogen flow = 2880 cc/min

Solvent is U.V. grade

Reaction temperature = 20.1 ± .1°C

Time (sec)	$\alpha MS \times 10^4$ $(\frac{\text{g-mole}}{\text{cc}})$
0	1.406
200	0.7883
400	0.263

$-r_A^x = 2.857 \times 10^{-7}$ $\frac{\text{g-mole}}{\text{cc-sec}}$

$-r_A = 0.0283$ $\frac{\text{g-mole}}{\text{sec-gr pd}}$

Exp. G-5

Catalyst loading = 4.33 grams

Reaction volume = 2300 cc

Hydrogen flow = 2880 cc/min

Solvent is U.V. grade

Reaction temperature = 25.2 ± .2°C

Time (sec)	$\alpha MS \times 10^4$ $(\frac{\text{g-mole}}{\text{cc}})$
0	2.1072
150	1.6703
300	1.109
450	0.626
600	0.229

$-r_A^x = 3.199 \times 10^{-7}$ $\frac{\text{g-mole}}{\text{cc-sec}}$

$-r_A = 0.034$ $\frac{\text{g-mole}}{\text{sec-gr pd}}$

Exp. G-6

Catalyst loading = 5 grams

Reaction volume = 2300 cc

Solvent is U.V. grade

Hydrogen flow = 2880 cc/min

Reaction temperature = 20.4 $\pm$ .1°C

Time (sec)	$\alpha MS \times 10^4$ $(\frac{\text{g-mole}}{\text{cc}})$
0	2.723
205	2.08
402	1.497
645	0.764

$-r_A^x = 3.03 \times 10^{-7}$ $\frac{\text{g-mole}}{\text{cc-sec}}$

$-r_A = 0.0278$ $\frac{\text{g-mole}}{\text{sec-gr pd}}$

Time (sec)	$\alpha MS \times 10^4$ $(\frac{\text{g-mole}}{\text{cc}})$
0	2.218
455	1.941
855	1.575
1250	1.1988

$$-r_A^x = 8.219 \times 10^{-8} \quad \frac{\text{g-mole}}{\text{cc-sec}}$$

$$-r_A = 0.0086 \quad \frac{\text{g-mole}}{\text{sec-gr pd}}$$

From experiments G-1 to G-8

t.°C	$\frac{1}{T} \times 10^3$ °K^{-1}	P_{H_2} (atm)	$-r_A$ $(\frac{\text{g-mole}}{\text{sec-gr pd}})$
15.1	3.47	1.023	0.021
20.2	3.41	1.023	0.027
25.2	3.35	1.023	0.034
20.2	-	0.5	0.0139
20.1	-	0.3	0.0086

$$E = 7.95 \sim 8.0 \ \frac{\text{Kcal}}{\text{mole}}$$

$$-r_A = K_p P_{H_2}$$

Exp. G-7

Solvent is U.V. grade

Catalyst loading = 4.7 grams

Reaction volume = 2300 cc

Hydrogen flow = 1420 cc/min

Nitrogen flow = 1480 cc/min

Reaction temperature = 20.2 $\pm$ .1°C

Time (sec)	$\alpha MS \times 10^4$ $(\frac{\text{g-mole}}{\text{cc}})$
0	1.871
245	1.607
500	1.145
770	0.812

$-r_A^x = 1.419 \times 10^{-7}$ $\frac{\text{g-mole}}{\text{cc-sec}}$

$-r_A = 0.0139$ $\frac{\text{g-mole}}{\text{sec-gr pd}}$

Exp. G-8

Catalyst loading = 4.4 grams

Solvent is U.V. grade

Reaction volume = 2300 cc

H_2 flow = 900 cc/min

N_2 flow = 2080 cc/min

Reaction temperature = 20.1°C

Exp. G-9

Catalyst loading = 5 grams

Reaction volume = 2300 cc

Reaction temperature = 20.2°C

Hydrogen flow = 2880 cc/min

Solvent is ACS grade

Time (sec)	$\alpha MS \times 10^4$ $(\frac{\text{g-mole}}{\text{cc}})$
0	3.044
200	2.891
450	2.588
750	2.232
1100	1.883

$-r_A^x = 1.086 \times 10^{-7}$ $\frac{\text{g-mole}}{\text{cc-sec}}$

$-r_A = 0.0099$ $\frac{\text{g-mole}}{\text{sec-gr pd}}$

$$\frac{(-r_A) \text{ U.V. grade solvent}}{(-r_A) \text{ ACS grade solvent}} = \frac{0.027}{0.0099} = 2.72$$

Set-H Experiments

Catalyst	= 0.5% pd on alumina
dp	= 0.005 cm
Agitation rate	= 1400 R.P.M.
Reactor pressure	= 1.023 atm
Hydrogen flow	= 2880 cc/min
Solvent	= Tetrahydrofurane and a mixture of tetrahydrofurane - cyclohexane.

Exp. H-1

Solvent	= pure tetrahydrofurane
Catalyst loading	= 4.9 grams
Reaction volume	= 2300 cc
Temperature	= 25°C

Time (sec)	$\alpha MS \times 10^4$ $(\frac{g\text{-mole}}{cc})$
0	2.575
260	2.536
600	2.314
1000	2.166
1625	2.04
2275	1.79
3000	1.583

$-r_A^x = 3.025 \times 10^{-8}$ $\frac{g\text{-mole}}{cc\text{-sec}}$

$-r_A = 0.00284$ $\frac{g\text{-mole}}{sec\text{-gr pd}}$

Exp. H-2

Solvent = 70% by volume cyclohexane and 30% tetrahydrofurane

Catalyst loading = 5.0174 grams

Reaction volume = 2300

Temperature = 15°C

Time (sec)	$\alpha MS \times 10^4$ $(\frac{\text{g-mole}}{\text{cc}})$
0	2.473
400	2.308
1000	2.0248
1500	1.832

$-r_A^x = 4.33 \times 10^{-8}$ $\frac{\text{g-mole}}{\text{cc-sec}}$

$-r_A = 0.00397$ $\frac{\text{g-mole}}{\text{sec-gr pd}}$

Exp. H-3

Same conditions as in H-2, except

Catalyst loading = 4.9 grams

Temperature = 20°C

Time (sec)	$\alpha MS \times 10^4$ $(\frac{\text{g-mole}}{\text{cc}})$
0	4.089
405	3.878
905	3.55
1700	3.121

$-r_A^x = 5.76 \times 10^{-8}$ $\frac{\text{g-mole}}{\text{cc-sec}}$

$-r_A = .0054$ $\frac{\text{g-mole}}{\text{sec-gr pd}}$

Exp. H-4

Same conditions as in H-2, except

Catalyst loading = 4.8 grams

Reaction volume = 2000 cc

Temperature = 24.9°C

Time (sec)	$\alpha MS \times 10^4$ $(\frac{g\text{-mole}}{cc})$
0	5.5
500	5.128
900	4.75
1700	4.1

$-r_A^x = 8.29 \times 10^{-8}$ $\frac{g\text{-mole}}{cc\text{-sec}}$

$-r_A = 0.0069$ $\frac{g\text{-mole}}{sec\text{-gr pd}}$

---

t°C	$\frac{1}{T} \times 10^3$ °K^{-1}	$-r_A$ $(\frac{g\text{-mole}}{sec\text{-gr pd}})$
15	3.472	.00397
20	3.41	.0054
24.9	3.356	.0069

$E = 9.44 \frac{Kcal}{mole}$

For 70% by volume cyclohexane and 30% tetrahydrofurane.

Set-I Experiments

Catalyst = 0.5% pd on alumina

dp = 0.005 cm

Solvent = Isobutyl alcohol

Reactor pressure = 1.023 atm

Hydrogen flow = 2880 cc/min

Reaction volume - 2300 cc

Exp. I-1

Catalyst loading = 5.002 grams

Reaction temperature = 15.4°C

Time (sec)	$\alpha MS \times 10^4$ $(\frac{g\text{-mole}}{cc})$
0	3.52
250	3.38
500	3.25
1100	2.96
2000	2.66
3500	2.32
5000	1.965
6500	1.67
8000	1.397
9500	1.13

neglected due to unequilibrium of the reaction mixture

$-r_A^x = 2.04 \times 10^{-8}$ $\frac{g\text{-mole}}{cc\text{-sec}}$

$-r_A = 0.00187$ $\frac{g\text{-mole}}{sec\text{-gr pd}}$

Exp. I-2

Catalyst loading = 4.8

Reaction temperature = 25.1 ± .1°C

Time (sec)	$\alpha MS \times 10^4$ $(\frac{g\text{-mole}}{cc})$
0	2.98
2000	2.32
4000	1.79
6000	1.32

$-r_A^x = 2.755 \times 10^{-8}$ $\frac{g\text{-mole}}{cc\text{-sec}}$

$-r_A = 0.00264$ $\frac{g\text{-mole}}{sec\text{-gr pd}}$

Exp. I-3

Reaction temperature = 35.3°C

Catalyst loading = 4.2 grams

Reaction volume = 2300 cc

Time (sec)	$\alpha MS \times 10^4$ $(\frac{g\text{-mole}}{cc})$
0	2.39
1000	1.93
2000	1.519
4000	0.906
5000	0.64

$-r_A^x = 3.454 \times 10^{-8}$ $\frac{g\text{-mole}}{cc\text{-sec}}$

$-r_A = 0.00378$ $\frac{g\text{-mole}}{sec\text{-gr pd}}$

Results of Experiment I-1 to I-3

t°C	$\frac{1}{T} \times 10^3$ °K^{-1}	$-r_A$ ($\frac{\text{g-mole}}{\text{sec-gr pd}}$)	Activation Energy
15.4	3.46	0.00187	E ($\frac{\text{Kcal}}{\text{mole}}$)
25.1	3.35	0.00264	6.33
35.3	3.24	0.00378	

BIBLIOGRAPHY

1. Van Deemter, J.J., "Trickle Hydrodesulfurization - A Case History", Third European Symp. Chem. Reaction Eng., 215 (1964).

2. Le Nobel, J.W., and J.H. Choufoer, "Development in Treating Processes for the Petroleum Industry", Fifth World Petr. Cong. Proc., Sec. III, Paper 18, Fifth World Petr. Cong., Inc., New York (1959).

3. Lister, A., "Engineering Design and Development of Desulphurizer Reactor", Third Eur. Symp. Chem. Reaction Eng., 225 (1964).

4. Brusie, J.P. and E.V. Hort, "Unsaturated Alcohols Manufacture", Kirk-Othmer Encyclopedia of Chem. Tech., 1, 2nd Edition, 609 (1963).

5. Bondi, A., "Handling Kinetics From Trickle-Phase Reactors", Chem. Tech., p. 185 (March 1971).

6. Kronig, W., "Hydrogenation of Acetylene in the Presence of Butadiene in Trickle-Flow Reactor", 6th World Petr. Cong., Sect. IV, paper 7 (1963).

7. Sirasubramanian, R. and B.L. Crynes, "Effect of Catalyst Support Properties on Hydrodenitrogenation of Coal Liquids", Paper presented at 69th Annual AIChE Meeting, Chicago, Ill., Nov. 28-Dec. 2 (1976).

8. Satterfield, C.N. "Trickle-Bed Reactors", AIChE J., 21, 209 (1975).

9. Hofman, H. "Hydrodynamics, Transport Phenomena, and Mathematical Models in Trickle-Bed Reactors", Int. Chem. Eng., 17, 19-28 (1977).

10. _____ "Multiphase Catalytic Packed Bed Reactors", Cat. Rev., Sci. ENG., 17(1), 71 (1978).

11. Goto, S., J.M. Smith and J. Levec, "Trickle-Bed Oxidation Reactors", Cat. Rev. Sci. ENG., 15(2), 187-247 (1977).

12. Herskowitz, M. "Performance of Trickle-Bed Reactor", Ph. D. Thesis, Univ. of California, Davis (1978).

13. Weekman, V.W., Jr., and J.E. Myers, "Fluid-Flow Characteristics of Concurrent Gas-Liquid Flow in Packed Beds", AIChE J., 10, 951 (1964).

14. Specchia, V., A. Rossini and G. Baldi, "Distribution and Radial Spread of Liquids in Two Phase Concurrent Flow in a Packed Bed", Quad. Ing. Chim., Ital., 10, 171 (1974).

15. Sylvester, N.D., and P. Pitayagulsarn, "Radial Liquid Distribution In Concurrent Two Phase Down Flow in Packed Beds", Can. J. Chem. Eng., 53, 599 (1975).

16. Reiss, L.P. "Concurrent Gas-Liquid Contacting In Packed Columns", Ind. Eng. Chem., Proc. Des. Dev., 6, 486 (1967).

17. Hochman, J.M. and E. Effron, "Two-Phase Concurrent Down Flow In Packed Beds", Ind. Eng. Chem., Fund. 8, 63 (1969).

18. Baldi, G. and V. Specchia, "Distribution and Radial Spread of Liquid in Packed Towers With Two-Phase Concurrent Flow: Effect of Packing Shape and Size", Quad. Ing. Chim. Ital., 12, 107 (1976).

19. Shah, Y.T., "Gas-Liquid-Solid Reactor Design", McGraw Hill Inc., 1979.

20. Charpentier, J.C. "Recent Progress in Two Phase Gas-Liquid Mass Transfer in Packed Beds", Chem. Eng. J., 11, 161-181 (1976).

21. Gianetto, A., V. Specchia and G. Baldi "Absorption in Packed Towers With Concurrent Downward High-Velocity Flow: I: Interfacial Areas", Quad. Ing. Chim. Ital., 6, 125 (1970).

22. "Absorption in Packed Towers with Concurrent Downward High-Velocity Flow: II: Mass Transfer", AIChE J., 19, 916 (1973).

23. Specchia, V., S. Sicardi, and A. Gianetto, "Absorption In Packed Towers With Concurrent Upward Flow", AIChE J., 20, 646 (1974).

24. Baldi, G., and S. Sicardi, "A Model For Mass Transfer With and Without Chemical Reaction in Packed Towers", Chem. Eng. Sci., 30, 617 (1975).

25. "A Model for Mass Transfer In Packed Towers: Mass Transfer With Controlling Resistance In the Gas Phase", Chem. Eng. Sci., 31, 651 (1976).

26. Sato, Y., T. Hirose, F. Takahashi, and M. Toda, "Pressure Loss and Liquid Holdup In Packed Bed Reactors With Cocurrent Gas-Liquid Down Flow", J. Chem. Eng., Japan, 6, 147 (1973).

27. Larkins, R.P., R.R. White, and D.W. Jeffrey, "Two Phase Concurrent Flow in Packed Beds", AIChE J., 7, 231 (1961).

28. Charpentier, J.C., and M. Favier, "Some Liquid Hold-up Experimental Data In Trickle Bed Reactors, For Foaming and Non-Foaming Hydrocarbons", AIChE J., 21, 1213 (1975).

29. Otake, T., and K. Okada, "Liquid Hold-up In Packed Towers", Kagaku Kaguku, 17, 176 (1963).

30. Way, P. "The Role Of Liquid Phase In the Performance Of A Trickle-Bed Reactor", Ph.D. Thesis, MIT, Cambridge (1971).

31. Davidson, J.F., E.J. Cullen, D. Harison, and D. Roberts "The Hold-Up and Liquid Film Coefficient Of Packed Towers, Part I: Behavior of a String of Spheres", Trans. Inst. Chem. Engrs., 37, 122 (1959).

32. Specchia, V., and G. Baldi, "Pressure Drop and Liquid Hold-Up For Two Phase Concurrent Flow In Packed Bed", Chem. Eng. Sc., 32, 515 (1977).

33. Colombo, A.J., G. Baldi, and S. Sicardi "Solid-Liquid Contacting Effectiveness In Trickle-Bed Reactors", Chem. Eng. Sc., 31, 1101 (1976).

34. Goto, S., and J.M. Smith, "Trickle Bed Reactor Performance, Part I: Hold-up and Mass Transfer", AIChE J., 21, 706 (1975).

35. _____ "Trickle Bed Reactor Performance, Part II: Reaction Studies", AIChE J., 21, 714 (1975).

36. Sylvester, N.D., and P. Pitayagulsarn, "Mass Transfer For Two-Phase Cocurrent Downflow In A Packed Bed", Ind. Eng. Chem., Proc. Des. Dev., 14, 421 (1975).

37. Sherwood, T.K. and F.A.L. Holloway, "Performance Of Packed Towers-Liquid Film Data For Several Packings", Trans. Am. Inst. Chem. Eng., 36, 39 (1940).

38. Ufford, R.C., and J.J. Perona, "Liquid Phase Mass Transfer With Cocurrent Flow Through Packed Towers", AIChE J., 19, 1223 (1973).

39. Van Krevelen, D.W., and J.T.C. Krekels "Rate of Dissolution of Solid Substances", Rec. Trav. Chim., 67, 512 (1948).

40. Sato, Y., T. Hirose, F. Takahashi, and M. Toda "Performance Of Fixed Bed Catalytic Reactor With Concurrent Gas-Liquid Flow", PACHEC, Section 8. 187, (1972).

41. Hirose, T., M. Toda and Y. Sato, "Liquid Phase Mass Transfer In Packed Bed Reactor With Concurrent Gas-Liquid Down Flow", J. Chem. Eng., Japan, 7, 187, (1974).

42. Evans, G.C., and C.F. Gerold, "Mass Transfer From Benzoic Acid Granules To Water In Fixed and Fluidized Beds At Low Reynolds Numbers", Chem. Eng. Progr., 49, 135 (1953).

43. Onda, K. E. Sada, and Y. Murase, "Liquid-Solid Mass Transfer Coefficients In Packed Towers", AIChE J., 5, 235 (1959).

44. Puranik, S.S. and A. Vogelpohl, "Effective Interfacial Area In Irrigated Packed Columns", Chem. Eng. Sc., 29, 501 (1974).

45. Shulman, K.L., C.F. Ulbrich, A.Z. Proulx, and J.O. Zimmerman "Performance Of Packed Columns. II. Wetted And Effective Interfacial Areas, Gas And Liquid Phase Mass Transfer Rates", AIChE J., 1, 253 (1955).

46. Dudukovič, M.P., "Catalyst Effectiveness Factor And Contacting Efficiency In Trickle Bed Reactors", AIChE J., 23, 940 (1977).

47. Mills, P.L., and M.P. Duduković, "A Dual-Series Solution For The Effectiveness Factor Of Partially Wetted Catalyst In Trickle Bed Reactors", Ind. Eng. Chem. Fund., 18, 139 (1979).

48. Schwartz, J.G., "The Efficiency Of Liquid-Solid Contacting In Trickle-Bed Reactors", D. Sc. Thesis, Washington University, St. Louis, MO.

49. Sedriks, W., and C.N. Kenney, "Partial Wetting In Trickle Bed Reactors: The Reduction Of Crotonaldehyde Over A Palladium Catalyst", Chem. Eng. Sc., 28, 559 (1973).

50. Jawad, A., "Catalytic Trickle-Bed Reactor Studies", Ph.D. Thesis, University of Birmingham, England, (1974).

51. Satterfield, C.N., "Mass Transfer In Heterogeneous Catalysis", MIT Press (1970).

52. Hoog, H., H.G. Klinkert, and A. Schaafsma, "Shell Hydrodesulfurization Process", Petrol. Ref., 32 (5), 137 (1953).

53. Van Zoonen, D., and C. Th. Douwes, "Effect Of Pellet Pore Structure On Catalyst Performance In The Hydrodesulfurization Of Straight-Run Gas Oil", J. Inst. Petroleum, 49, 383 (1963).

54. Van Deemter, J.J., 3rd Symposium on Chemical Reaction Eng., P. 215 (1964).

55. Adlington, D., and E. Thompson, "Desulfurization In Fixed And Fluidized Bed Catalyst System", 3rd Eur. Symp. Chem. Reaction Eng., P. 203 (1964).

56. Klassen, J., and R.S. Kirk, "Kinetics Of Liquid Phase Oxidation Of Ethanol", AIChE J., 1, 488 (1955).

57. Babcock, B.D., G.T. Mejdel, and O.A. Hougen, "Catalyzed Gas-Liquid Reaction In Trickle-Bed Reactors", AIChE J., 3, 366 (1957).

58. Johnson, D.L., H. Saito, J.D. Polejes, and O.A. Hougen, "Effects Of Bubbling And Stirring On Mass Transfer Coefficients In Liquids", AIChE J., 3, 411 (1957).

59. Sherwood, T.K. and E.J. Farkas, "Studies Of The Slurry Reactor", Chem. Eng. Sc. 21, 573 (1966).

60. White, D.E., M. Litt, and G.J. Heymach, "Diffusion Limited Heterogeneous Catalytic Reaction On A Rotating Disk. I. Hydrogenation Of α-Methylstyrene". Ind. Eng. Chem. Fund., 13, 143 (1974).

61. Biskis, E.G., and J.M. Smith, "Pulsation In A Fixed-Bed Reactor", AIChE J., 9, 677 (1963).

62. Satterfield, C.N., and P.E. Way, "The Role Of The Liquid Phase In The Performance Of A Trickle-Bed Reactor", AIChE J., 18, 305 (1972).

63. Germain, A.H., A.G. LeFebure, and G.A. L'Homme, "Experimental Study Of A Catalytic Trickle-Bed Reactor", Chem. Reaction Eng., - II, Adv. In Chem. Ser. No. 133, p. 164 (1974).

64. Ware, C.H. Jr., "Liquid Phase Catalytic Hydrogenation In A Trickle-Bed Reactor", Ph.D. Thesis, Univ. of Penn., University Park (1959).

65. Satterfield, C.N., and F. Ozel, "Direct Solid-Catalyzed Reaction Of A Vapor In An Apparently Completely Wetted Trickle-Bed Reactor", AIChE J., 19, 1259 (1973).

66. Satterfield, C.N., A.A. Pelossof, and T.K. Sherwood, "Mass Transfer Limitations In A Trickle-Bed Reactor", AIChE J., 15, 226 (1969).

67. Levec, J., and J.M. Smith, "Oxidation of Acetic Acid Solution In A Trickle-Bed Reactor", AIChE J., 22, 159 (1976).

68. Sylvester, N.D. and P. Pitayagulsarn, "Effect Of Transport Processes On Conversion In A Trickle-Bed Reactor", AIChE J., 19, 640 (1973).

69. Hanika, J., K. Sporka, and V. Ruzicka, "Investigation Of Hydrogenation In Liquid Phase. XVI. Theoretical Models Of Hydrogenation In Liquid Film. Flat Plate", Coll. Czech. Chem. Comm., 35, 2111 (1976).

70. _____ "Investigation of Hydrogenation in Liquid Phase. XVIII. Experimental Verification Of A Theoretical Model Of A Trickle Bed Reactor", Ibid., 36, 2903 (1971b).

71. _____ "Investigation Of Hydrogenation In Liquid Phase. XVII. Theoretical Model Of Hydrogenation In A Liquid Film In A Vertical Column Of Spheres", Ibid., 36, 1358 (1971a).

72. _____ and J. Krausova, "Qualitative Observations Of Heat And Mass Transfer Effects On The Behavior Of A Trickle-Bed Reactor", Chem. Eng. Commun. 2, 19 (1975).

73. Pelossof, A.A., Ph.D. Thesis, M.I.T., Cambridge, Mass. (1967).

74. Mears, D. "The Role Of Liquid Hold-Up And Effective Wetting On The Performance Of Trickle-Bed Reactor", Chem. Reaction Eng. II, Adv. In Chem. Ser. No. 133, p. 218 (1974).

75. Norman, W.S. "Absorption, Distillation And Cooling Towers", Longmans Press (1962).

76. Ma, Y.H. "Effectiveness Factor In A Liquid-Filled Porous Catalyst", D.Sc. Thesis, M.I.T., (1966).

77. Ross, L.D. "Performance Of Trickle-Bed Reactors", Chem. Eng. Prog., 61, 77 (1965).

78. Henry, H.C. and J.B. Gilbert, "Scale Up Of Pilot Plant Data For Catalytic Hydroprocessing", Ind. Eng. Chem. Proc. Des. Develop., 12, 328 (1973).

79. Suzuki, M., and J.M. Smith, "Effect Of Transport Processes On Conversion In A Fixed Bed Reactor", AIChE J., 16, 882 (1970).

80. Sylvester, N.D., and P. Pitayagulsarn "Effect Of Catalyst Wetting On Conversion In A Trickle-Bed Reactor", Can. J. Chem. Eng., 52, 539 (1974).

81. Lin, C.T., "A Model Reaction For Studying Trickle-Bed Reactor", M.Sc. Thesis, University of Mississippi, August (1974).

82. Furusawa, T. and J.M. Smith "Interparticles Mass Transport In Slurries By Dynamic Adsorption Studies", AIChE J., 20 (1), 88 (1974).

83. Rurusawa, T., and J.M. Smith, "Mass Transfer Rates In Slurries By Chromatography", Ind. Eng. Chem. Fundam., 12, 360 (1973).

84. Misic, D., and J.M. Smith, "Adsorption Of Benzene In Carbon Slurries", Ind. Eng. Chem., Fundam. 10, 380 (1971).

85. Tien, C., and G. Thodos, "Ion Exchange Kinetics For Systems Of Non-Linear Equilibrium Relationship", AIChE J., 5, 373 (1959).

86. Weber, W.J., Jr. and J.P. Gould, "Sorption Of Organic Pesticides From Aqueous Solutions", Amer. Chem. Soc. publication, Washington, D.C. (1966).

87. Miller, C.O., and C.W. Clump "A Liquid Phase Adsorption Study Of Rates Of Diffusion Of Phenol From Aqueous Solution into Activated Carbon", AIChE J., 16, 169 (1970).

88. Koymiyama, H., and J.M. Smith, "Sulfur Dioxide Oxidation In Slurries Of Activated Carbon, Part I. Kinetics", AIChE J., 21, 664 (1975).

89. Koymiyama, H., and J.M. Smith "Sulfur Dioxide Oxidation In Slurries of Activated Carbon, Part II, Mass Transfer Studies", AIChE J., 21 670 (1975).

90. Koymiyama, H., and J.M. Smith "Surface Diffusion In Liquid Filled Pores", AIChE J., 20, 1110 (1974).

91. Ramahandran, P.A., and J.M. Smith "Adsorption Of Hydrogen Sulfide In A Slurry Reactor", Ind. Eng. Chem. Fundam., 17, 17 (1978).

92. Niyama, H., and J.M. Smith, "Adsorption Of Nitric Oxide In Aqueous Slurries Of Activated Carbon: Transport Rates By Moment Analysis Of Dynamic Data", AIChE J., 22, 961 (1976).

93. Niyama, H., and J.M. Smith "Adsorption Rates of Oxygen In Aqueous Slurries of Activated Carbon", AIChE J., 23, 592 (1977).

94. Goto, S., and J.M. Smith, "Analysis Of Three-phase Packed-Bed Reactors", AIChE J., 24, 294 (1978).

95. Sylvester, N.D., and J. Carbary, "Slurry And Trickle-Bed Reactor Effectiveness", Cand. J. Chem. Eng., 53, 313 (1975).

96. Goto, S., S. Watabe, and M. Mastubara, "The Role Of Mass Transfer In Trickle-Bed Reactors", Can. J. Chem. Eng., 54, 551 (1976).

97. Cecil, R.R., Mayer, F.Z., and E.N. Cart Am. Inst. Chem. Eng. Meet. Los Angeles (1968).

98. Pexidr, V., A. Krejcirik, and J. Pasek, "Mass Transfer In A Catalytic Bubble-Phase Reactor", Int. Chem. Eng., 20 (1), 84 (1980).

99. Pruden, B.B., and M.E. Weber, "Evaluation Of Three Phase Transport Reactor", Can. J. Chem. Eng., 48, 162 (1970).

100. Snider, J.W., and J.J. Perona, "Mass Transfer In A Fixed Bed Gas-Liquid Catalytic Reactor With Concurrent Upflow", AIChE J., 20 (6), 1172 (1974).

101. Ramachandran, P.A., and J.M. Smith "Effectiveness Factors in Trickle-Bed Reactors" AIChE J., 25, 538 (1979).

102. Herskowitz, M., R.G. Carbonell, and J.M. Smith "Mass Transfer and Partial Wettings in Trickle-Bed Reactors", AIChE J., 25, 272, (1979).

103. Tan, C.S., and J.M. Smith, "Catalyst Particle Effectiveness With Unsymmetrical Boundary Conditions", unpublished manuscript.

104. Mills, P.L. and M.P. Duduković, "Analysis Of Catalyst Effectiveness In Trickle-Bed Reactors Processing Volatile Or Nonvolatile Reactants", Chem. Eng. Sc., "In press".

105. Gianetto, A., G. Baldi, V. Specchia, and S. Sicardi, "Hydrodynamics And Solid-Liquid Contacting Effectiveness In Trickle-Bed Reactors", AIChE J., 24, 1087 (1978).

106. Midoux, N., M. Favier, J.C. Charpentier, "Flow Pattern, Pressure Loss And Liquid Hold-up Data In Gas-Liquid Downflow Packed Beds With Foaming and Non-Foaming Hydrocarbons", J. Chem. Eng. Japan, 9, 350 (1976).

107. Chou, T.S., F.L. Worley, and D. Luss "Flow Regimes Transition In Trickle-Bed Reactors", Ind. Eng. Chem. Proc. Des. Develop., 16, 424 (1977).

108. Onda, K., H. Takeuchi, and Y. Okumoto, "Mass Transfer Coefficients Between Gas And Liquid Phases In Packed Columns", J. Chem. Eng., Japan, 1, 56 (1968).

109. Mahajani, V.V., and M.M. Sharma, "Effective Interfacial Area And Liquid Side Mass Transfer Coefficient In Trickle-Bed Reactor", Chem. Eng. Sc., 34, 1425 (1979).

110. Mills, P.L., "Catalyst Effectiveness And Solid-Liquid Contacting In Trickle-Bed Reactors", D. Sc. Thesis, Washington University, St. Louis, MO (1980).

111. Specchia, V., G. Baldi, and A. Gianetto, "Solid-Liquid Mass Transfer In Trickle-Bed Reactors", 4th ISCRE, Heidelberg, p. 656 (1976).

112. Onda, K., H. Takeuchi, and Y. Kayama, "Effect Of Packing Materials On The Wetted Surface Areas", Kagaku Kogaku, 31, 126 (1967).

113. Kruyer, S., and P.P. Nobel "Solubility Of Hydrogen In Benzene, Cyclohexane, Decalin, Phenol And Cyclohexanol", RECUEIL, 80, 1145 (1961).

114. Dwivedi, P.N., and S.N. Upadhyay, "Particle-Fluid Mass Transfer In Fixed And Fluidized Beds", Ind. Eng. Chem. Proc. Des. Develop., 16, 157, (1977).